Direct and indirect measurements in quantum mechanics

Thesis submitted to

Tata Institute of Fundamental Research, Mumbai, India
for the degree of
Doctor of Philosophy
in
Physics

by

Varun Dubey

International Centre for Theoretical Sciences
Tata Institute of Fundamental Research
Bangalore 560089, India

July 31, 2024

DECLARATION

This thesis is a presentation of my original research work. Wherever contributions of others are involved, every effort is made to indicate this clearly, with due reference to the literature, and acknowledgement of collaborative research and discussions.

This work was done under the guidance of Prof. Abhishek Dhar, at the International Centre for Theoretical Sciences, Tata Institute of Fundamental Research (ICTS-TIFR), Bangalore.

Varun Dubey

In my capacity as supervisor of the candidate's thesis, I certify that the above statements are true to the best of my knowledge.

Prof. Abhishek Dhar
July 31, 2024

ACKNOWLEDGEMENTS

List of Figures

Contents

Abstract

This thesis is a study of measurement of simple quantum systems. The general framework of projections (ideal measurements) on eigenspaces of an observable of a quantum system is employed to study the evolution of an object system that is under continuous monitoring. When these projections are on the subspaces of the object system, then the measurement is direct. If the projections are on the subspaces of an ancilla (i.e. a probe) coupled to the object system, then the measurement is indirect. When such measurements (direct or indirect) are performed repeatedly at a high rate, then the object system is said to be under continuous observation. The object systems and the measurement protocols that are studied here are simple enough to admit a thorough analysis by use of standard mathematical methods. For direct measurements, the findings of this thesis include closed form expressions for distribution of first arrival times and its asymptotic form. For indirect measurements, the jump events in a two state system are studied via *clicks* observed in a readout process. We obtain closed form expressions for expected number of such clicks.

CHAPTER 1

Introduction

Quantum mechanics has a special relationship with classical mechanics in that classical mechanics is realized as a certain limit of quantum theory, whereas the formulation of quantum mechanics itself requires classical mechanics [LL77]. This is quite unlike the situation where a more general theory (such as relativistic mechanics) can be obtained from its own set of principles independent of the theory it generalizes (Newtonian mechanics). From the point of view of the experimenter, a given system in general has some interesting properties whose quantitative description gives the experimenter an understanding of the behaviour of the system. Such quantitative description of properties is made possible by *measurement* of certain *observables* of the system under study. Quantum mechanics provides a framework for calculating the probability distribution of the measured value of an observable. In so far as the calculation of distributions is concerned, this framework is fully deterministic. The Schrödinger's equation describes the evolution of the state of the system, and the probability distribution of an observable in a given state is obtained from the Born rule. The verification of this distribution requires measurements to be performed on an ensemble of identically prepared systems. Any measurement procedure [Bal98] establishes a correlation between the measured observable of the system and a macroscopic indicator that can be directly observed. Such correlations inevitably disrupt the Schrödinger evolution of the system proper and bring it in a new state. The measurement procedure, whose description is not contained in the system's Schrödinger equation, verifies the distribution calculated using Schrödinger evolution and also changes this distribution irreversibly.

1.1. Brief overview of quantum measurements

The most complete description of the state of a closed system $\mathcal{S}$ in quantum theory is given by a normalized vector $|\psi\rangle$ (a pure state) that lies in the system Hilbert space $\mathcal{H}$. The Hilbert space $\mathcal{H}$ is a complex vector space which includes the totality of all the possible states of $\mathcal{S}$. The energy of the closed system $\mathcal{S}$ is an important observable. In quantum mechanics, this observable is a self-adjoint operator $\widehat{H}$ that acts on $\mathcal{H}$ and it generates the evolution of the system state $|\psi\rangle$ in accordance with the Schrödinger's equation (setting $\hbar = 1$)

$$\imath\, \partial_t |\psi\rangle = \widehat{H} |\psi\rangle. \tag{1.1}$$

Any other observable associated with $\mathcal{S}$ is similarly represented by a self-adjoint operator $\widehat{M}$ acting on $\mathcal{H}$. The spectrum Λ of $\widehat{M}$ consists of real values and the associated

orthonormal eigenstates $|\lambda\rangle$ form a complete system. These facts are expressed by

$$\widehat{M}|\lambda\rangle = \lambda|\lambda\rangle, \qquad \langle\lambda|\mu\rangle = \delta_{\lambda\mu}, \qquad \int_{\lambda\in\Lambda} |\lambda\rangle\langle\lambda|\,d\lambda = \mathbf{1},$$

where $\mathbf{1}$ stands for the identity operator on $\mathcal{H}$. The integration should be interpreted as a summation on part of the spectrum which is discrete. Suppose that $\Lambda = \bigcup_{k\geq 1} E_k$ of mutually disjoint subsets E_k, then the projectors π_k defined below are self-adjoint and satisfy the completeness and orthogonality relations

$$\pi_k := \int_{\lambda\in E_k} |\lambda\rangle\langle\lambda|\,d\lambda, \qquad \sum_{k\geq 1}\pi_k = \mathbf{1}, \qquad \pi_j\pi_k = \delta_{jk}\pi_k. \tag{1.2}$$

Now consider a measurement procedure intended to decide if the measured value M of $\widehat{M}$ for a given state $|\psi\rangle$ of the system lies in $E_k \subset \Lambda$. The probabilities $P_{|\psi\rangle}(M \in E_k)$ that the value of $\widehat{M}$ lies in E_k when the system state is $|\psi\rangle$, satisfy

$$P_{|\psi\rangle}(M \in E_k) = \langle\psi|\pi_k|\psi\rangle, \qquad \sum_{k\geq 1} P_{|\psi\rangle}(M \in E_k) = 1. \tag{1.3}$$

It should be pointed here that the measurement procedure only decides in which of the ranges E_k the value M lies, rather than the precise value M. The post measurement state of the system is

$$\frac{\pi_k|\psi\rangle}{\sqrt{P_{|\psi\rangle}(E_k)}}, \tag{1.4}$$

if it is known that the measurement reveals the value of M to be in E_k. The EQs. (1.3 and 1.4) together constitute Lüders-von Neumann projection postulate. If the spectrum Λ of $\widehat{M}$ is non-degenerate and discrete, then one can take $E_k = \{\lambda_k\}$ and a precise measurement of the value of $\widehat{M}$ is possible (Chapter III, [vN18]). In this case, EQs. (1.3 and 1.4) include the projection postulate of quantum mechanics, which is quoted below from [Sha94] with a slight change of notation.

> If the particle is in the state $|\psi\rangle$, measurement of the observable $\widehat{M}$ will yield one of the eigenvalues λ with probability $P(\lambda) \propto |\langle\lambda|\psi\rangle|^2$. The state of the system will change from $|\psi\rangle$ to $|\lambda\rangle$ as a result of the measurement.

It further follows from the above that if $\widehat{M}$ is immediately measured after the first measurement, then one gets the same result for the measured value. This is a repeatability condition on the measured value. The condition for repeatability of measurements of an observable with discrete spectrum under the Lüders-von Neumann projection postulate has been analysed in [BGL95]. It is further proposed there that repeatable measurements of observables with continuous spectra are possible with more generalized measurements as against the type of *ideal* measurements described above.

For observables with continuous spectra, von Neumann's projection postulate admits only approximate measurements. For example, if in the position measurement of a particle in state $|\psi\rangle$ in one dimension, it is found in the interval $(-\epsilon/2, +\epsilon/2)$, then the post

measurement state of the particle in coordinate representation is

$$
\begin{cases}
\dfrac{\psi(x)}{\sqrt{\int_{-\epsilon/2}^{\epsilon/2} |\psi(x')|^2 \, dx'}} & -\epsilon/2 < x < \epsilon/2, \\
0 & \mathbb{R} \setminus (-\epsilon/2, \epsilon/2).
\end{cases}
$$

One can now define a new observable $\widehat{X}_\epsilon$ which approximates the position operator $\widehat{X}$. The eigenvalues of $\widehat{X}_\epsilon$ are in the discrete set, $\{k\epsilon, k \in \mathbb{Z}\}$ and its spectral representation in terms of orthogonal projections is given by

$$
\widehat{X}_\epsilon = \sum_{k \in \mathbb{Z}} (k\epsilon)\pi_k, \qquad \pi_k = \int_{k\epsilon-\epsilon/2}^{k\epsilon+\epsilon/2} |x\rangle\langle x| \, dx. \tag{1.5}
$$

Measurement of $\widehat{X}_\epsilon$ corresponds to an approximate measurement of $\widehat{X}$. An exact measurement of $\widehat{X}_\epsilon$ is possible by what was stated above for observables with discrete spectra. Successive measurements of $\widehat{X}_\epsilon$ obey the projection postulate of quantum mechanics and therefore verify the repeatability condition for the position operator $\widehat{X}$ with precision ϵ. The projection postulate of quantum mechanics which is stated for all observables may be regarded true for an observable with continuous spectrum when von Neumann measurements of arbitrary precision for such an observable are possible. This idealisation puts strong demands on the measuring device's capabilities, such as the measurement procedure does not disturb the value of the measured quantity at arbitrary precision.

Let us recollect the results for ideal measurement of an observable $\widehat{M}$ described above and rewrite the expressions in terms of density matrices. An ideal measurement is performed by a collection of orthogonal projections π_k acting on the Hilbert space $\mathcal{H}$. π_k project vectors in $\mathcal{H}$ onto mutually orthogonal subspaces $\mathcal{H}_k$ such that

$$
\sum_{k \geq 1} \pi_k = \mathbf{1}, \qquad \pi_j \pi_k = \delta_{jk} \pi_k, \qquad \mathcal{H} = \bigoplus_{k \geq 1} \mathcal{H}_k. \tag{1.6}
$$

If the state of the system is described by the density matrix ρ, then the probability $P_\rho(M \in E_k)$ that the outcome of the measurement lies in E_k and the post measurement state $\widetilde{\rho}$ are given by

$$
\langle \widehat{M} \rangle = \mathbf{tr}[\rho\widehat{M}], \qquad P_\rho(M \in E_k) = \mathbf{tr}[\rho\pi_k], \qquad \widetilde{\rho} = \frac{\pi_k \rho \pi_k}{P_\rho(M \in E_k)}. \tag{1.7}
$$

In [**GLE57**], it was shown that every probability measure on mutually orthogonal closed subspaces of a Hilbert space of dimension 3 or higher is of the form in the second EQ. (1.7) for some density matrix ρ. This is the well known Gleason's Theorem for projective measurements.

Suppose $\widehat{M'}$ is another observable (i.e., a self-adjoint operator acting on $\mathcal{H}$) of the system $\mathcal{S}$. Then Λ', λ', E_j', π_j' and $\mathcal{H}_j'$ can be defined for $\widehat{M'}$ in the same manner as the unprimed counterparts are defined for $\widehat{M}$ and EQs. (1.6, 1.7) can be written for $\widehat{M'}$ and a given system state ρ. The individual probability distributions of $\widehat{M}$ and $\widehat{M'}$ in the state ρ are known from $P_\rho(M \in E_k)$ and, $P_\rho(M' \in E_j')$ respectively. A joint probability

distribution of $\widehat{M}$ and $\widehat{M}'$ in ρ specified by the probabilities $P_\rho(M \in E_k,\, M' \in E_j')$ can be obtained in the case when $\widehat{M}$ and $\widehat{M}'$ commute, i.e., when $[\widehat{M}, \widehat{M}'] = \widehat{M}\widehat{M}' - \widehat{M}'\widehat{M} = 0$. This is equivalent to commutability of the projections π_j' and π_k and in fact

$$\pi_j' \pi_k = \pi_k \pi_j' = \pi_{\mathcal{H}_j' \cap \mathcal{H}_k},$$
$$P_\rho(M \in E_k,\, M' \in E_j') = \mathbf{tr}[\rho\, \pi_{\mathcal{H}_j' \cap \mathcal{H}_k}]. \tag{1.8}$$

The order in which the observables are measured is immaterial as the resulting state $\widetilde{\rho}$ post a measurement of $\widehat{M}$ followed by $\widehat{M}'$ is the same as post a measurement of $\widehat{M}'$ followed by $\widehat{M}$. In this sense, the observables $\widehat{M}$ and $\widehat{M}'$ are simultaneously measurable. However, when $[\widehat{M}, \widehat{M}'] \neq 0$, the projectors may not commute. Then the products $\pi_j' \pi_k$ are not even self-adjoint and therefore cannot represent a compound property of the system (for necessary and sufficient conditions for commutability of projections, please see [**Reh80**]). In this case, $\widehat{M}$ and $\widehat{M}'$ are said to be incompatible and a joint probability distribution such as in EQ. (1.8) cannot be given. For canonically conjugate observables such as the particle position $\widehat{X}$ and the particle momentum $\widehat{P}$, one has the commutation relation and the well known Heisenberg's uncertainty relation

$$\left[\widehat{X}, \widehat{P}\right] = \imath, \qquad \sqrt{\langle (\widehat{X} - \langle \widehat{X} \rangle)^2 \rangle} \sqrt{\langle (\widehat{P} - \langle \widehat{P} \rangle)^2 \rangle} = \sigma(\widehat{X})\, \sigma(\widehat{P}) \geq \frac{1}{2}. \tag{1.9}$$

In the standard proof of the uncertainty relation, the RMS deviations $\sigma(\widehat{X})$ and $\sigma(\widehat{P})$ in the given state are calculated from the individual distributions of $\widehat{X}$ and $\widehat{P}$ in the given state, as against obtaining them as deviations in the marginals of a joint distribution. Statistically, this amounts to considering two ensembles of systems, all prepared in the same state and making ideal measurements of $\widehat{X}$ in one ensemble and that of $\widehat{P}$ in the other. Then the RMS deviations in the two distributions obtained satisfy the uncertainty relation. Since no joint distributions of conjugate variables can be obtained via the ideal measurements described thus far, generalized measurements are used for this purpose. Studies by Arthurs & Kelly [**AKJ65**] and by She & Heffner [**SH66**] address this problem.

In [**AKJ65**], the authors describe a joint measurement of $\widehat{X}$ and $\widehat{P}$ by coupling the object system to two one dimensional meter systems, which interact with the object system via an interaction Hamiltonian of the form

$$\widehat{H}_{\mathrm{int}} = K \left(\widehat{X}\, \widehat{p}_x + \widehat{P}\, \widehat{p}_y \right). \tag{1.10}$$

Here $(\widehat{x}, \widehat{p}_x)$ and $(\widehat{y}, \widehat{p}_y)$ are the conjugate pairs for the two meter systems and K is a coupling constant which is large enough so that $\widehat{H}_{\mathrm{int}}$ primarily evolves the total system during the measurement process via EQ. (1.1). For a proper choice of the initial states of the meter systems, a simultaneous measurement of $\widehat{x}$ and $\widehat{y}$ (this is possible as they commute) at $t = 1/K$ leads to an *indirect* measurement of $\widehat{X}$ and $\widehat{P}$ respectively. From the joint probability distribution $P(x, y)$, it is possible to show that $\langle \widehat{x} \rangle$ and $\langle \widehat{y} \rangle$ are respectively equal to the expected values $\langle \widehat{X} \rangle$ and $\langle \widehat{P} \rangle$ of the object system in its pre-measurement state. It is further shown that if the meter readings are x_0 and y_0, then the

post measurement state of the object system turns out to be

$$\left(\frac{1}{\pi b}\right)^{\frac{1}{4}} \exp\left[-\frac{1}{2b}(X-x_0)^2 + \imath y_0 X\right], \tag{1.11}$$

where b is a device parameter which encodes the relative precision with which $\widehat{x}$ and $\widehat{y}$ are measured. Notice that $\widehat{x}$ and $\widehat{y}$ are measurements on two separate meters, and each can be ideally measured with any desired accuracy in the context of quantum measurement of a single observable with a continuous spectrum (see discussion following EQ. (1.5)). Thus, the value of b is controlled by the experimenter. For the choice of $b = \sigma(\widehat{X})/\sigma(\widehat{P})$ (the ratio in the pre-measurement state of the object system), it can be shown that the uncertainty relation in this indirect simultaneous measurement is given by

$$\sigma(\widehat{x})\,\sigma(\widehat{y}) \geq \sigma(\widehat{X})\,\sigma(\widehat{P}) + \frac{1}{2} \geq 1$$

whose RHS is different from that of the standard uncertainty relation by a factor of 2. Unlike the case of ideal measurements, where the post measurement state of the object system is an eigenstate of the measured observable, we notice that simultaneous measurement of incompatible observables can leave the object system in a coherent state such as the expression in (1.11). The increased lower bound of the uncertainty product is due to the additional effect of the joint measurement bringing about a new state of the object system. She & Heffner [**SH66**] treat simultaneous measurement of conjugate observables as a single measurement of a non-Hermitian observable $\widehat{a}$ whose eigenstates $|\alpha\rangle$ are the coherent states.

$$\widehat{a} = \frac{1}{\sqrt{2\,b}}\left(\widehat{X} + \imath b\widehat{P}\right), \qquad \widehat{a}|\alpha\rangle = \alpha|\alpha\rangle. \tag{1.12}$$

If a measurement gives x_0 for $\widehat{X}$ and y_0 for $\widehat{P}$, then the post measurement state of the object system is the eigenstate in the expression (1.11). This state is an eigenstate of $\widehat{a}$ with eigenvalue $\alpha(x_0, y_0) = (x_0 + \imath by_0)/\sqrt{2\,b}$. If the pre-measurement state of the object system is $|\psi\rangle$ then the joint probability distribution for the position (x) and the momentum (y) in the indirect measurement is just $P(x, y) = |\langle\alpha(x, y)|\psi\rangle|^2$. The states $|\alpha\rangle$ are not orthogonal wrt to the inner product on the Hilbert space of square integrable functions. If another simultaneous measurement is performed immediately after the first, then $P(x', y') = |\langle\alpha(x', y')|\alpha(x, y)\rangle|^2$, which implies that these simultaneous measurements do not have the repeatability property of ideal measurements. The states $|\alpha\rangle$ however do satisfy the completeness relation

$$\frac{1}{\pi}\int_{\alpha \in \mathbb{C}} |\alpha\rangle\langle\alpha|\, d^2\alpha = \mathbf{1}. \tag{1.13}$$

It is interesting to note that the system of coherent states $\{|\alpha\rangle,\ \alpha \in \mathbb{C}\}$ is in fact over-complete, i.e., if a finite collection of states $\{|\alpha_1\rangle, \ldots, |\alpha_n\rangle\}$ are removed, then the system

is again complete. In [**Per71**], it has been shown that states with

$$\alpha_{m,n} = \sqrt{\frac{\pi}{b}}(m + \imath\, b\, n), \qquad m,\, n \in \mathbb{Z},\ (m,n) \neq (0,0),$$

form a minimal collection of coherent states which is complete.

Thus, we see that with non-ideal measurements, it is possible to give a joint probability distribution $P(x,y)$ for the simultaneously measured values of particle position $\widehat{X}$ and particle momentum $\widehat{P}$. This description of simultaneous measurement is true only about those measurement procedures which lead the object system into minimum uncertainty states. It is conceivable to have measurement procedures which leave the object system in a mixed state. All such cases are covered in the theory of generalized measurements.

A generalized measurement is effected by a positive operator valued measure (POVM). A POVM is a collection of operators $\{\Pi_k\}$ acting on the Hilbert space $\mathcal{H}$ of the object system. $\{\Pi_k\}$ possess the following properties,

$$\sum_k \Pi_k = \mathbf{1}, \qquad \langle\psi|\Pi_k|\psi\rangle \geq 0 \quad \forall\ |\psi\rangle \in \mathcal{H}. \tag{1.14}$$

The index k enumerates the measurement outcomes. We note that the decomposition in EQ. (1.2) for projective measurements is a special case of EQ. (1.14) wherein the orthogonality condition has been dropped for $\{\Pi_k\}$. Further, the coherent state decomposition in EQ. (1.13) is an example of a POVM in which the measurement outcomes are continuously indexed by complex numbers α. It should be noted that while in the case of EQ. (1.13), the operators $\Pi_\alpha = |\alpha\rangle\langle\alpha|$ are projections on coherent states, in the general case of POVM, the operators Π_k need not be projections. A generalization of the Gleason's Theorem for POVM is due to P. Busch [**Bus03**]. The probability of the outcome k in measurement effected by $\{\Pi_k\}$ on the object system in state ρ is

$$P_k = \mathbf{tr}[\rho\,\Pi_k]. \tag{1.15}$$

The POVM $\{\Pi_\alpha\}_{\alpha \in \mathbb{C}}$ in the Arthurs-Kelly protocol is obtained by performing commuting projective measurements on $\mathcal{H} \otimes \mathcal{H}_x \otimes \mathcal{H}_y$ ($\mathcal{H}_x$, $\mathcal{H}_y$ being the Hilbert spaces of the meter systems) and the post measurement states are the coherent states $|\alpha\rangle \in \mathcal{H}$. We shall encounter a similar effect in continuous monitoring of a qubit, to be discussed in the Chapter 3. In general, the knowledge of $\{\Pi_k\}$ is not sufficient to obtain the post measurement state of the system, as it may be possible to obtain the same POVM by a different extension to a larger Hilbert space. Thus, we see that the system dynamics may be influenced in a desired way via measurements by an appropriate choice of system-device interaction. Properly shaped system-device interactions can be employed for steering a quantum system towards a target state via successive measurements [**RCGG20**].

1.2. Continuous time measurements and the Zeno effect

Single measurements on a quantum system were discussed in the previous section. In the manner of their description, these measurements are *instantaneous*, i.e., the duration

it takes to carry out the measurement is vanishingly small. It is maybe possible to model more realistic measurements that require finite time within the scheme of generalized measurements. The optimal POVM that gives an estimate of the measured quantity would be the one which has a probability distribution on its outcomes peaked around the true value of the measured quantity. The question of choosing the best estimator for the quantity to be measured leads one to the very interesting field of quantum estimation theory [Hel76]. Problems of this nature are not studied here, and it will be assumed that the measurements are sharp. On the other hand, the case where the observed system is continuously monitored is the main aspect of the problems we consider. This corresponds to the situation where the measurement process is such that a readout is continuously generated as the apparatus interacts with the object system over time.

Continuous monitoring via ideal measurements leads to the well known quantum Zeno effect [MS77]. This effect can be illustrated for the simplest case quite readily. Consider a sequence of ideal measurement of an observable $\widehat{M}$ with a simple discrete spectrum $\{\lambda_k\}_{k\geq 1}$. The spectral representation of $\widehat{M}$ is

$$\widehat{M} = \sum_{k\geq 1} \lambda_k |\lambda_k\rangle\langle\lambda_k|.$$

The time interval between successive measurements is τ. During each such interval, the system evolves via the Hamiltonian $\widehat{H}$. Continuous measurement of $\widehat{M}$ would correspond to the case where $\tau \to 0$. Assume that at $t = 0$, the state of the system is $|\psi(0)\rangle = |\lambda_m\rangle$. Then, in accordance with Schrödinger's equation one has

$$|\psi(\tau)\rangle = \exp\left[-\imath\tau\widehat{H}\right]|\lambda_m\rangle,$$
$$\Rightarrow |\psi(\tau)\rangle = \left[\mathbf{1} + (-\imath\tau\widehat{H}) + \frac{(-\imath\tau\widehat{H})^2}{2} + \dots\right]|\lambda_m\rangle. \tag{1.16}$$

Now, an an ideal measurement is performed on the system to determine if the state is still $|\lambda_m\rangle$, i.e., if the measured value lies in $\{\lambda_m\}$. The amplitude of this state in $|\psi(\tau)\rangle$ is

$$\langle\lambda_m|\psi(\tau)\rangle = 1 - \imath\tau\langle\widehat{H}\rangle_m - \frac{\tau^2}{2}\langle\widehat{H}^2\rangle_m + \dots$$

where the subscript m indicates the expectation of the operator in the state $|\lambda_m\rangle$. One is interested in the probability $p_m(\tau)$ that the measured value is in $\{\lambda_m\}$. This is given by

$$p_m(\tau) = |\langle\lambda_m|\psi(\tau)\rangle|^2 = 1 - \tau^2 \underbrace{(\langle\widehat{H}^2\rangle_m - \langle\widehat{H}\rangle_m^2)}_{(\sigma(\widehat{H})_m)^2} + \mathcal{O}(\tau^4). \tag{1.17}$$

Thus the short time behaviour of $p_m(\tau)$ is quadratic in τ. In this regime, the following approximation holds

$$p_m(\tau) \approx \exp(-\tau^2\sigma(\widehat{H})_m)^2). \tag{1.18}$$
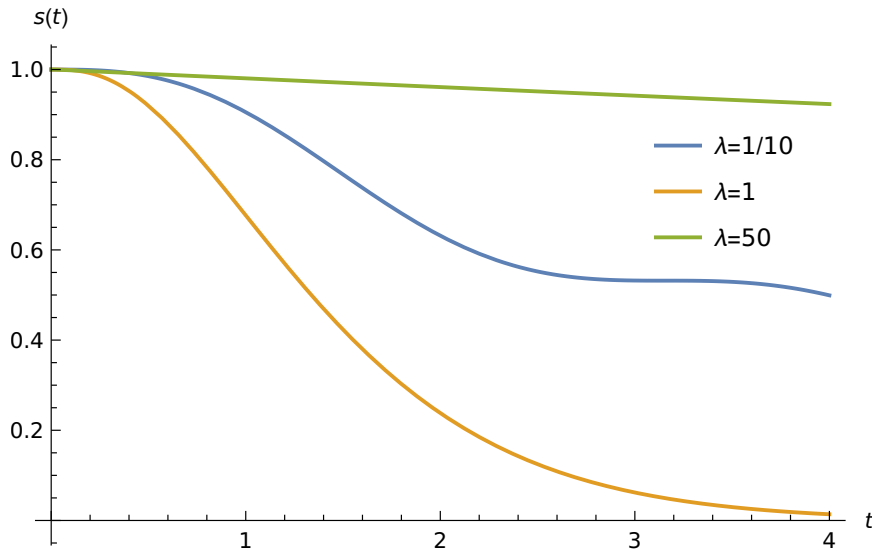
FIGURE 1. Plot of Survival probability as a function of time and measurement strength λ.

If N successive measurements are performed at intervals of τ, then the probability that every measurement result reveals the system to be in $|\lambda_m\rangle$ is

$$p_m(N\tau) = p_m(\tau)^N.$$

Fix a time $t = N\tau$. If N is made sufficiently large so that the approximation in EQ. (1.18) is good, then one may write

$$p_m(t) \approx \left[\exp(-\tau^2 \sigma(\widehat{H})_m)^2) \right]^N = \exp(-t^2 \sigma(\widehat{H})_m^2/N). \tag{1.19}$$

Because N can be arbitrarily large, the above indicates that $\lim_{N\to\infty} p_m(t) = 1$. Therefore, in the limit of continuous measurements, the system stays in the initial state. [MS77] cautions to not interpret $\lim p_m(t)$ as the probability that the system would be found in its initial state after time t. In fact, in the above derivation, $p_m(\tau)$ is such a probability.

The freezing of evolution due to continuous ideal measurements is the standard definition of the quantum Zeno effect. In [Wol01] chapter 3, authors have argued that a more admissible definition maybe adopted in which the observations are not ideal. Of relevance to the problems to be considered in this thesis, this broader definition would include the slowdown in evolution of a system which is observed continuously via generalized measurements. In these problems, the measurements would be characterized by a certain strength, whose value when increased, causes the state evolution of the object system to either slowdown or even get restricted to a smaller part of the Hilbert space. When the measurement strength is increased in an unrestricted manner, the slowdown would be absolute, reminiscent of freezing of evolution in the purely theoretical case of ideal measurements. The graph in Fig.(1) is a plot of expressions in EQ. (3.23) for

various values of the measurement strength λ. The effect of increasing the strength of measurement on state evolution is clearly seen.

In the continuous monitoring process, the object system is in a continual interaction with the measuring apparatus and also possibly with an environment. A readout of the apparatus is the observational record of a physical quantity of interest in the object system. This record reveals to the experimenter the trajectory of the value of the measured quantity and therefore provides partial information about the state evolution of the object system for the duration of the experiment. Of interest to the current thesis are those continuous measurements which involve counting of a certain type of events that occur in the system. A typical example of such a continuous measurement is the direct detection of photons emitted by an atom which is driven by a resonant source [**BP02**]. This example of resonance fluorescence also serves as motivation for the model considered in chapter (3).

Consider a two state atom with Hamiltonian H_S which is driven by a resonant laser source. The interaction with the laser can be described by an effective Hamiltonian H_L acting on the atom's Hilbert space. The Hamiltonians are

$$H_S = \frac{\omega_0}{2}\sigma_z, \qquad H_L = -\frac{\gamma_0}{2}\,\sigma_x.$$

γ_0 is a positive frequency which depends upon the intensity of the light. The environment of the atom consists of the electromagnetic field vacuum, whose Hamiltonian is given by

$$H_E = \sum_j \omega_j\,\hat{a}_j^\dagger\,\hat{a}_j.$$

Take the temperature to be 0 so that the only significant process between the atom and the environment is the excitation of the field vacuum via emissions from the atom. The driving laser causes Rabi oscillations in the atom at a frequency of γ_0. The lowering and the raising operators for the atomic states are respectively

$$\sigma_- = \begin{bmatrix} 0 & 0 \\ 1 & 0 \end{bmatrix}, \qquad \sigma_+ = \begin{bmatrix} 0 & 1 \\ 0 & 0 \end{bmatrix}.$$

If γ be the effective dissipation rate into the field vacuum then using the above jump operators, a Lindblad master equation for the density matrix of the atom in the interaction picture can be written as

$$\frac{d}{dt}\rho = i\frac{\gamma_0}{2}[\,\sigma_x,\rho\,] + \gamma\left(\sigma_-\,\rho\,\sigma_+ - \frac{\{\sigma_+\,\sigma_-,\rho\}}{2}\right). \qquad (1.20)$$

The emission spectrum from the atom would be that of a dipole radiation obtained by coupling of the dipole operator of the atom to the reservoir modes. The experimenter may perform a photon counting experiment by placing detectors at various orientations and of various sensitivities (for light frequency). Such continuous monitoring in real time generates a readout which allows for expressing the quantum state evolution of the atom via a stochastic equation due to Barchielli & Belavkin [**BB91**].

It is well known [Car99] in the theory of resonance fluorescence that at sufficiently low laser intensity, i.e. $\gamma_0 \ll \gamma$, the emission spectrum is sharply peaked at the transition frequency ω_0. While there is always some incoherent component in the spectrum leading to broadening, as a simplification, assume only coherent scattering of the laser occurs when $\gamma_0 \ll \gamma$. Further assume that the photodetector is capable of detecting the scattered ω_0 photons with full efficiency in the whole 4π solid angle around the atom. A detection event would consist of an absorption of a photon by the detector screen, thereby producing a spike in the output signal of the apparatus. Thus, a continuous measurement record consists of a sequence of spikes in the output signal with irregular time gaps between consecutive spikes. If $w(\tau)$ represents the probability distribution of time gap between successive detection events, then experiments have confirmed [Car99](and references therein) that, even for low laser intensities, $w(\tau)$ goes rapidly to 0 as τ goes to 0. This is regarded as evidence that detection of a photon is accompanied by a quantum jump to the ground state of the atom. For then, it would take some time for the laser to sufficiently energise the atom to make another photon emission. Therefore, if detection of the photons is efficient, then the experimenter has a record of instances when the atom jumped to its ground state. Between consecutive detection events, the atom evolves under null measurements, i.e., under continuous measurement registering no photoemissions. Using second order perturbation theory, it has been shown in [BP02] that for this detection scheme, the two level atom evolves via the stochastic differential equation

$$d|\psi(t)\rangle = -\imath \left[H_L - \imath \frac{\gamma}{2} \left(\sigma_+ \sigma_- - ||\sigma_- |\psi(t)\rangle||^2 \right) \right] |\psi(t)\rangle \, dt \;\; + \;\; \left[\frac{\sigma_- |\psi(t)\rangle}{||\sigma_- |\psi(t)\rangle||} - |\psi(t)\rangle \right] dN_t.$$

(1.21)

The operator in the first bracket of the RHS evolves the state under null measurements. The term in the second bracket describes a jump to the ground state post detection of a photon. The process N_t is a counting process which counts the number of photons detected till time t from the start of the experiment. Thus, the above equation expresses the state vector $|\psi(t)\rangle$ as a stochastic process in the system Hilbert space. In chapter (3), a similar equation would be obtained and solved for counting statistics of the process N_t in the model considered there.

When the apparatus is imperfect, description of the system's evolution as a stochastic process in the Hilbert space is no longer possible. This would be an example of the case when state reduction post measurement via a POVM does not lead to a pure state but to a mixed state. The Belavkin equation in such a situation would describe a stochastic process in the space of density matrices.

1.3. Related experiments

After the foregoing cursory account of the theory of quantum measurements, this section provides a summary discussion of some experiments that demonstrate aspects of quantum measurements stated above. This summary is limited to two foundational

(A) Energy level diagram.

(B) Fluorescence intensity profile.
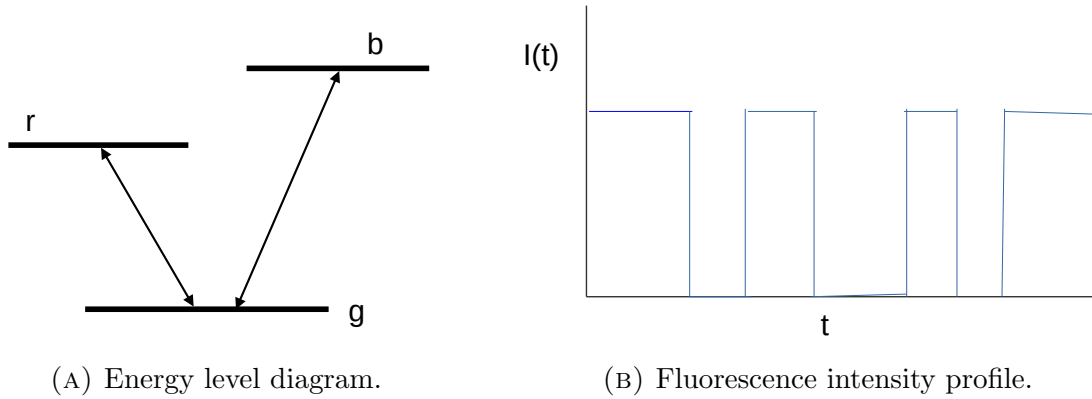
FIGURE 2. Three level electron shelving

experiments. There is an ever-growing body of literature on experiments related to measurement theory, especially in the area of quantum optics, which has for long provided a suitable avenue for formulation and performance of these experiments.

1.3.1. Electron shelving. The idea of electron shelving was proposed by HG Dehmelt as a tool for spectroscopy in 1975 [**LBMW03**]. One considers a three level atom with states $\{|g\rangle, |r\rangle, |b\rangle\}$ as shown in Fig. (2a). The state $|r\rangle$ is metastable, i.e., its spontaneous decay rate is orders of magnitude smaller than that of the state $|b\rangle$. In this sense, the $|g\rangle \leftrightarrow |b\rangle$ transitions are intense whereas the $|g\rangle \leftrightarrow |r\rangle$ transitions are weak. Suppose the atomic electron is initially in the ground state $|g\rangle$. Now a blue laser causing $|g\rangle \leftrightarrow |b\rangle$ transitions is switched on. Similarly, a second laser drives the $|g\rangle \leftrightarrow |r\rangle$ transitions. In accordance with the discussion of resonance fluorescence in the previous section, there will be coherent scattering of blue light due to action of the blue laser. If there happens a transition to the $|r\rangle$ state, then the blue fluorescence stops. Then the electron remains in the metastable shelf state $|r\rangle$ for an extended time, after which it decays to $|g\rangle$. After the decay, the blue fluorescence restarts. In this manner, the experimenter observes periods of brightness interspersed by periods of darkness in the blue fluorescent signal, as seen in the Fig. (2b). It has been shown in [**CTD86**] that the mean duration of the dark periods can be as large as half of the mean duration of the bright periods when the $|g\rangle \leftrightarrow |b\rangle$ is driven by a low intensity laser and the red laser is tuned perfectly to the $|g\rangle \leftrightarrow |r\rangle$ transition. In case of high intensity blue laser, this ratio can be as high as $1/4$ for a certain amount of detuning of the red laser. While the mean duration of dark periods should obviously depend upon the stimulated and spontaneous emission rates in the $|r\rangle$ state, one sees that the photon statistics in the fluorescent signal can be affected by controlling the intensities of the driving lasers.

The experimental realisation of Dehmelt's proposal was made by Nagourney *et al.* [**NSD86**] by utilizing transitions in Ba$^+$. In [**Coo88**], R.J.Cook proposed an experiment to test the validity of the quantum Zeno effect by employing electron shelving. Consider a two state atom coherently driven by a perfectly tuned laser. For the time dependent Hamiltonian of the atom, the Schrödinger equation is exactly solvable [**LL77**](Chapter

VI). If an energy measurement is made on the atom, then it will be found in one of the two states. If the atom continues to evolve for a short time interval τ after the measurement, then the probability $p(\tau)$ that it would transition to the other state is proportional to τ^2. If τ is very small, and a transition does indeed happen, i.e. a second energy measurement reveals this, then such a transition can be operationally called a quantum jump [Coo88]. From this discussion, it follows that the rate of quantum jumps ($p(\tau)/\tau$) in a frequently monitored two level atom driven by a tuned laser is inversely proportional to the frequency of the energy measurements. In Cook's proposal, the $|g\rangle \leftrightarrow |r\rangle$ system is the two state system under observation and illuminating the $|g\rangle \leftrightarrow |b\rangle$ system with a short pulse of a resonant laser constitutes a measurement. If during a pulse, there is fluorescence, then the electron is in the $|g\rangle \leftrightarrow |b\rangle$ manifold (or equivalently in level $|g\rangle$). If during a pulse, there is no fluorescence, then the electron is shelved in $|r\rangle$. To test the Zeno effect, start with an electron in the state $|g\rangle$. Then the $|g\rangle \leftrightarrow |r\rangle$ transitions are driven for half a cycle with a square pulse. If this perturbation was the only drive on the atom, then it is easily seen that the electron would end in the state $|r\rangle$ at the end of the half cycle. However, during this half cycle, the $|g\rangle \leftrightarrow |b\rangle$ transition is also driven by n equally spaced short pulses of resonant laser. Observance of continued fluorescence for large n would be validation of the Zeno effect. Itano *et al.* [IHBW90] confirmed the observation of Zeno effect on an experimental setup similar to that of Cook's proposal.

1.3.2. Progressive state collapse. In the discussion of electron shelving, the concept of a quantum jump was important. These quantum jumps can be regarded as much a property of the measuring process as they are of the system itself. There are other measurements which affect the measured system's state in a gradual manner than by abrupt jumps. The important experiment by Haroche *et al.* [GBD+07] is one example of such measurements. The objective of the experiment is to non-destructively measure the photon number in the electromagnetic field stored in a cavity. The field in the cavity is prepared in the coherent state

$$|\alpha\rangle = e^{-|\alpha|^2/2} \sum_{n \geq 0} \frac{\alpha^n}{\sqrt{n!}} |n\rangle = \sum_{n \geq 0} c_n |n\rangle. \tag{1.22}$$

It is of interest to note how such a field could in fact be prepared in the cavity [Car09]. For simplicity, neglect thermal fluctuations and assume a cavity of resonant frequency ω_C being pumped by a classical laser $E_0 \exp(-\imath \omega_C t)$. Let $\hat{a}$ and $\hat{a}^\dagger$ be the creation and annihilation operators of the cavity mode. If κ is the dissipation rate for the cavity mode and ρ its density matrix, then in the Schrödinger picture, the master equation is

$$\begin{aligned} \frac{d}{dt}\rho = &- \imath \omega_C \left[\hat{a}^\dagger \hat{a}, \rho \right] - \imath \left[E_0 \exp\left(-\imath \omega_C t\right) \hat{a}^\dagger + E_0^* \exp\left(\imath \omega_C t\right) \hat{a}, \rho \right] \\ &+ \kappa \left(2\hat{a}\rho\hat{a}^\dagger - \hat{a}^\dagger\hat{a}\rho - \rho\hat{a}^\dagger\hat{a} \right). \end{aligned} \tag{1.23}$$

If at $t = 0$, $\rho = |0\rangle\langle 0|$ then the above operator equation can be solved for $\rho(t)$ as a coherent state in the form of EQ. (1.22) with

$$\alpha = \imath (E_0/\kappa) e^{-\imath \omega_C t} (1 - e^{-\kappa t}).$$

In the experiment [GBD+07], excited states with principal quantum numbers 50 and 51 of Rubidium atoms serve as a two level system. The atom can then be treated as a spin-1/2 particle whose spin orientation rotates on the Bloch sphere. With the spin properly oriented, the atom passes through the cavity field. The time of flight of the atom through the cavity is a fixed time interval. Interaction between the atom and the field is so tuned that a single photon would rotate the spin polarization by a certain angle $\delta = \pi/q$ in a fixed plane, where q is a positive integer. Since the cavity field is in a coherent state, at the end of the interaction between the atom and the cavity field, they are in an entangled state $\sum_{n \geq 0} c_n |\delta_n\rangle \otimes |n\rangle$. Here $|\delta_n\rangle$ represents the state of the atom in which the polarization has rotated by an angle $n\delta$. The value of n is therefore known only modulo $2q$. For this to be possible, the interaction H_I between the atom and the field would have to satisfy the non-demolition condition $[\hat{a}^\dagger \hat{a}, H_I] = 0$ [RBH01]. Unlike the case of resonance fluorescence where photons were directly absorbed by the detector, here the photons are preserved in the measurement process, and it is important that the interaction Hamiltonian commute with the number operator if the interaction were to leave the photon number unchanged. After the interaction, the polarization of the atom is measured in a random direction (at an angle $\phi = k\delta$) from the original direction of the spin in the fixed plane, and it is ascertained whether the atom is in the up state ($j = 0$, corresponding to the spin aligning with the direction of axis ϕ) or in the down state ($j = 1$, for the opposite direction of the axis)

Let us introduce some notation to ascertain the impact of the information gained from the measurement of the spin state of the outgoing atom. $P_0(n) = |c_n|^2$ is the Poisson distribution for the number n of photons in the cavity before the measurement. $P(j, \phi|n) = \cos^2\left(\dfrac{n\pi}{2q} + \dfrac{j\pi - \phi}{2}\right)$ is the probability of the outcome of the measurement if there were n photons in the cavity. $P_1(j, \phi) = \sum_m P_0(m) P(j, \phi|m)$ is the total probability of the outcome. $P_1(n) = P(n|j, \phi)$ is the updated probability distribution of the photon numbers after the measurement. Then an application of the Bayes' theorem gives

$$P_1(n) = P_0(n) \frac{P(j, \phi|n)}{P_1(j, \phi)}.$$

The updated probability distribution is conditioned on the information obtained from the first measurement. Now one could send a sequence of probes and update the probability distribution conditioned on the outcome of the measurement at each step. It follows that after N probes have interacted with the cavity field, the probability distribution of the photon numbers after these interactions, conditioned on the measurement record

$\{\phi_k, j_k\}_{k=1}^N$ is given by

$$P_N(n) = P_{N-1}(n) \frac{P(j_N, \phi_N | n)}{\sum_m P_{N-1}(m) P(j_N, \phi_N | m)} = P_0(n) \prod_{k=1}^{N} \frac{P(j_k, \phi_k | n)}{\sum_m P_{k-1}(m) P(j_k, \phi_k | m)}$$

$$(1.24)$$

It was observed in the experiment that as N increases, the distributions $P_N(n)$ become more and more peaked at some value of an integer indicating convergence to this limit. If the cavity is prepared in the same way many times over and a measurement record generated each time, then the limits would be distributed according to the original Poisson distribution of the coherent state in EQ. (1.22). Each measurement record signifies a stochastic evolution of the cavity field, wherein the field starts in the coherent state and through the sequence of iterated measurement, goes to a state with a definite number of photons in it, i.e., a Fock state. It should be pointed out that in actual practise, the Fock state will not be long-lived as dissipation eventually takes the cavity to the vacuum state as noted in [GBD$^+$07]. Recursively defined probability distributions of the type in EQ. (1.24) has been considered in [BBB13,BBB12] and it is shown that the convergence observed experimentally can in fact be proven to be in accordance with the Born rule.

This chapter has presented a short summary of quantum measurement theory, which covers all the basic tools that will be necessary to state and solve the problems to be considered in the next two chapters. Continuous measurements will be central to both the problems. Counting processes in measurements has been emphasized through the example of photo detection in case of resonance fluorescence. Some experiments that have motivated us in modelling the measurement problems were described. Now we turn to the details of these problems and their solution.

CHAPTER 2

Direct Measurements

This chapter presents the results in [**DBD21**] and the technical methods employed to obtain these results. The principal quantity of interest is the distribution of time of arrival of a quantum particle at a detector. The classical notion of the time of arrival has several important experimental applications. The event of arrival in an experiment is indicated by a certain change in the state of the detector, such as in the scintillation of a fluorescent screen set up near a radioactive preparation [**BBSR89**]. Measurement of time delay between arrival of ion pulses of a nearly mono-energetic beam of ions [**CE48**] formed the basis for development of the important field of time of flight mass spectrometry (TOFMS). In [**YKH$^+$09**], time of flight measurements on ultra-cold atoms were employed to measure their temperature towards development of optical lattice clocks. In these experiments and possibly several other similar ones, motion of the detected particles is ballistic and simple kinematic calculations give very good estimates.

The classical case of thermal motion leads to the well studied theory of Brownian motion [**KS88**]. For a classical particle moving in a 1 dimensional noisy medium, starting from $x = 0$, the distribution of times for first arrival at $x = a$ is given by

$$F_c(t) = \frac{|a|}{\sqrt{2\pi t^3}} \exp\left(-\frac{a^2}{2t}\right).$$
(2.1)

If t_a represents the time of first arrival at $x = a$ and $P[t_a < t]$, the probability of the event that the first arrival at a occurs at a time less than t from the start of the motion, then one has

$$P[t_a < t] = P[t_a < t, x_t > a] + P[t_a < t, x_t < a],$$
$$= 2P[t_a < t, x_t > a],$$
$$\Rightarrow P[t_a < t] = \frac{1}{\sqrt{2\pi t}} \int_a^\infty e^{-x^2/2t} dx.$$

The second equality in the above is a consequence of the strong Markov property of the Brownian motion x_t (with $x_0 = 0$). $P[t_a \geq t]$ can be interpreted as the survival probability, i.e., the probability S_t that the particle survives detection at a in the time interval $[0, t)$. A differentiation of the above equation wrt to t gives the expression in EQ. (2.1). We note this as a definition for the distribution of first arrival times

$$F(t) := -\frac{dS_t}{dt}.$$
(2.2)

   The problem of first arrival to a particular state is meaningful only if the system is continuously monitored. In classical mechanics, such monitoring presents no difficulty in principle. In the quantum case however, the process of detection has irreversible effects on the monitored system and must be considered in conjunction with the system's dynamics. The first important question is whether, in the standard framework of quantum mechanics, there exists a physically observable *time* variable with a corresponding self-adjoint operator T acting on the system Hilbert space, and which encodes the information about the arrival of a particle at specific location? The answer to this was given in the negative by Pauli, and the question has received considerable attention over time. Allcock [**All69a**] has argued that under the assumption of time translation invariance, the operator T cannot have mutually orthogonal eigenstates and hence cannot be self-adjoint. On the other hand, if a self-adjoint T exists for a system with the Hamiltonian H which is conjugate to T, then in canonical quantization one has

$$[H, T] = \imath, \qquad [H, T^n] = \imath\, n\, T^{n-1}.$$

If $|E\rangle$ is an eigenstate of H and ϵ a real, then an application of the above commutations gives

$$H\big[e^{\imath \epsilon T}|E\rangle\big] = (E - \epsilon)\big[e^{\imath \epsilon T}|E\rangle\big].$$

It follows that the Hamiltonian is unbounded from below, which is physically unacceptable. This was essentially Pauli's argument as explicated by Delgado and Muga in [**DM97**]. If no such self-adjoint T exists, then it is clear that the distribution of arrival times can not be inferred in terms of probability amplitudes of eigenstates of T. A number of workarounds have been proposed. For example, [**DM97**] defines a self-adjoint T conjugate to an unbounded operator related to the system Hamiltonian. [**ML00**] provides a discussion of various other approaches to the problem.

   Despite theoretical challenges in a proper definition of time of arrival for the quantum case, experimental measurements of time of flight of atomic species in various settings have been made. In view of this, one may adopt EQ. (2.2), which is true in the classical case, as an *operational* definition of the distribution of times of first arrival even in the quantum case. The evaluation of the survival probability $S(t)$ would of course require the knowledge of system dynamics and the measurement protocol employed for the purpose of detection. Discrete time quantum walks [**ABN+01**, **Kon02**, **Kem03**] on finite or infinite lattices serve as good starting point to study the problem of arrival times. In [**icvcvJK08**], a related problem of recurrence of initial state in a quantum walk was studied without monitoring of the system. In [**GVWW13**], monitoring was incorporated at every time step using a renewal approach to show that recurrent states of a quantum walk have finite expected recurrence time and that these times are quantized. Using this approach, a number of interesting physical results on first passage in the lattice Schrödinger problem have been obtained in [**FKB16**, **FKB17**, **TBK18**, **TK20**, **TMKB20**]. In particular, it has been shown that the return probability on an infinite one-dimensional (1D) lattice

is less than one, and we do not have the Polya recurrence of the 1D random walk. The distribution of first detection times has been shown to scale as $1/t^3$. Different aspects of the equivalence to the non-Hermitian Hamiltonian have been explored in [**LD19**, **TK20**, **TKB20**].

The discrete time quantum walk models have generalization to the continuous time quantum walks (CTQW) [**Kem03**]. Farhi and Gutmann [**FG98**] study the penetration of a finite graph by a CTQW whose Hamiltonian is decided by the connectivity of the graph. Measurements are not incorporated, say, at any specific node of the graph. In this respect, the model is similar to the recurrence problem studied in [**icvcvJK08**] mentioned above. One of the principal contributions of our work in [**DBD21**] was to incorporate continuous measurement at a specific site to detect the arrival of the quantum particle at the detector.

To model continuous measurement, consider a sequence of projective measurements done on the system at regular intervals of time τ. $\tau \to 0$ corresponds to continuous measurement but when this limit is taken in an unregulated fashion, then one runs into the quantum Zeno effect. This problem can be avoided if the system-detector coupling strength scales as $\sim 1/\sqrt{\tau}$. We employed this scaling to show the equivalence between the repeated projection dynamics and an effective evolution via a non-Hermitian Hamiltonian. Finally, for the lattice models we consider, we obtain the space continuum limit and show that the evolution is described by a Schrödinger equation with complex Robin boundary condition at the location of the detector.

2.1. Continuous projective measurements

To study the measurement problem in the context of detection of first arrival events, a tight binding model for 1 dimensional lattice was employed. In the following, this model is described in detail, and it is shown how a proper choice of scaling for detector-system coupling leads to a non-Hermitian description.

2.1.1. A discrete time measurement model. Consider a quantum system whose states belong to the Hilbert space $\mathcal{H}$. We assume that $\mathcal{H} = \mathcal{S} \oplus \mathcal{D}$ can be written as the sum of two orthogonal complementary subspaces, where $\mathcal{S}$ is a "system" subspace and $\mathcal{D}$ a "detector" subspace. If P and Q are orthogonal projections on the subspaces $\mathcal{D}$ and $\mathcal{S}$ respectively, then

$$P + Q = \mathbf{1}. \tag{2.3}$$

Now consider an experiment where the initial state $|\psi(0)\rangle$ belongs to $\mathcal{S}$ and evolves unitarily for a time τ via the operator U_τ. At this instance, a direct measurement is performed on the system to ascertain whether the system has arrived in the detector subspace $\mathcal{D}$. The probability $S(\tau)$ that the detection fails after time τ and the subsequent normalized state post a failed detection are given by

$$S(\tau) = |QU_\tau|\psi(0)\rangle|^2, \qquad \widetilde{\psi}(\tau) = QU_\tau|\psi(0)\rangle/\sqrt{S(\tau)}.$$

This procedure is repeated at every time step τ till a successful detection is made at which point the experiment stops. Noting that $Q|\psi(0)\rangle = |\psi(0)\rangle$ and applying the procedure inductively, one obtains for n consecutive failed detection events

$$S(n\tau) = |\widetilde{U}_\tau^n|\psi(0)\rangle|^2, \qquad \widetilde{\psi}(n\tau) = \widetilde{U}_\tau^n|\psi(0)\rangle/\sqrt{S(n\tau)}, \qquad \widetilde{U}_\tau = QU_\tau Q. \tag{2.4}$$

The above result is due to [**DDDS15**]. It may be noted that $\widetilde{U}_\tau$ is a norm reducing, i.e. a contraction operator. The normalized state $|\widetilde{\psi}(n\tau)\rangle$ evolves in a complicated manner at every time step, but the difference equation for the un-normalized state $|\psi(n\tau)\rangle = \widetilde{U}_\tau^n|\psi(0)\rangle$ takes the simple form

$$\frac{|\psi(n\tau + \tau)\rangle - |\psi(n\tau)\rangle}{\tau} = \left[\frac{\widetilde{U}_\tau - \mathbf{1}}{\tau}\right]|\psi(n\tau)\rangle. \tag{2.5}$$

Further note that in terms of the un-normalized state $|\psi(n\tau)\rangle$, the expression for the survival probability is written as

$$S(n\tau) = \langle\psi(n\tau)|\psi(n\tau)\rangle. \tag{2.6}$$

2.1.2. Continuous measurement & effective non-Hermitian Hamiltonian. In order to model a system under continuous measurement, the measurement interval τ should be made arbitrarily small. We begin by describing the Hilbert space $\mathcal{H}$ along with the proper choice of the Hamiltonian for which the limiting procedure works. Let $\{|i\rangle\}$ and $\{|\alpha\rangle\}$ form orthonormal bases for $\mathcal{S}$ and $\mathcal{D}$ respectively, so that the states $\{|i\rangle, |\alpha\rangle\}$ together form a complete orthonormal basis of $\mathcal{H}$. Then one has

$$P = \sum_\alpha |\alpha\rangle\langle\alpha|, \qquad Q = \sum_i |i\rangle\langle i|. \tag{2.7}$$

The most general Hamiltonian (measured in units of $\hbar$) describing such a system is given by

$$H = H^{(\mathcal{S})} + H^{(\mathcal{D})} + H^{(\mathcal{SD})}, \tag{2.8}$$

$$H^{(\mathcal{S})} = \underbrace{\sum_{i,j} H_{ij}^{(S)}|i\rangle\langle j|}_{\text{System}}, \qquad H^{(\mathcal{D})} = \underbrace{\sum_{\alpha,\beta} H_{\alpha\beta}^{(D)}|\alpha\rangle\langle\beta|}_{\text{Detector}}, \tag{2.9}$$

$$H^{(\mathcal{SD})} = \underbrace{\sum_{i,\alpha}\left[H_{i\alpha}^{(\mathcal{SD})}|i\rangle\langle\alpha| + H_{\alpha i}^{(\mathcal{SD})}|\alpha\rangle\langle i|\right]}_{\text{System-Detector}}. \tag{2.10}$$

It was numerically demonstrated in [**DDD15**, **DDDS15**, **LD19**] that for the case where the time between measurements τ is small (compared to typical time scales in the unitary evolution), the above dynamics is accurately described by a continuous time evolution with a non-Hermitian effective Hamiltonian. However, the limit $\tau \to 0$ leads to the Zeno effect when the coupling coefficients ($H_{i\alpha}^{(\mathcal{SD})}$ and $H_{\alpha i}^{(\mathcal{SD})}$) are held constant. To obtain a

limiting behaviour, one takes

$$H_{i\alpha}^{(\mathcal{SD})} = \sqrt{\frac{\gamma_{i\alpha}}{\tau}}, \quad H_{\alpha i}^{(\mathcal{SD})} = \sqrt{\frac{\gamma_{\alpha i}}{\tau}}. \tag{2.11}$$

Further, denoting $H_{ij}^{(\mathcal{S})} = \gamma_{ij}$ and $H_{\alpha\beta}^{(\mathcal{D})} = \gamma_{\alpha\beta}$ we note the form of the Hamiltonian H

$$H = \underbrace{\sum_{i,j} \gamma_{ij} \ket{i}\bra{j}}_{H^{\mathcal{S}}} + \underbrace{\sum_{\alpha,\beta} \gamma_{\alpha\beta} \ket{\alpha}\bra{\beta}}_{H^{\mathcal{D}}} + \underbrace{\sum_{i,\alpha} \left[\sqrt{\frac{\gamma_{i\alpha}}{\tau}} \ket{i}\bra{\alpha} + \sqrt{\frac{\gamma_{\alpha i}}{\tau}} \ket{\alpha}\bra{i} \right]}_{H^{\mathcal{SD}}}. \tag{2.12}$$

The γ coefficients (assumed positive) in the above expression have unit of frequency. With the above definition of the Hamiltonian, the following commutation relations are obtained.

$$QH^{(\mathcal{S})}Q = H^{(\mathcal{S})}, \qquad QH^{(\mathcal{D})}Q = QH^{(\mathcal{SD})}Q = 0,$$
$$Q\left[H^{(\mathcal{S})}\right]^2 Q = \left[H^{(\mathcal{S})}\right]^2, \qquad Q\left[H^{(\mathcal{D})}\right]^2 Q = 0,$$
$$Q\left[H^{(\mathcal{SD})}\right]^2 Q = \frac{1}{\tau} \sum_{i,j,\alpha} \ket{i}\bra{j} \sqrt{\gamma_{i\alpha}\gamma_{\alpha j}}. \tag{2.13}$$

For the contraction operator $\widetilde{U}_\tau$, a series expansion with the aid of above commutations gives

$$\widetilde{U}_\tau = Q\exp\left[-\imath\tau H\right]Q = \mathbf{1} - \imath\tau H^{\mathcal{S}} - \tau V^{\mathcal{S}} + \mathcal{O}(\tau^2), \tag{2.14}$$

where

$$V_{ij}^{\mathcal{S}} = \frac{1}{2} \sum_\alpha \sqrt{\gamma_{i\alpha}\gamma_{\alpha j}}. \tag{2.15}$$

Taking the continuum limit $\tau \to 0$, $n \to \infty$ while keeping $t = n\tau$ finite in EQ. (2.5) gives a new Schrödinger's equation with an effective non-Hermitian Hamiltonian H^{eff}

$$\imath\frac{\partial\ket{\psi(t)}}{\partial t} = H^{\text{eff}}\ket{\psi(t)}, \quad H^{\text{eff}} = H^{\mathcal{S}} - \imath V^{\mathcal{S}}. \tag{2.16}$$

Therefore, conditioned on non-detection, the un-normalized state evolves in $\mathcal{S}$ via a non-Hermitian Hamiltonian. In this limit, EQ. (2.6) becomes

$$S_t = \braket{\psi(t)|\psi(t)} \tag{2.17}$$

and from EQs. (2.2, 2.16) one obtains the form of the first arrival distribution

$$F(t) = 2\braket{\psi(t)|V^{\mathcal{S}}|\psi(t)}. \tag{2.18}$$

One notes that $V^{\mathcal{S}}$ has the form of a Gram matrix [HJ85] and is therefore non-negative. It follows that the decay rate $F(t)$ is non-negative, as expected physically.

2.2. Quantum particle on one dimensional lattice

The framework developed in the previous section will now be applied to physical cases. It is assumed that a quantum particle hops on a 1 dimensional lattice containing a site $\ket{0}$ where detection is performed. Thus, $P = \ket{0}\bra{0}$ and $\ket{i}$ are position eigenstates indexing
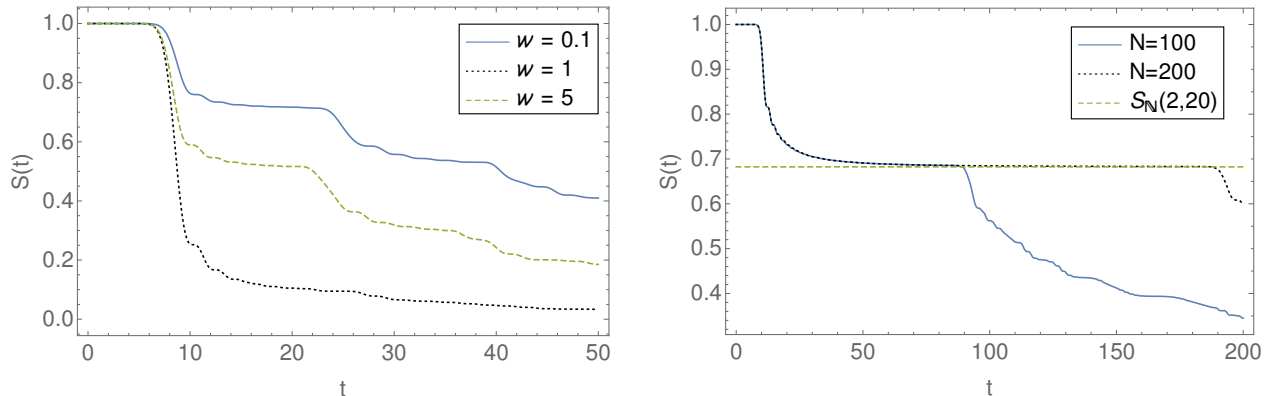
FIGURE 3. In the graph on the left, the survival probability $S(t)$ is plotted for $N = 15$, $\psi_i(0) = \delta_{i,15}$ and for different values of w. In the graph to the right, the survival probability $S(t)$ is plotted for lattice sizes $N = 100$ and $N = 200$. In both cases $\psi_i(0) = \delta_{i,20}$, $w = 2$. The dashed line is the value of survival probability S_∞ obtained from EQ. (2.41) for the $\mathbb{N}$ Lattice.

the remaining sites of the lattice. A constant potential exists across the lattice, except at those sites which are in the immediate vicinity of the detector. The dimensionless parameter β is used to encapsulate the deformation in the potential at such sites.

2.2.1. Finite lattice. Consider a lattice indexed by the states $\{|0\rangle, |1\rangle, \ldots, |N\rangle\}$ with $N \geq 2$. Taking the Hamiltonian as

$$H = -\gamma_0 \sum_{n=2}^{N} \left[|n\rangle\langle n-1| + |n-1\rangle\langle n| - 2|n\rangle\langle n| \right] + (2+\beta)\gamma_0|1\rangle\langle 1| - \sqrt{\frac{2\alpha\gamma_0}{\tau}} \left(|0\rangle\langle 1| + |1\rangle\langle 0| \right) \tag{2.19}$$

and defining

$$H_N := \frac{H^{\mathrm{eff}}}{\gamma_0}, \tag{2.20}$$

a simple calculation with EQs. (2.15, 2.16) for H in EQ. (2.19) gives

$$H_N = -\sum_{n=2}^{N} \left[|n\rangle\langle n-1| + |n-1\rangle\langle n| - 2|n\rangle\langle n| \right] + (2 - \imath w)|1\rangle\langle 1| \tag{2.21}$$

$$` \Rightarrow H_N = -\Delta_N - \imath w|1\rangle\langle 1|.$$

where $w = \alpha + \imath\beta$ and Δ_N is the discrete Laplacian of size $N \times N$. In the Schrödinger's equation for H_N, time is dimensionless. In case of no measurement, i.e. $w = 0$, H_N has the well known spectrum $\epsilon(k) = -2(1 - \cos k)$ for $k = s\pi/(N+1), s \in \{1, 2, \ldots, N\}$.

Before studying the spectral properties of H_N for non-zero w, it is useful to see some numerical results concerning the survival probability for motion that occurs under H_N. The numerical results are obtained by a direct solution of the non-Hermitian Schrödinger equation. In Fig. 3 (left panel) we plot the decay of survival probability on a system for which $N = 15$ for three different values of w. The survival probability cascades to 0 over time. We observe a non-monotonic dependence with $S(t)$ decaying slowly for both very

small $w = 0.1$ as well large $w = 5$. The several plateaus in the survival probability can be understood as arising from ballistic propagation of the particle with a group velocity ≈ 2, such that as the wave packet hits the detector, the survival probability plunges considerably. The velocity 2 corresponds to the maximum group velocity $d\epsilon(k)/dk$.

Returning to spectral properties of H_N for non-zero w, first observe that if λ is an eigenvalue of $-\imath H_N$ associated to some eigenvector, $|\psi\rangle$ then one has that

$$\lambda \langle \psi | \psi \rangle = \imath \, \langle \psi | \Delta_N | \psi \rangle - w \, |\langle 1 | \psi \rangle|^2.$$

Because the Laplacian is negative semi-definite, the first term in the RHS of above has real part 0. The case $\langle 1 | \psi \rangle = 0$ is excluded because then $|\psi\rangle$ would be an eigenfunction of $-\imath H_N$, but no eigenfunction of $-\imath H_N$ has $\langle 1 | \psi \rangle = 0$. Therefore, the real part of λ has then the same sign at $-\alpha$ and one concludes that the spectrum of $-\imath H_N$ is contained in $\{z \in \mathbb{C} \,;\, \Re(z) < 0\}$. By using the Jordan-Chevalley decomposition of $-\imath H_N$, it follows that for any $|\psi(0)\rangle$,

$$S(t) = \langle \psi(t) | \psi(t) \rangle = O(e^{-\mu t})$$

for some real $\mu > 0$. Hence, the survival probability $S(t)$ goes to 0 as $t \to \infty$ exponentially fast. This decay rate will be dependent on that eigenvalue of $-\imath H_N$ which has real part of minimum magnitude.

From EQ. (2.18), it follows that the first passage time distribution is given by $F(t) = 2\alpha |\psi_1(t)|^2$, with the notation $\psi_i = \langle i | \psi \rangle$. One can write a formal solution for $\psi_1(t)$, by using the information on the spectrum of the Hermitian part of the effective Hamiltonian, which in this case is the lattice Laplacian. For the Schrödinger equation

$$\imath \frac{\partial |\psi(t)\rangle}{\partial t} = -\Delta_N |\psi(t)\rangle - \imath \, w \, \psi_1(t) |1\rangle,$$

taking the Laplace transform on both sides with the notation $|\tilde{\psi}(s)\rangle = \int_0^\infty dt e^{-st} |\psi(t)\rangle$, one obtains

$$-|\psi(0)\rangle + s |\tilde{\psi}(s)\rangle = \imath \Delta_N |\tilde{\psi}(s)\rangle - w \, \tilde{\psi}_1(s) |1\rangle.$$

Defining the Green's function $G(s) = [s - \imath \Delta_N]^{-1}$, the following formal solution is achieved.

$$|\tilde{\psi}(s)\rangle = G(s)|\psi(0)\rangle - w \, \tilde{\psi}_1(s) G(s) |1\rangle. \tag{2.22}$$

Assuming an initial wave function, $|\psi(0)\rangle = |\ell\rangle$, localized at a site ℓ, project the above equation on the state $|1\rangle$ to get the Laplace transform $\tilde{\psi}_1(s)$ of $\psi_1(t)$ in the form

$$\tilde{\psi}_1(s) = \frac{G_{1\ell}(s)}{1 + w G_{11}(s)}, \tag{2.23}$$

where the matrix elements $G_{ij}(s) = \langle i | G(s) | j \rangle$ can be written in terms of the eigenfunctions $\phi_k(j) = \sqrt{2/(N+1)} \sin(kj)$ of the Laplacian Δ_N, and corresponding eigenvalues $\epsilon_k = -2(1 - \cos k)$ with $k = s\pi/(N+1)$, $s = 1, 2, \ldots, N$. One gets

$$G_{ij}(s) = \sum_k \frac{\phi_k(i)\,\phi_k(j)}{s - \imath \, \epsilon_k},$$

and hence an explicit expression for the Laplace transform $\tilde{\psi}_1(s)$. By using an inverse Laplace transform formula we can then get an explicit formula for the first passage time distribution $F(t)$, which remains however difficult to exploit, even qualitatively. Similar expressions have recently been discussed in [**TK20**] who also point the analogy with the renewal approach for the repeated measurement problem.

The case $\beta = 0$. It has been observed above that the closed form expression for the eigenvalues of H_N in case of general w are not obtainable. It should be pointed out that in the simpler case $w = \alpha$, further analysis is indeed possible. This is accomplished by studying the root locus of the characteristic polynomial of the operator H_N. This analysis reveals interesting features of the spectrum of H_N, such as the existence of critical value α_c for which the operator becomes non-diagonalizable and how the spectrum differs from one side of α_c to the other. A further advantage of this study is that it allows to pass to the limit $N \to \infty$ and obtain the spectrum for the semi-infinite lattice, a case that will be examined in detail in the next subsection. Please see Appendix (A) for the study of the root locus.

A notable feature of the analysis done so far for the finite lattice case is that the survival probability cascades to 0 as $t \to \infty$. This is not generally true, and the model described in sec. (2.1.2) admits other possibilities. Consider a ring of lattice sites as shown in the figure below.
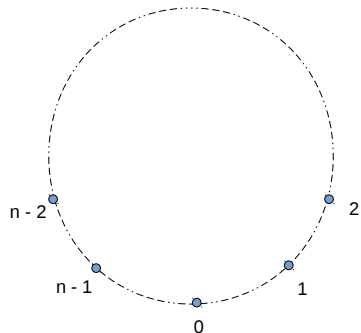
FIGURE 4. A ring of lattice sites with nearest neighbour hopping and detection at site 0.

For sake of concreteness, let $n = 4$ and the Hamiltonian for discrete time evolution be given by

$$H = -\gamma_0 \Bigg[|1\rangle\langle 2| + |2\rangle\langle 1| + |2\rangle\langle 3| + |3\rangle\langle 2| - 2|1\rangle\langle 1| - 2|2\rangle\langle 2| - 2|3\rangle\langle 3| \Bigg]$$
$$- \sqrt{\frac{2\alpha\gamma_0}{\tau}} \Bigg[|0\rangle\langle 1| + |1\rangle\langle 0| + |0\rangle\langle 3| + |3\rangle\langle 0| \Bigg]. \tag{2.24}$$

β has been taken to be 0 so that in the terminology of EQ. (2.21), $w = \alpha$. The detector site $|0\rangle$ only interacts with positions $|1\rangle$ and $|3\rangle$ while the remote site $|2\rangle$ has no direct interaction with the detector. The first line in the RHS of the above equation is to be regarded as $H_{\mathcal{S}}$ where as the lower line is $H_{\mathcal{SD}}$. Following EQ. (2.15), the effective Hamiltonian that describes continuous non Hermitian evolution conditioned on non-detection

is easily seen to be

$$H_3(\alpha) = \gamma_0 \begin{bmatrix} 2 - \imath\alpha & -1 & -\imath\alpha \\ -1 & 2 & -1 \\ -\imath\alpha & -1 & 2 - \imath\alpha \end{bmatrix}. \tag{2.25}$$

The eigenvalues of H_3/γ_0 are $\{2 \pm \sqrt{2 - \alpha^2} - \imath\alpha, 2\}$. Notice that, for $\alpha = \sqrt{2}$, H_3 becomes non-diagonalizable. For $\alpha > \sqrt{2}$, all the three eigenvalues have real part equal to 2. The propagator matrix $\exp(-\imath\gamma_0 t H_3)$ can be easily calculated for general α.

The important difference that arises due to the presence of symmetry can be easily seen for the non-diagonalizable case $\alpha = \sqrt{2}$. In this case, H_3 has the Jordan decomposition

$$\begin{bmatrix} 1 & 0 & -1 \\ -\imath\sqrt{2} & -1 & 0 \\ 1 & 0 & 1 \end{bmatrix} \begin{bmatrix} 2 - \imath\sqrt{2} & 1 & 0 \\ 0 & 2 - \imath\sqrt{2} & 0 \\ 0 & 0 & 2 \end{bmatrix} \begin{bmatrix} 1 & 0 & -1 \\ -\imath\sqrt{2} & -1 & 0 \\ 1 & 0 & 1 \end{bmatrix}^{-1},$$

from where the propagator is obtained to be

$$\exp(-\imath\gamma_0 t H_3) = \frac{e^{-(2\imath+\sqrt{2})\gamma_0 t}}{2} \begin{bmatrix} 1 + e^{\sqrt{2}\gamma_0 t} - \sqrt{2}\gamma_0 t & \imath 2\gamma_0 t & 1 - e^{\sqrt{2}\gamma_0 t} - \sqrt{2}\gamma_0 t \\ \imath 2\gamma_0 t & 2(1 + \sqrt{2}\gamma_0 t) & \imath 2\gamma_0 t \\ 1 - e^{\sqrt{2}\gamma_0 t} - \sqrt{2}\gamma_0 t & \imath 2\gamma_0 t & 1 + e^{\sqrt{2}\gamma_0 t} - \sqrt{2}\gamma_0 t \end{bmatrix}. \tag{2.26}$$

The normalized states

$$\chi_1 = \frac{1}{2} \begin{bmatrix} 1 \\ -\imath\sqrt{2} \\ 1 \end{bmatrix}, \quad \chi_2 = \begin{bmatrix} 0 \\ -1 \\ 0 \end{bmatrix}, \quad \chi_3 = \frac{1}{\sqrt{2}} \begin{bmatrix} -1 \\ 0 \\ 1 \end{bmatrix}, \tag{2.27}$$

form a complete (though not orthogonal) system for $H_3(\sqrt{2})$. If the general initial normalized state $\psi(0)$, supported in $\{|1\rangle, |2\rangle, |3\rangle\}$, is expressed as

$$\psi(0) = c_1\chi_1 + c_2\chi_2 + c_3\chi_3, \tag{2.28}$$

and detection of strength $\alpha = \sqrt{2}$ is done at $|0\rangle$, then EQs. (2.16, 2.17 , 2.26) can be employed to obtain a general form of the survival probability $S(t)$. This general form is somewhat tedious, and it is more useful to look at the cases as below

$$S(t) = \begin{cases} \exp(-2\sqrt{2}\gamma_0 t) & \text{for } c_1 = 1,\ c_2 = c_3 = 0 \\ \exp(-2\sqrt{2}\gamma_0 t)\left(2\gamma_0^2 t^2 + (1 + \sqrt{2}\gamma_0 t)^2\right) & \text{for } c_2 = 1,\ c_1 = c_3 = 0 \ . \\ 1 & \text{for } c_3 = 1,\ c_1 = c_2 = 0 \end{cases} \tag{2.29}$$

Thus one sees that the effect of symmetry in the considered topology is the existence of a *dark* state [**TMM$^+$20**] χ_3 - a state in which, if the system is initialized, the particle would never be detected with probability 1. This dark state exists also for the diagonalizable cases when, $\alpha \neq \sqrt{2}$ and in every case corresponds to the real eigenvalue of 2 of $H(\alpha)$.

In [**TMM$^+$20**], the dark states were investigated for their role in suboptimal detection in quantum walk on finite graphs. The underlying symmetry of the Hamiltonian leads

to existence of such states, and the detection probability (related to $S(t)$ in our study) was shown to be generically independent of the frequency with which detection was performed. In our study, the measurement is continuous in time. The symmetry of the effective Hamiltonian H_3 leads to existence of dark state χ_3 and for any generic state such as in EQ. (2.28), one has

$$\lim_{t \to \infty} S(t) = |c_3|^2.$$

It may be noted that the state χ_3 is completely antisymmetric wrt to inversion about $|2\rangle$. To elaborate this, consider the inversion operator $\hat{C}_2$ and its properties as below

$$\hat{C}_2 = \begin{bmatrix} 0 & 0 & -1 \\ 0 & -1 & 0 \\ -1 & 0 & 0 \end{bmatrix}, \quad \hat{C}_2^2 = \mathbf{1}, \quad \left[H_3(\alpha), \hat{C}_2 \right] = 0, \quad \hat{C}_2 \chi_3 = \chi_3, \quad \hat{C}_2 \chi_{1,2} = -\chi_{1,2}.$$

Thus, the effective Hamiltonian H_3 has inversion symmetry, and it will evolve antisymmetric states into antisymmetric states without effecting the norm. More general graphs with other non-trivial symmetries could possibly be considered by an appropriate choice of the $\gamma-$coefficients in EQ. (2.12).

2.2.2. $\mathbb{N}$ Lattice. This is the case of a semi-infinite lattice and differs from the finite case in that $N \to \infty$. The effective Hamiltonian therefore has the form

$$H_\mathbb{N} = -\sum_{n \geq 2} \left[|n\rangle\langle n-1| + |n-1\rangle\langle n| - 2|n\rangle\langle n| \right]. + (2 - \imath w)|1\rangle\langle 1| \tag{2.30}$$

With the notation $\psi_n(t) = \langle n|\psi(t)\rangle$ and by introducing the fictitious Dirichlet boundary condition $\psi_0(t) = 0$, the Schrödinger equation corresponding to the effective Hamiltonian $H_\mathbb{N}$ can be written as

$$\imath \frac{\partial \psi_n}{\partial t} = 2\psi_n - \psi_{n-1} - \psi_{n+1} - \imath w \delta_{n,1} \psi_1, \quad n \geq 1. \tag{2.31}$$

Similar equation has been studied in [**KLM14**] and we follow their approach of solution. If $\hat{\psi}(k,t)$ is the sine transform of $\psi_n(t)$, then for $k \in [0, \pi]$ one has that

$$\psi_n(t) = \sqrt{\frac{2}{\pi}} \int_0^\pi dk \, \hat{\psi}(k,t) \sin(n\,k), \qquad \hat{\psi}(k,t) = \sqrt{\frac{2}{\pi}} \sum_{n=1}^\infty \psi_n(t) \, \sin(n\,k).$$

Observe that the Dirichlet boundary condition is automatically satisfied. Assume $\psi_n(0) = \delta_{n,n_0}$ so that $\hat{\psi}(k,0) = \sqrt{\frac{2}{\pi}} \sin(n_0 k)$. Then it follows from EQ. (2.31) that

$$\imath \frac{\partial \hat{\psi}}{\partial t}(k,t) - 2(1 - \cos(k))\hat{\psi}(k,t) = -\imath w \sqrt{\frac{2}{\pi}} \psi_1(t) \sin(k). \tag{2.32}$$

The Laplace transforms of $\hat{\psi}(k,t)$ and $\psi_1(t)$ are by definition given by

$$\tilde{\psi}(k,s) = [\mathcal{L}\hat{\psi}(k,t)](s) = \int_0^\infty dt \, \exp(-st)\hat{\psi}(k,t), \tag{2.33}$$
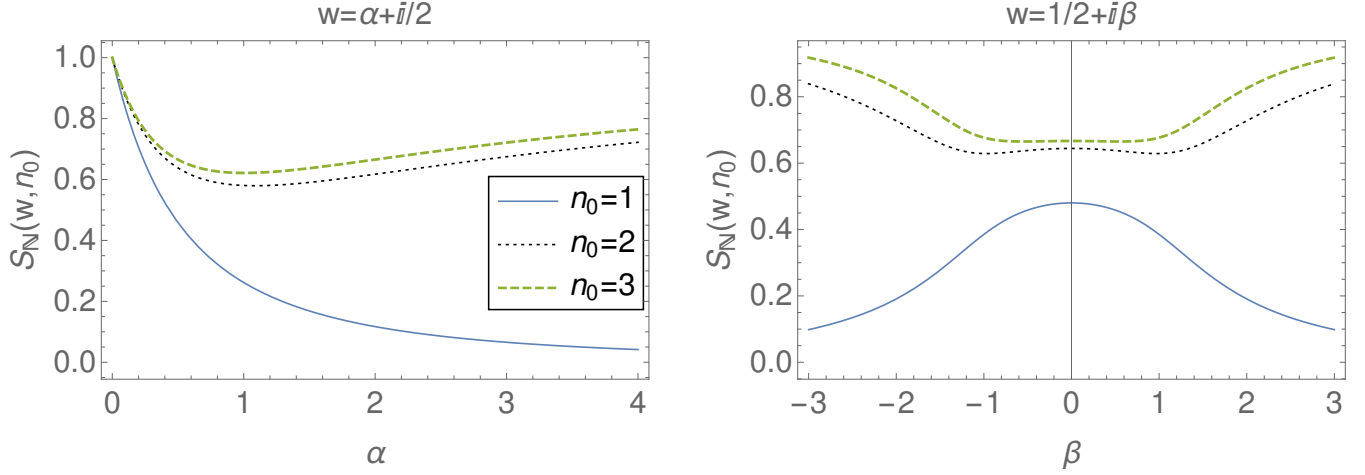
FIGURE 5. Plots showing variation of $S_\mathbb{N}$ (EQ. (2.41)) with w for various starting positions n_0. The left plot is for $w = \alpha + i/2$ and the right plot for $w = 1/2 + i\beta$.

$$[\mathcal{L}\psi_1](s) = \int_0^\infty dt\ \exp(-st)\,\psi_1(t)$$

$$= \sqrt{\frac{2}{\pi}} \int_0^\pi dk\,\tilde{\psi}(k,s)\,\sin(k). \tag{2.34}$$

Taking the Laplace Transform of EQ. (2.32) and by use of the above equations

$$\tilde{\psi}(k,s) = i\sqrt{\frac{2}{\pi}}\,\frac{\sin(n_0 k) - w\sin(k)\,[\mathcal{L}\psi_1](s)}{is - 2(1 - \cos(k))}. \tag{2.35}$$

The two relations, EQ. (2.34) and EQ. (2.35) between $\tilde{\psi}(k,s)$ and $[\mathcal{L}\psi_1](s)$ above give

$$[\mathcal{L}\psi_1](s) = i\,\frac{\dfrac{2}{\pi}\displaystyle\int_0^\pi dk\,\dfrac{\sin(k)\sin(n_0 k)}{is - 2(1 - \cos(k))}}{1 + i\dfrac{2w}{\pi}\displaystyle\int_0^\pi dk\,\dfrac{\sin^2 k}{is - 2(1 - \cos(k))}}. \tag{2.36}$$

The integrals involved in EQ. (2.36) can be evaluated by means of contour integration for any complex number s such that $\Re(s) > 0$, see section B. We get then that

$$[\mathcal{L}\psi_1](s) = -i\,\frac{i^{n_0}\left[-\left(\frac{s}{2}+i\right) + \sqrt{\left(\frac{s}{2}+i\right)^2 + 1}\right]^{n_0}}{1 + w\left[-\left(\frac{s}{2}+i\right) + \sqrt{\left(\frac{s}{2}+i\right)^2 + 1}\right]} \tag{2.37}$$

where $\sqrt{z}$ denotes the principal square root of $z \in \mathbb{C}\backslash\mathbb{R}_-^*$ (using the non-positive real axis as a branch cut). We have hence obtained an explicit expression of the Fourier-Laplace transform $\tilde{\psi}$ of the wave function ψ by plugging EQ. (2.37) into EQ. (2.35).

Turning to computation of the survival probability, from EQ. (2.17), the survival probability after time t is $S(t) = \sum_{n=1}^{\infty} |\psi_n(t)|^2$. From EQ. (2.31), one has

$$\imath \frac{\partial}{\partial t} |\psi_n|^2 = \begin{cases} -2\imath\Re(w)|\psi_1|^2 + 2\imath\Im(\psi_1\psi_2^*), & n = 1, \\ 2\imath\Im\left(-\psi_{n-1}\psi_n^* + \psi_n\psi_{n+1}^*\right), & n \geq 2. \end{cases}$$

Since ψ_n goes to 0 as $n \to \infty$, the equations can be summed to obtain $dS/dt = -2\Re(w)|\psi_1|^2$. Integrating, we get the survival probability

$$S_\infty = \lim_{t\to\infty} S(t) = 1 - 2\Re(w)\int_0^\infty dt\, |\psi_1(t)|^2. \tag{2.38}$$

For square integrable function ψ_1, one has [Hoc89]

$$\int_0^\infty dt\, |\psi_1(t)|^2 = \lim_{\epsilon\to 0^+} \frac{1}{2\pi\imath}\int_{\epsilon-\imath\infty}^{\epsilon+\imath\infty} ds\, |[\mathcal{L}\psi_1](s)|^2. \tag{2.39}$$

For $s = \epsilon + 2\imath(x-1)$ in the limit $\epsilon \to 0^+$, by EQ. (2.37)

$$|[\mathcal{L}\psi_1](s)|^2 = \begin{cases} \dfrac{\left(x+\sqrt{x^2-1}\right)^{2n_0}}{1+|w|^2\left(x+\sqrt{x^2-1}\right)^2 + 2\Im(w)\left(x+\sqrt{x^2-1}\right)}, & x < -1, \\[20pt] \dfrac{1}{1+|w|^2 + 2\left[\Re(w)\sqrt{1-x^2} + \Im(w)\,x\right]}, & -1 \leq x \leq 1, \\[20pt] \dfrac{\left(x-\sqrt{x^2-1}\right)^{2n_0}}{1+|w|^2\left(x-\sqrt{x^2-1}\right)^2 + 2\Im(w)\left(x-\sqrt{x^2-1}\right)}, & x > 1. \end{cases} \tag{2.40}$$

Denote by $S_{\mathbb{N}}(w, n_0)$ the survival probability given by EQ. (2.38) corresponding to the initial condition $|\psi(0)\rangle = |n_0\rangle$, where the detection parameter is $\alpha = \Re(w)$ and the impurity parameter is $\beta = \Im(w)$. From EQ. (2.38) and EQs. (2.39, 2.40), after simplification one gets

$$S_{\mathbb{N}}(w, n_0) = 1 - \frac{\Re(w)}{\pi|w|}\int_{-\frac{\pi}{2}}^{\frac{\pi}{2}} d\theta \frac{\cos\theta}{\frac{1}{2}\left(|w| + \frac{1}{|w|}\right) + \cos(\theta-\varphi)}$$
$$- \frac{2\Re(w)}{\pi}\int_0^1 du \frac{u^{2n_0-2}(1-u^2)(1+|w|^2 u^2)}{(1+|w|^2 u^2)^2 - (2\Im(w)u)^2}. \tag{2.41}$$

where $\varphi = \mathrm{Arg}(w)$. Figure (5) shows the variation of $S_{\mathbb{N}}(w, n_0)$ for some choices of w and starting positions n_0. In the left panel, we see that for $n_0 = 1$, the survival probability goes to 0 with increasing strength α of detection. For $n_0 > 1$ the survival probability attains a minimum. This can be compared with the results obtained in [KLM14] (Fig. 3). As noted earlier [see comment after EQ. (2.31)], [KLM14] solves the case with an imaginary potential at the origin of a $\mathbb{Z}$-lattice, and so the similarity of our result to theirs is expected. In the right panel, we see that $S_{\mathbb{N}}$ is symmetric in β for all starting
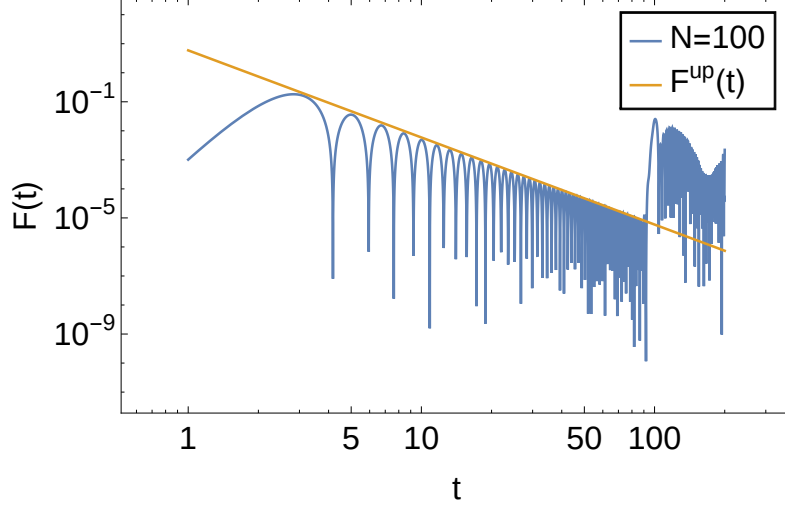
FIGURE 6. The figure shows variation of $F(t)$ with time for $w = 1/2$ and initial position $n_0 = 5$. The blue curve is obtained from simulation on a finite lattice of size $N = 100$, also with $n_0 = 5$. The first peak in $F(t)$ is around $t = 2.5$ and the jump in $F(t)$ at $t = 100$ corresponds approximately to the instance when the particle hits the detector a second time. The orange line is the upper envelope obtained in equation (2.45) which is valid for semi-infinite lattice.

positions n_0 for a fixed α. For purely real $w(=\alpha)$, EQ. (2.41) simplifies to

$$S_{\mathbb{N}}(\alpha, n_0) = \frac{2}{\pi}\left[2\left(\frac{\alpha^2 + 1}{\alpha^2 - 1}\arctan\frac{\alpha - 1}{\alpha + 1}\right) - \alpha\int_0^1 du\, u^{2n_0 - 2}\frac{1 - u^2}{1 + \alpha^2 u^2}\right]. \qquad (2.42)$$

From the above expression one has

$$S(\alpha, 1) = \frac{2}{\pi}\left[2\left(\frac{\alpha^2 + 1}{\alpha^2 - 1}\arctan\frac{\alpha - 1}{\alpha + 1}\right) + \frac{\alpha - (1 + \alpha^2)\arctan\alpha}{\alpha^2}\right]$$

and it is easy to see from here that indeed $\lim_{\alpha \to \infty} S_{\mathbb{N}}(\alpha, 1) = 0$ as observed in the Figure (5) left panel for the case $n_0 = 1$.

It is now possible to obtain an explicit form for $\psi_1(t)$ and hence also for $S_{\mathbb{N}}(t) = 1 - 2\Re(w)\int_0^t dt'\, |\psi_1(t')|^2$. The following form is obtained (as shown in section B)

$$\psi_1(t) = -2i^{n_0 + 1}e^{-2it}\sum_{k=0}^{\infty}(k + n_0)(-w)^k\frac{J_{k+n_0}(2t)}{2t}. \qquad (2.43)$$

The asymptotic form of $J_k(2t)$ for large t give by

$$[J_k(2t)]_{t \gg 1} \asymp \frac{1}{\sqrt{\pi t}}\cos\left(2t - \frac{\pi}{4} - \frac{k\pi}{2}\right) = \frac{e^{i\left(2t - \frac{\pi}{4} - \frac{k\pi}{2}\right)} + e^{-i\left(2t - \frac{\pi}{4} - \frac{k\pi}{2}\right)}}{2\sqrt{\pi t}}.$$

Substituting this in the expression for $\psi_1(t)$, after some simplification

$$\psi_1(t) \asymp \frac{(-i)^{n_0 + 1}e^{-i2t}}{2\sqrt{\pi t^3}}\left[e^{i\left(2t - \frac{\pi}{4} + \frac{in_0\pi}{2}\right)}f(n_0, w) + e^{-i\left(2t - \frac{\pi}{4} + \frac{in_0\pi}{2}\right)}f(n_0, w^*)^*\right] \qquad (2.44)$$

where
$$f(n_0, w) = \frac{n_0 - \imath(n_0 - 1)w}{(1 - \imath w)^2}.$$

For $t \gg 1$, an upper envelope for $F(t) = 2\Re(w)|\psi_1(t)|^2$ can be obtained from above

$$0 \leq F(t) \leq \frac{4\gamma_0 \lambda}{\pi(\gamma_0 t)^3} \frac{n_0^2 + 4(n_0 - 1)^2 \lambda^2}{(1 + 4\lambda^2)^2} = F^{\mathrm{up}}(t). \tag{2.45}$$

Equation (2.45) shows $1/t^3$ behaviour in $F(t)$ at large times. This however is not universal as can be seen from the fact that if the system is prepared in the state $|\psi(0)\rangle = \eta^b$, then $F(t)$ falls off exponentially. It is conceivable that other initial state preparations allow decay rates faster than $1/t^3$ and slower than exponential. This is shown to be the case for detection on the semi axis in section (2.3.1).

It remains to consider the spectral properties of the operator $H_{\mathbb{N}}$ (defined in EQ. (2.30)). From the study of root locus for H_N in the previous section, some properties are already known for the case when $w = \alpha$. $H_{\mathbb{N}}$ is non-diagonalizable for $\alpha = 1$. For $\alpha \in [0, 1)$, the eigenvalues of $H_{\mathbb{N}}$ are the continuous set $(0, 4)$. For $\alpha > 1$, the spectrum consists of the set $(0, 2) \cup (2, 4)$ and an isolated eigenvalue $\lambda_p = 2 - \imath(\alpha - \alpha^{-1})$. For the general case of complex w, it is seen below that $H_{\mathbb{N}}$ is non-diagonalizable for all points on the unit semicircle in the right half of the $w-$plane.

If $|\psi_E\rangle$ is an eigenfunction of $H_{\mathbb{N}}$ with eigenvalue E (possibly complex), then let $\psi_n = \langle n|\psi_E\rangle$, $n \geq 1$ so that the eigenvalue equation reads

$$\begin{aligned} (2 - \imath w)\psi_1 - \psi_2 &= E\psi_1, \\ 2\psi_n - \psi_{n-1} - \psi_{n+1} &= E\psi_n, \quad n > 1. \end{aligned} \tag{2.46}$$

This is equivalent to solving the second equation for $n \geq 1$ with the boundary condition

$$\psi_0 + \xi(\psi_1 - \psi_0) = 0, \quad \xi = \frac{-\imath w}{1 - \imath w}. \tag{2.47}$$

The most general scattering solutions are of the form $\psi_n = Ae^{\imath kn} + Be^{-\imath kn}$. This satisfies the second equation of EQ. (2.46) with $E_s(k) = 2(1 - \cos(k)) = 4\sin^2(k/2)$. Then the boundary condition EQ. (2.47) above gives $B = -A\frac{1 - \xi + \xi e^{\imath k}}{1 - \xi + \xi e^{-\imath k}}$. This gives us all the scattering solutions, and we define for each $k \in (0, \pi)$ the eigenfunction η^k associated to the eigenvalue $2(1 - \cos(k))$ by

$$\eta_n^k = \frac{\imath\left[(1 - \xi + \xi e^{-\imath k})e^{\imath kn} - (1 - \xi + \xi e^{\imath k})e^{-\imath kn}\right]}{\sqrt{2\pi(1 - \xi + \xi e^{\imath k})(1 - \xi + \xi e^{-\imath k})}}, \quad n \geq 1. \tag{2.48}$$

A bound state solution will have the form e^{-nk} with $\Re(k) > 0$. Then the eigenvalue is $2(1 - \cosh k)$ and the boundary condition gives $e^{-k} = 1 - \xi^{-1} = 1/(\imath w)$. Thus, the bound state exists only when $|w| > 1$ for only then is $\Re(k) > 0$. Thus for $|w| > 1$, the bound state with isolated eigenvalue $E_b = 2 - \imath(w - w^{-1})$ is given by

$$\eta_n^b = \frac{(1 - \xi^{-1})^n}{\sqrt{1 - (1 - \xi^{-1})^2}}, \quad n \geq 1. \tag{2.49}$$

Further notice that if w is on the unit circle in the right half of the $w-$plane, then for some $k \in (0, \pi)$ one has $e^{\imath k} = \imath w$ and for this k, the scattering state disappears since the denominator in EQ. (2.48) vanishes. Thus $|w| = 1, \Re(w) > 0$ are the exceptional points [**Hei04**] of $H_{\mathbb{N}}(w)$.

The orthonormality and completeness relations (whose verification requires contour integration results in the Section B) are given by

$$\sum_{n \geq 1} \eta_n^k \eta_n^{k'} = \delta(k - k'), \qquad \sum_{n \geq 1} \eta_n^k \eta_n^b = 0, \qquad \sum_{n \geq 1} \left[\eta_n^b \right]^2 = 1,$$

$$\int_0^\pi \eta_m^k \eta_n^k \, dk = \delta_{m,n} \text{ for } |w| < 1, \qquad \int_0^\pi \eta_m^k \eta_n^k \, dk + \eta_m^b \eta_n^b = \delta_{m,n} \text{ for } |w| > 1. \tag{2.50}$$

The operator $H_{\mathbb{N}}$ being complex symmetric admits a diagonalization only by orthogonal transformation [**HJ85**] in contrast to self-adjoint operators which admit diagonalization by unitary transformation. Hence, the absence of conjugation in any of the above relations.

2.2.3. $\mathbb{Z}$ Lattice. In this example, motion occurs on the infinite lattice indexed by integers, with detection at site 0. The Hamiltonian is taken to be

$$H = -\gamma_0 \sum_{n \in \mathbb{Z}\backslash\{0\}} \left[(1 - \delta_{n,1})|n\rangle\langle n-1| + (1 - \delta_{n,-1})|n\rangle\langle n+1| - 2|n\rangle\langle n| \right]$$

$$+ \sum_{n \in \{\pm 1\}} \left[-\sqrt{\frac{2\alpha\gamma_0}{\tau}} \left(|0\rangle\langle n| + |n\rangle\langle 0| \right) + \beta\gamma_0 |n\rangle\langle n| \right]. \tag{2.51}$$

The dimensionless effective Hamiltonian turns out

$$H_{\mathbb{Z}} = -\sum_{n \in \mathbb{Z}\backslash\{0\}} \left[(1-\delta_{n,1}) |n\rangle\langle n-1| + (1-\delta_{n,-1}) |n\rangle\langle n+1| - 2 |n\rangle\langle n| \right] - \imath w \sum_{n,n' \in \{-1,1\}} |n\rangle\langle n'|. \tag{2.52}$$

The calculations here are along the same lines as for the $\mathbb{N}$ Lattice case. For the effective Hamiltonian $H_{\mathbb{Z}}$ given by EQ. (2.52) the Schrödinger equation is equivalent to

$$\imath \frac{\partial \psi_n}{\partial t} = 2\psi_n - \psi_{n+1} - \psi_{n-1} - \imath w (\delta_{n,-1} + \delta_{n,1})(\psi_{-1} + \psi_1), \quad n \in \mathbb{Z}\backslash\{0\} \tag{2.53}$$

with $\psi_0(t) = 0$. Let us define

$$\hat{\psi}^{\pm}(k, t) = \sqrt{\frac{2}{\pi}} \sum_{n=1}^{\infty} \psi_{\pm n}(t) \sin(n\,k)$$

$$\Rightarrow \quad \psi_{\pm n}(t) = \sqrt{\frac{2}{\pi}} \int_0^\pi dk\, \hat{\psi}^{\pm}(k, t) \sin(n\,k)$$

which both satisfy the same equation,

$$\imath \frac{\partial \hat{\psi}^{\pm}}{\partial t}(k, t) - 2(1 - \cos(k))\hat{\psi}^{\pm}(k, t) = -\imath w \sqrt{\frac{2}{\pi}} \left[\psi_1(t) + \psi_{-1}(t) \right] \sin(k). \tag{2.54}$$

We assume that $\psi_n(0) = \delta_{n,n_0}$ with $n_0 \geq 1$ so that $\hat{\psi}^+(k,0) = \sqrt{\dfrac{2}{\pi}} \sin(n_0 k)$ and $\hat{\psi}^-(k,0) = 0$. The Laplace transforms of $\hat{\psi}^\pm(k,t)$ and $\psi_{\pm 1}(t)$ are by definition

$$\tilde{\psi}^\pm(k,s) = [\mathcal{L}\hat{\psi}^\pm(k,t)](s) = \int_0^\infty dt \, \exp(-st)\hat{\psi}^\pm(k,t), \qquad (2.55)$$

$$[\mathcal{L}\psi_{\pm 1}](s) = \int_0^\infty dt \, \exp(-st) \, \psi_{\pm 1}(t)$$

$$\Rightarrow [\mathcal{L}\psi_{\pm 1}](s) = \sqrt{\frac{2}{\pi}} \int_0^\pi dk \, \tilde{\psi}^\pm(k,s) \, \sin(k). \qquad (2.56)$$

Taking the Laplace Transform of EQ. (2.54) and by use of the above equations

$$\begin{aligned}
\tilde{\psi}^+(k,s) &= \imath \sqrt{\frac{2}{\pi}} \frac{\sin(n_0 k) - w \sin(k) \, \mathcal{L}[\psi_{-1} + \psi_1](s)}{\imath s - 2(1 - \cos(k))}, \\
\tilde{\psi}^-(k,s) &= -\imath \sqrt{\frac{2}{\pi}} \frac{w \sin(k) \, \mathcal{L}[\psi_{-1} + \psi_1](s)}{\imath s - 2(1 - \cos(k))}.
\end{aligned} \qquad (2.57)$$

Then we get

$$[\mathcal{L}(\psi_{-1} + \psi_1)](s) = \imath \, \frac{\dfrac{2}{\pi} \displaystyle\int_0^\pi dk \, \dfrac{\sin(k) \sin(n_0 k)}{\imath s - 2(1 - \cos(k))}}{1 + \imath \dfrac{4w}{\pi} \displaystyle\int_0^\pi dk \, \dfrac{\sin^2 k}{\imath s - 2(1 - \cos(k))}} \qquad (2.58)$$

from which follows the explicit expression for the Fourier-Laplace transform of the wave function. This is the same expression as EQ. (2.36) where w has been replaced by $2w$. Proceeding as in the derivation of EQ. (2.38), in this case the expression for the survival probability is

$$S_\infty = \lim_{t\to\infty} S(t) = 1 - 2\Re(w) \int_0^\infty dt \, |\psi_{-1}(t) + \psi_1(t)|^2. \qquad (2.59)$$

If $S_\mathbb{Z}(w, n_0)$ denotes the survival probability S_∞ corresponding to this initial condition $\psi_n(0) = \delta_{n,n_0}$ we get that

$$S_\mathbb{Z}(w, n_0) = S_\mathbb{N}(2w, n_0). \qquad (2.60)$$

The spectral properties of $H_\mathbb{Z}$ can be ascertained in the same way as was done for $H_\mathbb{N}$. By introducing, $\zeta = \dfrac{-2\imath w}{1 - 2\imath w}$ we deduce that the spectrum of $H_\mathbb{Z}$ is composed of:

- Symmetric scattering states $\hat{\eta}^k$ for each $k \in (0, \pi)$ associated to the eigenvalue $2(1 - \cos(k))$ and defined for $|n| \geq 1$ by

$$\hat{\eta}_n^k = \frac{\imath \left[(1 - \zeta + \zeta e^{-\imath k}) e^{\imath k |n|} - (1 - \zeta + \zeta e^{\imath k}) e^{-\imath k |n|} \right]}{\sqrt{4\pi(1 - \zeta + \zeta e^{\imath k})(1 - \zeta + \zeta e^{-\imath k})}}. \qquad (2.61)$$

- Anti-symmetric scattering states σ^k for each $k \in (0, \pi)$ associated to the eigenvalue $2(1 - \cos(k))$ and defined for $|n| \geq 1$ by

$$\sigma_n^k = \frac{1}{\sqrt{\pi}} \sin(kn). \qquad (2.62)$$

- A symmetric bound state $\hat{\eta}^b$ associated to the eigenvalue $E_b = 1 + \zeta^{-1}$ if $|1 - \zeta^{-1}| < 1$ or equivalently $|2w| > 1$. It is defined by

$$\hat{\eta}_n^b = \frac{(1 - \zeta^{-1})^{|n|}}{\sqrt{2(1 - (1 - \zeta^{-1})^2)}}. \tag{2.63}$$

The orthonormality and completeness relations are

$$\sum_{n \geq 1} \hat{\eta}_n^k \hat{\eta}_n^{k'} = \sum_{n \geq 1} \sigma_n^k \sigma_n^{k'} = \delta(k - k'), \qquad \sum_{n \geq 1} \left[\hat{\eta}_n^b\right]^2 = 1,$$

$$\sum_{n \geq 1} \hat{\eta}_n^k \hat{\eta}_n^b = \sum_{n \geq 1} \hat{\eta}_n^k \sigma_n^k = \sum_{n \geq 1} \sigma_n^k \hat{\eta}_n^b = 0,$$

$$\int_0^\pi [\eta_m^k \eta_n^k + \sigma_m^k \sigma_n^k] \, dk = \delta_{m,n} \qquad \text{for } |w| < 1/2,$$

$$\int_0^\pi [\eta_m^k \eta_n^k + \sigma_m^k \sigma_n^k] \, dk + \eta_m^b \eta_n^b = \delta_{m,n} \qquad \text{for } |w| > 1/2. \tag{2.64}$$

$|w| = 1/2, \Re(w) > 0$ are the exceptional points of $H_{\mathbb{Z}}(w)$.

2.2.4. Green's function approach. The closed form expressions of survival probability and detection time distribution for the $\mathbb{N}$ and $\mathbb{Z}$ lattices were obtained using a Fourier-Laplace transform of the effective equations of motion. The knowledge of the spectra of these operators provides a more direct method to obtain these results. As an illustration of the idea, EQ. (2.43) for the case of $\mathbb{N}$ lattice is obtained below.

If $|\psi(0)\rangle$ is the initial state, then the time evolution to $|\psi(t)\rangle$ is given by

$$|\psi(t)\rangle = G(t)|\psi(0)\rangle, \tag{2.65}$$

where the infinite matrix $G(t)$ is given by

$$G_{nm} = \int_0^\pi dk \, \eta_n^k \eta_m^k \, e^{-\imath E_s(k)t} \; + \; \Theta(|w| - 1) \, \eta_n^b \eta_m^b \, e^{-\imath E_b(\xi)t}. \tag{2.66}$$

Θ denotes the Heaviside step function. In particular, starting with an initial condition, $|\psi(0)\rangle = |n_0\rangle$ one has that $\psi_1(t) = G_{1,n_0}(t)$. By using the explicit forms of $\{\eta^k \; ; \; k \in (0, \pi)\}$, $E_s(k)$ in EQ. (2.48) and using that $\xi/(1 - \xi) = -\imath w$ we get

$$\eta_1^k \eta_{n_0}^k \, e^{-\imath E_s(k)t} = -\frac{\imath}{\pi} e^{-2\imath(1 - \cos(k))t} \, \sin(k) \times \left[\frac{e^{\imath n_0 k}}{1 - \imath w e^{\imath k}} - \frac{e^{-\imath n_0 k}}{1 - \imath w e^{-\imath k}}\right].$$

Assuming $|w| < 1$, transforming the previous expression in series since $|\imath w e^{\pm \imath k}| < 1$, exchange the sum with the integrals, and by using symmetries one has

$$\int_0^\pi dk \, \eta_n^k \eta_m^k \, e^{-\imath E_s(k)t} = -\frac{\imath e^{-2\imath t}}{\pi} \sum_{p=0}^\infty (\imath w)^p I_{n_0 + p} \tag{2.67}$$

$$I_n = \int_{-\pi}^\pi dk \, e^{2\imath \cos(k)t} \, \sin(k) e^{\imath n k}.$$

But from the properties of Bessel functions of the first type, $I_n = \pi \imath^n t n J_n(2t)/t$. Substituting this in the above, EQ. (2.43) is obtained immediately. For the case $|w| > 1$,

one has to take into account the existence of a bound state but for the rest we proceed similarly by rewriting for $|z| = 1$

$$\frac{1}{1 - \imath wz} = \frac{\imath}{wz} \frac{1}{1 + \frac{\imath}{wz}} = \frac{\imath}{wz} \sum_{p=0}^{\infty} (-1)^p \left(\tfrac{\imath}{wz}\right)^p.$$

Then we get the same expression as before EQ. (2.43) for $\psi_1(t)$. The expression for $|w| = 1$ is obtained from the previous expression by a continuity extension.

2.3. Space continuum limit

We now seek to extend the results to the case of motion in continuous space in one dimension by taking appropriate limits of the discrete models. This will be done by taking lattice spacing $\epsilon \to 0$.

2.3.1. Real semi-axis. Start with the Schrödinger equation for the $\mathbb{N}$ lattice.

$$\imath \frac{\partial \psi_n}{\partial t} = \begin{cases} (2 - \imath w)\psi_1 - \psi_2, & n = 1, \\ 2\psi_n - \psi_{n-1} - \psi_{n+1}, & n \geq 2. \end{cases}$$

Letting $\psi_0 = \imath w \psi_1$, the above system can be rewritten with a boundary condition as

$$\imath \frac{\partial \psi_n}{\partial t} = 2\psi_n - \psi_{n+1} - \psi_{n-1}, \ n \geq 1; \qquad \psi_0 - \frac{\imath w}{1 - \imath w}(\psi_1 - \psi_0) = 0. \tag{2.68}$$

Now define a lattice spacing parameter ϵ and the continuous wave function Ψ as

$$\Psi(x, t) = \lim_{\epsilon \to 0} \epsilon^{-1/2} \psi_{[x/\epsilon]}\big(t\epsilon^{-2}\big). \tag{2.69}$$

Consider the limit

$$\zeta = \lim_{\epsilon \to 0^+} \epsilon \frac{\imath w}{\imath w - 1}. \tag{2.70}$$

For this limit to be non-zero, w should be regulated with ϵ so that for small ϵ, one has $\imath w(\epsilon) \approx 1 + \epsilon/\zeta$ to leading order in ϵ. This implies that $\Re(w(\epsilon)) \approx -\epsilon \Im(\zeta)/|\zeta|^2$. In the model of $\mathbb{N}$ lattice, $\Re(w) = \alpha > 0$ and therefore $\Im(\zeta) < 0$. With this assumption on w, the discrete EQs. (2.68) in conjunction with EQ. (2.69), in the limit $\epsilon \to 0^+$ take the form

$$\imath \frac{\partial \Psi}{\partial t} = -\frac{\partial^2 \Psi}{\partial x^2}, \quad \text{with Robin b.c.} \quad \left[\Psi + \zeta \frac{\partial \Psi}{\partial x}\right]_{x=0} = 0, \quad x \geq 0, \Im(\zeta) < 0. \tag{2.71}$$

The operator appearing in EQ. (2.71) has a bound eigenstate for $\Re[\zeta] > 0$ given by

$$\eta^b(x) = \sqrt{\frac{2}{\zeta}} e^{-x/\zeta}. \tag{2.72}$$

Here $\sqrt{z}$ denotes the principal square root of $z \in \mathbb{C} \backslash \mathbb{R}_-$ using the non-positive real axis as a branch cut. The scattering solutions are given by

$$\eta^k(x) = \frac{\imath \left[(1 - \imath k\zeta)e^{\imath kx} - (1 + \imath k\zeta)e^{-\imath kx}\right]}{\sqrt{2\pi(1 + \zeta^2 k^2)}}, \quad k > 0. \tag{2.73}$$
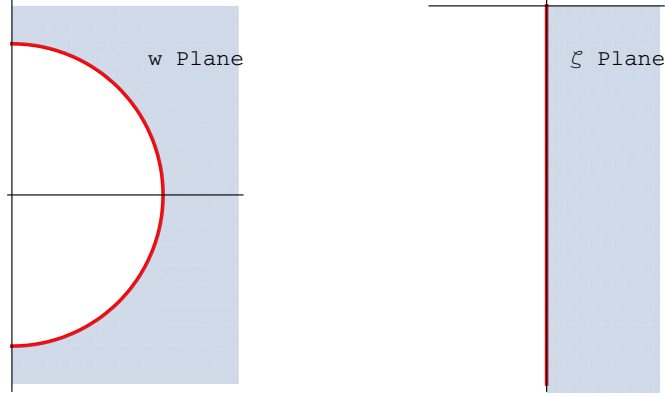
FIGURE 7. The admissible values of the measurement parameters, w (right half plane) for the $\mathbb{N}$ lattice case and ζ (lower half plane) for the half line case. See eq. (2.70) for a relation between the parameters in the two cases.

The states $\{\eta_k, \eta_b\}$ satisfy the boundary condition at $x = 0$ and the orthonormality conditions:

$$\int_0^\infty dx\ [\eta^b(x)]^2 = 1, \qquad \int_0^\infty dx\ \eta^k(x)\eta^b(x) = 0,$$

$$\int_0^\infty dx\ \eta^k(x)\eta^{k'}(x) = \delta(k - k').$$

$$(2.74)$$

This is easily proved using the identity $\int_0^\infty dx e^{\imath kx} = \imath P(1/k) + \pi\delta(k)$, where P denotes the principal part. One also has the completeness relation:

$$\int_0^\infty dk\ \eta^k(x)\eta^k(x') = \delta(x - x') \qquad \text{for } \Re[\zeta] < 0,$$

$$\int_0^\infty dk\ \eta^k(x)\eta^k(x') + \eta^b(x)\eta^b(x') = \delta(x - x') \text{ for } \Re[\zeta] > 0.$$

$$(2.75)$$

To prove this, we note that

$$\int_0^\infty dk\ \eta^k(x)\eta^k(x')$$

$$= -\frac{1}{2\pi}\int_0^\infty dk \frac{1}{(1 + \zeta^2 k^2)}\left[(1 - \imath k\zeta)e^{\imath kx} - (1 + \imath k\zeta)e^{-\imath kx}\right]\left[(1 - \imath k\zeta)e^{\imath kx'} - (1 + \imath k\zeta)e^{-\imath kx'}\right]$$

$$= \delta(x - x') - \frac{1}{2\pi}\int_0^\infty dk \left[\frac{(1 - \imath k\zeta)^2 e^{\imath k(x+x')}}{(1 + \zeta^2 k^2)} + \frac{(1 + \imath k\zeta)^2 e^{-\imath k(x+x')}}{(1 + \zeta^2 k^2)}\right]$$

$$= \delta(x - x') - \frac{1}{2\pi}\int_{-\infty}^\infty dk\frac{(1 - \imath k\zeta)e^{\imath k(x+x')}}{(1 + ik\zeta)} = \delta(x - x') - \frac{1}{\pi}\int_{-\infty}^\infty dk\frac{e^{\imath k(x+x')}}{1 + ik\zeta},$$

where in the last step, we used the fact that $\int_{-\infty}^\infty dk e^{\imath k(x+x')} = 0$, since $x, x' > 0$. Performing the final integration, we then get the completeness relations in EQ. (2.75).

The detection problem on the half line has been obtained as a limit of the problem on the $\mathbb{N}$ lattice. Fig. (7) compares the admissible values of the measurement parameters in both cases. The operator $H_{\mathbb{N}}$ and the operator defined in EQ. (2.71) are both non-Hermitian. In the measurement model under study, the parameter w takes values in the

right half of the complex plane while ζ takes values in the lower half of the complex plane. The unshaded regions in Fig. (7) for both cases correspond to those values of the measurement parameters for which only scattering solutions exist while, for values in the shaded region, there is in addition a bound state. The red unit semicircle and the red negative imaginary axis are the values of the measurement parameters for which the respective operators are non-diagonalizable.

If $\Psi_0(x)$, $x \geq 0$ is some initial state, then its time development in accordance with EQ'. (2.71) can be completely specified in terms of the basis states described above. This solution is given by

$$\Psi(x,t) = \int_0^\infty dk \; c(k)\eta^k(x)e^{-\imath k^2 t} + c_b \eta^b(x)e^{\imath t/\zeta^2},$$

$$c(k) = \int_0^\infty dx \; \Psi_0(x)\eta^k(x), \quad c_b = \int_0^\infty dx \; \Psi_0(x)\eta^b(x). \tag{2.76}$$

The coefficients $c(k)$ as well as the oscillating integrals above are well-defined for any initial wave function Ψ_0 which is sufficiently smooth, since then the $c(k)$'s have a fast decay in k. If $\Psi_0 \in \mathbb{L}^2([0,\infty))$ is only square integrable, the previous formula has to be understood by using an approximation of the initial condition by smooth initial conditions. The approximation scheme propagates in time thanks to the decay EQ. (2.81) of the $\mathbb{L}^2$-norm.

With the full solution of EQs. (2.71) known, one can obtain a saddle point approximation to $\Psi(x,t)$ for large t (see sec. C). This turns out to be

$$\Psi_\infty(x,t) = -\frac{1}{\sqrt{2t}}c\left(\tfrac{x}{2t}\right)\frac{\left(1 - \imath\zeta\tfrac{x}{2t}\right)}{\sqrt{1 + \zeta^2\tfrac{x^2}{4t^2}}}\exp\left[\imath\left(\tfrac{x^2}{4t} - \tfrac{\pi}{4}\right)\right]. \tag{2.77}$$

For $x \lesssim \sqrt{t}$ we need the form of $c(k)$ at $k \to 0$. Using the explicit form of the wave functions in EQ. (2.73) we find immediately that

$$c(k) \sim \frac{2\imath k}{\sqrt{2\pi}}m_{\Psi_0}, \text{ where } m_{\Psi_0} = \int_0^\infty dx\,(x - \zeta)\Psi_0(x).$$

Hence, we have for $x \lesssim \sqrt{t}$

$$\Psi_\infty(x,t) \approx m_{\Psi_0}\frac{x}{\sqrt{4\pi t^3}}\exp\left[\imath\left(\tfrac{x^2}{4t} + \tfrac{3\pi}{4}\right)\right], \tag{2.78}$$

which has a universal structure apart from the factor m_{Ψ_0}.

As an explicit numerical example, we now consider the evolution of an initial wave function of the form

$$\Psi_0(x) = 1, \text{ for } 1 < x < 2,$$

and zero elsewhere. In this case the basis expansion coefficients are given:

$$c(k) = \frac{k\zeta\cos(3k/2) - \sin(3k/2)}{\sqrt{2\pi(1 + k^2\zeta^2)}}\frac{\sin(k/2)}{k/2}, \qquad c_b = \sqrt{2\zeta}e^{-2/\zeta}(-1 + e^{1/\zeta}).$$
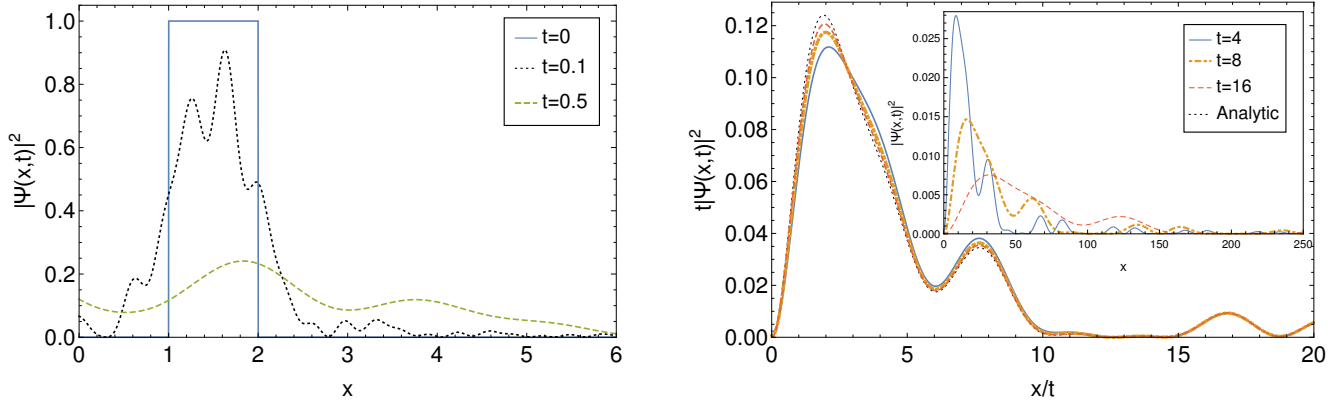
FIGURE 8. Plot showing $|\Psi(x,t)|^2$ at times $t = 0, 0.1, 0.5$, obtained from the solution in eq. (2.76) with the square initial condition $\Psi(x,0) = 1$ for $1 < x < 2$ and zero elsewhere. The parameter value $\zeta = 0.2 - 0.5i$ was taken.
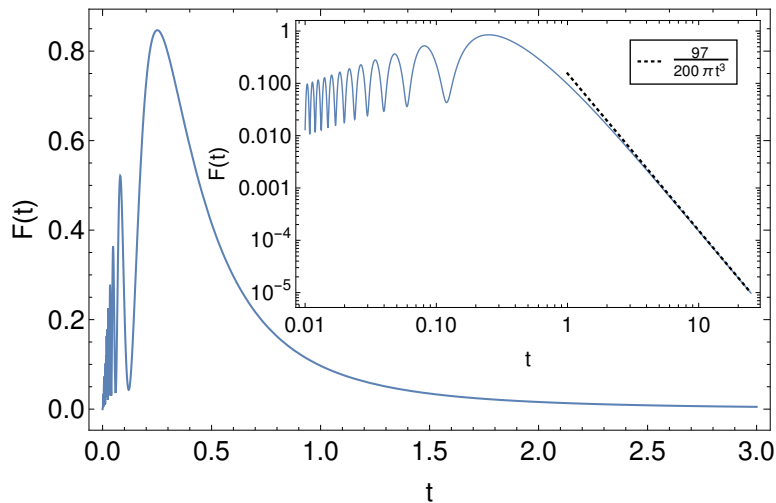
FIGURE 9. The first passage time distribution $F(t)$ for the initial wave packet and parameter values considered in Fig. (8). The inset shows the decay $F(t) \sim t^{-3}$ at large times, with a pre-factor given by eq. (2.83).

We choose $\zeta = 0.2 - 0.5i$. In Fig. (8) we show the evolution of the wave function at early (a) and late times (inset of b). For the scaled wave function in Fig. 8b and we see an excellent agreement with the analytic form in EQ. (2.77).

The survival probability $S(t)$ is given by

$$S(t) = \int_0^\infty dx \, |\Psi(x,t)|^2 \tag{2.79}$$

and after some straightforward manipulations one can show, using EQ. (2.71) that

$$S(t) = 1 + 2\frac{\Im(\zeta)}{|\zeta|^2} \int_0^t dt' \, |\Psi(0,t')|^2 \tag{2.80}$$

which is the continuous counterpart of EQ. (2.38). For purely real ζ, i.e. $\alpha = 0$ which corresponds to non-measurement, the system EQ. (2.71) determines unitary evolution on half line. We note that the first passage time distribution is given by

$$F(t) = -\frac{dS(t)}{dt} = -2\frac{\Im(\zeta)}{|\zeta|^2}|\Psi(0,t)|^2 > 0. \tag{2.81}$$

From the asymptotic scaling form in EQ. (2.77) we find that

$$S_\infty = \lim_{t \to \infty} S(t) = \int_0^\infty dk \left|\frac{1 - \imath\zeta k}{1 + \imath\zeta k}\right| |c(k)|^2. \tag{2.82}$$

We are not able to find more explicit forms for $F(t)$ or $S(t)$. However, we can obtain the asymptotic long time form of $F(t)$. We need the wave function at the origin, $\Psi(0,t)$. This can be obtained from the scaling solution in EQ. (2.78) by use of the boundary condition $\Psi(0,t) = -\zeta\left[\frac{\partial\Psi}{\partial x}\right]_{x=0}$. This gives us, for $t \to \infty$, $\Psi(0,t) = [m_{\Psi_0}\zeta/\sqrt{4\pi t^3}]e^{-\imath 3\pi/4}$. Hence, we get

$$\lim_{t \to \infty} t^3 F(t) = -\frac{\Im(\zeta)}{2\pi}|m_{\Psi_0}|^2. \tag{2.83}$$

In Fig. (9) we plot $F(t)$ for the same parameters and initial wave function used in Fig. (8). At large times, we verify the above asymptotic form given in EQ. (2.83).

We observe that the RHS of EQ. (2.83) may vanish for some special initial condition Ψ_0. This means that the asymptotic decay of the first passage time distribution is not universal. An exhaustive study can be performed showing that it is always possible to start with a special initial wave function Ψ_0 such that the asymptotic decay of the first passage time distribution will be of order $t^{-(2s+1)}$ for some integer $s \geq 1$. The detailed study is performed in sec. (C).

2.3.2. Real axis. The Schrödinger EQ. (2.53) can be rewritten in the form

$$\imath\frac{\partial\psi_n}{\partial t} = 2\psi_n - \psi_{n+1} - \psi_{n-1}, \quad n \in \mathbb{Z}$$
$$\psi_0 = \imath w(\psi_{-1} + \psi_1). \tag{2.84}$$

Assuming that $\imath w = \frac{1}{2} + \frac{\epsilon}{\zeta}$ where ζ is a complex number and defining the continuous wave function Ψ as

$$\Psi(x,t) = \lim_{\epsilon \to 0} \epsilon^{-1/2}\psi_{[x/\epsilon]}(t\epsilon^{-2}),$$

we get in the limit, $\epsilon \to 0$ the above equation reduces to the Schrödinger equation with a complex Robin boundary condition at the origin

$$\imath\frac{\partial\Psi}{\partial t} = -\frac{\partial^2\Psi}{\partial x^2},$$
$$2\Psi|_{x=0} + \zeta\left[\frac{\partial\Psi}{\partial x}|_{x=0^+} - \frac{\partial\Psi}{\partial x}|_{x=0^-}\right] = 0. \tag{2.85}$$

The solution of EQ. (2.85) can be obtained in the following way. Let us define

$$\Psi^s(x,t) = \frac{\Psi(x,t) + \Psi(-x,t)}{2}, \quad \Psi^a(x,t) = \frac{\Psi(x,t) - \Psi(-x,t)}{2},$$

the symmetric and antisymmetric part of the wave function Ψ. Both functions are uniquely determined by their restrictions to the half line $[0, \infty)$. EQ. (2.85) implies that on $[0, \infty)$, Ψ^s is solution of the Schrödinger EQ. (2.71) with a complex Robin boundary condition at the origin and that on $[0, \infty)$, Ψ^a is a solution of the Schrödinger equation with the Dirichlet boundary condition $\Psi^a(0, t) = 0$. To solve the latter, we observe that it is in fact sufficient to solve the free Schrödinger equation on the real line with the initial antisymmetric wave function Ψ^a, since this property will be preserved by the free propagator and in particular the solution will vanish on 0 at any time $t > 0$. It follows that the solution of EQ. (2.85) is given by,

$$\Psi(x, t) = \int_0^\infty dk \left[\hat{c}(k)\hat{\eta}^k(x) + a(k)\sigma^k(x)\right] e^{-\imath k^2 t} + \hat{c}_b \hat{\eta}^b(x) e^{\imath \frac{t}{\zeta^2}}, \qquad (2.86)$$

where

$$\hat{c}(k) = \int_{-\infty}^\infty dx\, \Psi_0(x)\hat{\eta}^k(x), \quad a(k) = \int_{-\infty}^\infty dx\, \Psi_0(x)\sigma^k(x), \quad \hat{c}_b = \int_{-\infty}^\infty dx\, \Psi_0(x)\hat{\eta}^b(x). \tag{2.87}$$

$\hat{\eta}^k, \sigma^k$ are the scattering states of the operator in EQ. (2.85) with explicit forms

$$\hat{\eta}^k(x) = \frac{\imath\left[(1 - \imath\zeta k)e^{\imath k|x|} - (1 + \imath\zeta k)e^{-\imath k|x|}\right]}{\sqrt{4\pi(1 + \zeta^2 k^2)}}, \quad \sigma^k(x) = \frac{1}{\sqrt{\pi}}\sin(k\,x), \qquad k > 0. \quad (2.88)$$

The bound state $\hat{\eta}^b(x)$ of the operator appears only when $\Re(\zeta) > 0$ and its form is

$$\hat{\eta}^b(x) = \frac{1}{\sqrt{\zeta}}\exp\left(-\frac{|x|}{\zeta}\right). \tag{2.89}$$

Observe that, up to a multiplicative constant, $\hat{\eta}^k$ and $\hat{\eta}^b$ are respectively the symmetrization of η^k and η^b states of the semi-axis case. The eigenfunctions σ^k are odd while $\hat{\eta}^k, \hat{\eta}^b$ are even. All the functions $\hat{\eta}^b$, $\hat{\eta}^k$ and σ^k satisfy the boundary condition in EQ. (2.85). Actually σ^k satisfy the boundary condition somewhat trivially since they are smooth and $\sigma^k(0) = 0$. All these eigenfunctions also satisfy the orthonormality conditions:

$$\int_{-\infty}^\infty dx\, [\hat{\eta}^b]^2 = 1,$$
$$\int_{-\infty}^\infty dx\, \hat{\eta}^k\hat{\eta}^{k'} = \int_{-\infty}^\infty dx\, \sigma^k\sigma^{k'} = \delta(k - k'), \quad k, k' > 0, \qquad (2.90)$$
$$\int_{-\infty}^\infty dx\, \sigma^k\hat{\eta}^{k'} = \int_{-\infty}^\infty dx\, \sigma^k\hat{\eta}^b = \int_{-\infty}^\infty dx\, \hat{\eta}^k\hat{\eta}^b = 0$$

and the completeness relations:

$$\int_0^\infty dk\, [\hat{\eta}^k(x)\hat{\eta}^k(x') + \sigma^k(x)\sigma^{k'}(x)] = \delta(x - x'),\ \text{for } \Re[\zeta] < 0$$
$$\int_0^\infty dk\, [\hat{\eta}^k(x)\hat{\eta}^k(x') + \sigma^k(x)\sigma^{k'}(x)] + \hat{\eta}^b(x)\hat{\eta}^b(x') = \delta(x - x'),\ \text{for } \Re[\zeta] > 0. \qquad (2.91)$$

The survival probability $S(t)$ is given by

$$S(t) = \int_{-\infty}^{\infty} dx \, |\Psi(x,t)|^2 \tag{2.92}$$

and after some straightforward manipulations one can show, using EQ. (2.85) that

$$S(t) = 1 + 4\frac{\Im(\zeta)}{|\zeta|^2} \int_0^t dt' \, |\Psi(0,t')|^2 \,. \tag{2.93}$$

Since $\sigma^k(0) = 0$ and $\hat{\eta}^k$, $\hat{\eta}^b$ are even, we conclude that the first passage time distribution $F = -\partial S/\partial t$ is up to a multiplicative constant the same as the one for the half-line, but starting from the wave function Ψ_0^s (instead of Ψ) restricted to the half-line. We observe in particular that if we start with an antisymmetric wave function $\Psi = \Psi^a$, then the particle is never detected.

2.4. Comparison of results

The previous sections of the current chapter offer a solution to the problem of continuous monitoring of a quantum system to detect the arrival of a particle at the detector. The object systems and the measurement protocol studied were simple enough to admit a thorough analysis by use of standard complex-analytic methods. The distribution of arrival times in each of the considered cases was obtained. Now, we shall briefly discuss some works in relation to our results, especially for the half line case of sec. (2.3.1).

A model for arrival time observable was given by Werner in [**Wer87**]. For a closed quantum system, the Hamiltonian, which is the generator of the system's unitary evolution is Hermitian. Werner gives an idealized description of the evolution of a *microsystem* (which can be taken to be a scalar particle on the half line) based on the existence of a contraction semigroup, up until the time it is absorbed by a *counter* placed at the origin $x = 0$. The instance of the absorption event is the arrival time of the particle. It is further assumed that the interaction of the counter with the microsystem is minimal, in the sense that pure states of the microsystem stay pure during the evolution. The description of continuous projective measurements in sec. (2.1) comports well with both the assumptions of Werner. In the particular case of detection on the half line (sec. (2.3.1)), the operator in EQ. (2.71) is a non-Hermitian extension of the one dimensional Laplacian ∂_{xx} and serves as the generator of Werner's semigroup, determining the evolution up to the instance of absorption. Let us establish that this is indeed the case. An operator L is dissipative (as defined in [**Wer87**]) if for all ψ in the domain of L ,

$$\langle \imath L\psi | \psi \rangle + \langle \psi | \imath L\psi \rangle \geq 0. \tag{2.94}$$

For the operator defined in EQ. (2.71), the above condition reads

$$\langle -\imath \partial_{xx}\psi | \psi \rangle + \langle \psi | -\imath \partial_{xx}\psi \rangle \geq 0,$$

which after partial integration and application of boundary condition in EQ. (2.71) gives

$$-2\frac{|\psi(0)|^2}{|\zeta|^2}\Im(\zeta) \geq 0.$$

Thus, the EQ. (2.94) is just the condition for positivity of the decay rate in EQ. (2.81).

Allcock [**All69b**] considers a different measurement scheme from the one used in our study. It is assumed in [**All69b**] that the free motion of the particle occurs in the region $x < 0$ (the incident channel) while in the region $x > 0$ (the measurement channel), there exists a uniform complex potential $-\imath V$ where V is a positive constant. The wave function $\phi(x, t)$ follows the equation

$$\imath\frac{\partial\phi}{\partial t} = -\frac{1}{2}\frac{\partial^2\phi}{\partial x^2} - \imath V\phi$$

in the region $x > 0$. The rate at which probability enters the measurement channel from the incident channel at the time t can be seen from the above equation to be

$$2V\int_0^\infty |\phi(x, t)|^2\, dx.$$

It follows from the above that the dissipation rate of survival probability has a time constant of $T \sim 1/(2V)$. Therefore, any registration of a detection event in the region $x > 0$ is known only to within an uncertainty of T. This is in contrast to our model, where the detection events are instantaneous.

Tumulka has considered the more general case of quantum motion in a three-dimensional domain Ω [**Tum22c**, **Tum22b**] with detectors placed everywhere on the boundary of the domain. An absorbing rule (ABR) is imposed on the domain boundary $\partial\Omega$ in the form

$$\hat{n}.\nabla\psi = \imath\kappa\psi,$$

where $\hat{n}(\boldsymbol{r})$ is the outward normal to the boundary at the boundary point $\boldsymbol{r}$. It is shown that ABR defines a probability distribution by exhibiting a projection operator valued measure on $\mathbb{R}_+ \times \partial\Omega$. It should be noted that Werner has shown that such projection operator valued measure is guaranteed to exist for any contraction map generated by a dissipative operator under the assumptions specified above EQ. (2.94). The measurement model considered in sec. (2.1 - 2.3) is an example of *hard* detection, whereas Allcock's model is that of *soft* detection. [**Tum22a**] analyses this distinction in more detail and obtains the hard detection model as a limit of the soft detection model in which the potential strength $V \to \infty$ and the width of the region of the complex potential $l \to 0$ such that $lV = \kappa$ up to a constant multiplier.

CHAPTER 3

Indirect Measurements

The measurement process discussed in the previous chapter involved a direct interaction between the measuring device with the object system. Conditioned on non-detection, the object system evolved through pure states in the model that was considered. In more general cases, the randomness introduced by the measurement performed on the system may not allow state evolution to remain pure. It may further be desirable that the evolution continue post a successful detection. For this to occur, the measurement protocol should preserve the system, unlike the case of detection via absorption at a screen.

Indirect measurements of a quantum system involve an interaction of the system with a quantum probe followed by projective measurement on the probe. Braginsky, Khalili & Thorne [**BKT92**] attribute this model of successive indirect measurements to Mandelstam [**Man71**]. Quantum non-demolition measurements (a type of indirect measurements) have proved useful in the important photon counting experiment of Haroche *et al.* [**GBD$^+$07**]. Other experiments [**MWMS13**, **MMS$^+$19**, **RSM$^+$14**] have looked at the trajectory of quantum systems under repeated indirect measurements. It should be further noted that in quantum measurement theory, *instruments* represent measurement procedures [**Bar93**]. It is a known result [**Oza84**] that any instrument can be realized via an indirect measurement scheme.

In this chapter, the results obtained in [**DCD23**] are presented. The object system that is measured is a 2−state system. It is allowed to interact for a period τ with a probe, which is also a two state system. The state of the probe is measured projectively after the interaction. Depending upon the result of this measurement, one obtains partial information about the state of the object system [**Bar93**]. If this process is repeated with identically prepared probes, then the object system evolves stochastically. It has been shown in [**Bru02**] for a two-state object system interacting with a sequence of identically prepared probes (which are also two-state systems), that the state of the object system evolves via a stochastic Schrödinger equation with jumps. Further, it has been shown in [**Bru02**] that when the interaction strength between the object system and the probes scales as, $\frac{1}{\sqrt{\tau}}$ then the reduced density matrix of the object system evolves via a Lindblad equation.

The basis of our study is the model described in [**SKR20**]. In this work, the authors have considered a measurement problem on a two-state system similar to the one described in the last paragraph. Their principal conclusion is that upon variation of the relative strength λ (defined below, see EQ.(3.10)) of measurement, the system exhibits transitions which mark various stages in the onset of the quantum Zeno effect.

Note that usual Zeno effect refers to the phenomena whereby a system's dynamics gets frozen as a result of continuous measurements on it. This Zeno effect is avoided with the choice of interaction strength scaling as $\tau^{-1/2}$. But what [**SKR20**] finds for their model is that in the limit of infinite measurement strength there is again a freezing of the dynamics. Interestingly, signatures of this freezing appear even at large but finite measurement strengths, with parts of the Hilbert space becoming inaccessible — this is referred to as the Zeno effect appearing in stages. Following [**SKR20**], we model the detector readout as a counting process and investigate the onset of the Zeno regime in the counting statistics of the readout process. Similar investigations have been carried out in [**LRS14**]. However, in the model we consider, the intensity of the counting process is state dependent [**Haw71**].

The aforementioned *stages* in the onset of Zeno effect are essentially topological transitions observed when measurement strength is changed. Measurement induced entanglement transitions and topological phase transitions based on Zeno physics have gained considerable attention, in particular we note the recent studies [**LCF18**, **TBF**+**21**, **BS21**, **NRSR21**, **IGG**+**21**]. These transitions have been identified with the presence of exceptional points [**GG21**] in the spectrum of non-Hermitian Hamiltonian, which evolves the quantum state under continuous measurement and post-selection. In [**RTLG18**], the spectral approach is employed to investigate the properties of Markov processes that are reset to a fixed state at times picked from an exponential distribution. [**MMCN19**, **MMC**+**20**] consider exceptional points of non-Hermitian Hamiltonians as well Liouvillians governing open system dynamics.

The results contained in this chapter are directly related to the problem of photodetection in experimental optics. In our study, we obtain expressions for survival probability (EQ. (3.23) below) which is well known in quantum optics. The review [**PK98**] and the works [**Car99**, **Car09**] are extensive surveys that have motivated the following study.

In the following pages, first a discrete model is developed in which the measurements are performed at times intervals of τ. Then a continuous time limit is obtained in a manner that the detector readout becomes a counting process. This counting process is the main object of the study for the rest of the chapter, where we develop the statistical functions associated with it. We adopt two complementary approaches. Firstly, the stochastic differential equation is written and analysed. Then the master equation is studies through the tools of spectral analysis.

3.1. Description of the measurement model

In this section, the basic measurement model is discussed first for the discrete time measurements and then the appropriate equations for continuous measurement are obtained.

3.1.1. Discrete time measurement model. Consider a $2-$state system $\mathcal{S}$ whose Hilbert space $\mathcal{H}_{\mathcal{S}}$ is spanned by the vectors

$$|\psi_0\rangle = \begin{bmatrix} 1 \\ 0 \end{bmatrix}, \quad |\psi_1\rangle = \begin{bmatrix} 0 \\ 1 \end{bmatrix}. \tag{3.1}$$

The system evolves with the Hamiltonian

$$H_{\mathcal{S}} = \begin{bmatrix} 0 & \gamma_0 \\ \gamma_0 & 0 \end{bmatrix} = \gamma_0 \sigma_x \tag{3.2}$$

where γ_0 is a positive frequency and σ_x, σ_y, σ_z represent the Pauli matrices. At any instance t, the state of $\mathcal{S}$ is given by the normalized vector

$$|\psi(t)\rangle = a(t)|\psi_0\rangle + b(t)|\psi_1\rangle = \begin{bmatrix} a(t) \\ b(t) \end{bmatrix}. \tag{3.3}$$

At this instance, $\mathcal{S}$ is allowed to interact with another $2-$level system $\mathcal{D}$ for a short time interval τ. The Hilbert space $\mathcal{H}_{\mathcal{D}}$ is spanned by $\{|\chi_0\rangle, |\chi_1\rangle\}$, defined similarly as in EQ. (3.1). At the start of the interaction, $\mathcal{D}$ is assumed to be in the state $|\chi_0\rangle$. The combined state of the system $\mathcal{S}$ and the detector $\mathcal{D}$ is the uncorrelated vector

$$|\Psi(t)\rangle = |\psi(t)\rangle \otimes |\chi_0\rangle \tag{3.4}$$

in the tensor product space $\mathcal{H} = \mathcal{H}_{\mathcal{S}} \otimes \mathcal{H}_{\mathcal{D}}$. We adopt the convention that for states or operators in $\mathcal{H}$, the first factor corresponds to $\mathcal{S}$ and the second factor to $\mathcal{D}$ in all summands. The state $|\Psi(t)\rangle$ evolves in the interval τ by the Hamiltonian

$$H = H_{\mathcal{S}} \otimes I + \sqrt{\frac{\gamma}{\tau}} \pi_1 \otimes \sigma_y. \tag{3.5}$$

The interaction part of the Hamiltonian is scaled as $1/\sqrt{\tau}$ and γ is a non-negative coupling frequency. In EQ. (3.5), the projector $\pi_1 = |\psi_1\rangle\langle\psi_1|$ and I is the identity operator. It follows that the combined state after the interval τ is given by

$$|\Psi(t+\tau)\rangle = \exp\left[-\imath\tau H\right]|\Psi(t)\rangle$$

$$\Rightarrow |\Psi(t+\tau)\rangle = |\psi(t)\rangle \otimes |\chi_0\rangle + (-\imath\tau)\left[\left(H_{\mathcal{S}} - \imath\frac{\gamma}{2}\pi_1\right)|\psi(t)\rangle\right] \otimes |\chi_0\rangle \tag{3.6}$$

$$-\imath\sqrt{\gamma\tau}\left[\pi_1|\psi(t)\rangle\right] \otimes \left[\sigma_y|\chi_0\rangle\right] + \mathcal{O}(\tau^{\frac{3}{2}}).$$

The overall state $|\Psi(t+\tau)\rangle$ can be regarded as the *a priori* state, i.e. the state before the result of the measurement is known. This result is known via a projective measurement on the outgoing probe post interaction. The measurement basis (or the pointer states) is taken to be $\{|\chi_0\rangle, |\chi_1\rangle\}$. Depending upon the result of the projective measurement on the probe, the state of the object system can be inferred from the above form of $|\Psi(t+\tau)\rangle$ along with the probabilities of these outcomes.
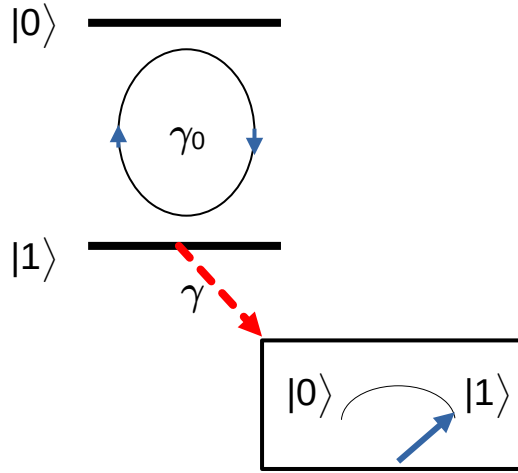
FIGURE 10. The observed system is a qubit with an internal transition frequency γ_0. The probe is also a qubit with pointer states $|0\rangle$ and $|1\rangle$. The probe is initially prepared in the state $|0\rangle$. During the interaction with the probe, the state $|1\rangle$ of the observed system couples to the probe with a rate proportional to $\sqrt{\gamma}$. A 'click' happens when the post interaction state of the probe is measured to be $|1\rangle$. Upon a click, the observed system collapses to the state $|1\rangle$.

If the probe is found to be in the state $|\chi_0\rangle$, then the un-normalized state $|\tilde{\psi}(t + \tau)\rangle$ of the object system $\mathcal{S}$ up to first order in τ is given by

$$|\tilde{\psi}(t + \tau)\rangle \approx \left[I - \imath\tau \left(H_{\mathcal{S}} - \imath\frac{\gamma}{2}\pi_1 \right) \right] |\psi(t)\rangle. \tag{3.7}$$

The probability of this event, i.e, of the readout to be $|\chi_0\rangle$, up to first order in τ is given by

$$p_0 \approx 1 - \gamma\tau\langle\psi|\pi_1|\psi\rangle = 1 - \gamma\tau|b(t)|^2. \tag{3.8}$$

If the readout is $|\chi_1\rangle$, then the un-normalized state and the probability of the readout are

$$|\widetilde{\psi}(t + \tau)\rangle \approx \sqrt{\gamma\tau}\pi_1|\psi(t)\rangle, \qquad p_1 \approx \gamma\tau\langle\psi|\pi_1|\psi\rangle = \gamma\tau|b(t)|^2. \tag{3.9}$$

This completes the description of one measurement cycle. For the two possible readouts, $|\chi_0\rangle$ corresponds to an incremental change in the state of the object system in accordance with EQ. (3.7) whereas $|\chi_1\rangle$ corresponds to a jump of the object system to the state $|\psi_0\rangle$ in accordance with EQ. (3.9). This jump event can be regarded as a *click* of the apparatus. Subsequently, the object system is coupled to another detector initialized in $|\chi_0\rangle$ and the process is repeated sequentially. A measurement record consists of a sequence of clicks separated by arbitrary integral multiples of interaction time τ.

3.1.2. Limit to continuous measurements. The choice of the interaction part of the Hamiltonian in EQ. (3.5) has already presented the EQ. (3.6) in a form for which the limit of continuous measurements corresponding to $\tau \to 0$ is easily obtained. The normalized *a posteriori* state after a jump is simply $|\psi_1\rangle$. For the case of incremental

evolution via EQ. (3.7), one has up to first order in τ

$$p_0 = \langle \widetilde{\psi}(t+\tau)|\widetilde{\psi}(t+\tau)\rangle \approx 1 + i\gamma_0\tau\langle\psi(t)|H_{\text{eff}}^{\dagger} - H_{\text{eff}}|\psi\rangle$$

where we have used the fact $\langle\psi(t)|\psi(t)\rangle = 1$ along with the definitions

$$H_{\text{eff}} = \frac{H_{\mathcal{S}}}{\gamma_0} - i\frac{\gamma}{2\gamma_0}\pi_1 = \begin{bmatrix} 0 & 1 \\ 1 & -2i\lambda \end{bmatrix}, \qquad \lambda = \frac{\gamma}{4\gamma_0}. \tag{3.10}$$

The parameter λ can be regarded as the strength of the measurement. An explicit calculation with above gives EQ. (3.8). In the limit, $\tau = dt \to 0$ the stochastic evolution of the normalized state is thus given by,

$$|\psi(t+dt)\rangle = \begin{cases} |\psi(t)\rangle - i\gamma_0 dt\left(H_{\text{eff}} + i\frac{\alpha_t}{2\gamma_0}\right)|\psi(t)\rangle, & \text{with prob. } p_0 = 1 - \alpha_t dt, \\ |\psi_1\rangle, & \text{with prob } p_1 = \alpha_t dt, \end{cases} \tag{3.11}$$

where

$$\alpha_t := \gamma\langle\psi(t)|\pi_1|\psi(t)\rangle = \gamma|b(t)|^2. \tag{3.12}$$

EQ. (3.11) is the continuous measurement limit of the discrete time model described in sec. (3.1.1). As in the discrete time case, the jump events can be regarded as clicks of the measuring apparatus. The time interval between consecutive clicks is of course non-deterministic. If N_t represents the number of clicks registered in time t from the start of the monitoring, then N_t is a counting process similar to the standard Poisson process. The important difference however is that the intensity α_t of the process N_t is not constant, but is in fact dependent upon the state of the monitored system via $b(t) = \langle\psi_1|\psi(t)\rangle$. The state $|\psi(t)\rangle$ in turn depends upon the time elapsed since the last click via the first case in EQ. (3.11).

The following assumptions, which are true for the standard Poisson process, are made for the process N_t on physical grounds that one does not expect N_t to explode in finite time.

$$dN_t = N_t - N_{t-}, \qquad dN_t\,dN_t = dN_t, \qquad dN_t\,dt = 0, \tag{3.13}$$

Here $N_{t-} = \lim_{t'\to t-} N_{t'}$ (the trajectories of N_t are right continuous with left limits). The expected value of the Poisson increment, conditioned upon the fact that the state of the system is $|\psi(t)\rangle$ is equal to

$$\mathbb{E}\left[dN_t\right] = \alpha_t dt = \gamma|b(t)|^2 dt. \tag{3.14}$$

The conditional EQ. (3.11) can now be written as a non-linear stochastic differential equation,

$$d|\psi(t)\rangle = -i\gamma_0\left(H_{\text{eff}} + i\frac{\alpha_t}{2\gamma_0}\right)|\psi(t)\rangle\,dt + \left(\sqrt{\gamma}\frac{\pi_1}{\sqrt{\alpha_t}} - I\right)|\psi(t)\rangle\,dN_t. \tag{3.15}$$

Note that for the second outcome in EQ. (3.11) one should include a factor $b(t)/|b(t)|$. However, rigorously, we should interpret the equation EQ. (3.15) for the corresponding

one-point projector $|\psi(t)\rangle\langle\psi(t)|$. More explicitly

$$d\begin{pmatrix} a(t) \\ b(t) \end{pmatrix} = \left[\begin{pmatrix} \frac{\gamma}{2}|b(t)|^2 & -i\gamma_0 \\ -i\gamma_0 & -\frac{\gamma}{2}+\frac{\gamma}{2}|b(t)|^2 \end{pmatrix} dt + \begin{pmatrix} -1 & 0 \\ 0 & -1+\frac{1}{|b(t)|} \end{pmatrix} dN_t \right] \begin{pmatrix} a(t) \\ b(t) \end{pmatrix}. \tag{3.16}$$

Equations (3.15, 3.16) are sometimes called stochastic Schrödinger equations [WM09, BB91] or quantum trajectory for pure state. This type of equation with Poisson noise in this set-up has been discussed in [Dio86, DCM92]. Since then, different justifications have been given for the fact that they model quantum systems which are subject to continuous indirect measurements. The general case of quantum trajectories is for mixed states and includes also Gaussian white noise [JS06, WM09, BP02].

Physically, two phenomena are in competition in EQ. (3.16) :

(1) Collapsing in basis $\{|\psi_0\rangle, |\psi_1\rangle\}$ thanks to continuous measurement. More precisely, when $\gamma_0 \to 0$ (i.e. $H_{\mathcal{S}} \to 0$), EQ. (3.16) models the continuous measurement of π_1. As π_1 is a diagonal matrix in the basis $\{|\psi_0\rangle, |\psi_1\rangle\}$, this basis is said to be of non-demolition form with respect to the measurement [WM09]. This will lead at large time to [BB11, ABBH01] the collapse in the basis $|\psi_0\rangle, |\psi_1\rangle$ with the born law with respect to the initial state $|\psi(0)\rangle$, i.e. :

$$\lim_{t\to\infty} |\psi(t)\rangle = \begin{cases} |\psi_0\rangle & \text{with probability } |\langle\psi_0|\,\psi(0)\rangle|^2 \\ |\psi_1\rangle & \text{with probability } |\langle\psi_1|\,\psi(0)\rangle|^2 \end{cases}. \tag{3.17}$$

(2) Rabi (coherent) oscillation due to unitary evolution. More precisely, when $\gamma = 0$, then from EQs. (3.13,3.37) one has $dN_t = 0$ and the EQ. (3.16) is the free (unitary) evolution with Rabi Hamiltonian, $H_{\mathcal{S}}$ which leads to classical Rabi oscillation [LB06].

In the general case with finite γ_0 and γ, as the commutator $[H_S, \pi_1] \neq 0$, the unitary evolution comes to prevent the asymptotic collapse in EQ. (3.17). The asymptotic behaviour will then be a smooth invariant density that will be obtained below. The competition between continuous non-demolition measurement and thermalization (instead of free unitary evolution here) has recently been extensively studied in [BBT15a, BBT15b, BBC$^+$21].

EQ. (3.15) describes the stochastic evolution of the state vector $|\psi(t)\rangle$ under continuous indirect measurements. Each measurement record of the state trajectory consists of a sequence of times at which clicks are registered by the apparatus. In the absence of a record, as in the case of blind measurements, one considers an overage over the outcomes and the density matrix $\rho(t)$ of the object system evolves as

$$\partial_t \rho(t) = -i[H_S, \rho(t)] + \frac{\gamma}{2}\left(2\pi_1\rho(t)\pi_1 - \{\pi_1, \rho(t)\}\right). \tag{3.18}$$

This is a Lindblad equation [Lin76, GKS76] with only one Kraus operator π_1 which is moreover self-adjoint. For a derivation, see sec. (D).

3.2. No click dynamics

From EQs. (3.7, 3.10) one sees that conditioned on no jump events during continuous monitoring, the un-normalized state $|\widetilde{\psi}(t)\rangle$ evolves in accordance with This evolution equation is

$$\imath \frac{\partial |\widetilde{\psi}\rangle}{\partial t} = \gamma_0 H_{\text{eff}} |\widetilde{\psi}\rangle. \tag{3.19}$$

This effective evolution has the same form as was derived in sec. (2.1.2) for direct measurements, and more specifically for the finite lattice case in sec. (2.2.1) with $N = 2$ and real $w = 2\lambda$. The survival probability $S(t)$, i.e., the probability of no clicks in the interval, $[0, t)$ is then given by

$$S(t) = \langle \tilde{\psi}(t) | \tilde{\psi}(t) \rangle. \tag{3.20}$$

3.2.1. Calculation of survival probability. Since H_{eff} is of order 2×2, EQ. (3.19) can be easily solved via matrix exponentiation. Suppose the object system $\mathcal{S}$ is prepared in the state $|\psi_0\rangle$ at $t = 0$ when continuous monitoring starts. For simplifying the expressions to be obtained below, introduce the notation $\beta^2 = -\beta'^2 = 1 - \lambda^2$, $\sin\phi = \beta$ and $\sinh\phi' = \beta'$.

When $0 \leq \lambda < 1$, then H_{eff} admits the orthogonal decomposition

$$\frac{1}{2\beta} \begin{bmatrix} c & c^* \\ -c^* & c \end{bmatrix} \begin{bmatrix} -(c^*)^2 & 0 \\ 0 & c^2 \end{bmatrix} \begin{bmatrix} c & -c^* \\ c^* & c \end{bmatrix}$$

where $c = \exp\left[\imath\left(\frac{2\phi-\pi}{4}\right)\right]$. From the above and the fact that $c^2 + (c^*)^2 = 2\beta$, one has

$$e^{-\imath\gamma_0 t H_{\text{eff}}} = \frac{1}{2\beta} \begin{bmatrix} c & c^* \\ -c^* & c \end{bmatrix} \begin{bmatrix} \exp[\imath\gamma_0 t(c^*)^2] & 0 \\ 0 & \exp[-\imath\gamma_0 t c^2] \end{bmatrix} \begin{bmatrix} c & -c^* \\ c^* & c \end{bmatrix}.$$

With the initial condition $|\psi(0)\rangle = |\psi_0\rangle$, from EQ. (3.19) one has

$$|\widetilde{\psi}(t)\rangle = e^{-\imath\gamma_0 t H_{\text{eff}}} |\psi_0\rangle = \frac{1}{\beta} \begin{bmatrix} \Re[c^2 \exp(\imath\gamma_0 t(c^*)^2)] \\ -\imath \Im[\exp(\imath\gamma_0 t(c^*)^2)] \end{bmatrix}. \tag{3.21}$$

The calculations in the case $\lambda > 1$ are similar to those for $0 \leq \lambda < 1$.

For $\lambda = 1$, as noted earlier (see discussion below EQ. (A.6)) H_{eff} is non-diagonalizable. The Jordan decomposition of H_{eff} is

$$\begin{bmatrix} 1 & \imath \\ 0 & 1 \end{bmatrix} \begin{bmatrix} -\imath & 0 \\ 1 & -\imath \end{bmatrix} \begin{bmatrix} 1 & -\imath \\ 0 & 1 \end{bmatrix}.$$

Once again, matrix exponentiation gives

$$e^{-\imath\gamma_0 t H_{\text{eff}}} = e^{-\gamma_0 t} \begin{bmatrix} 1 + \gamma_0 t & -\imath\gamma_0 t \\ -\imath\gamma_0 t & 1 - \gamma_0 t \end{bmatrix}.$$

With the same initial condition as before, one obtains

$$|\widetilde{\psi}(t)\rangle = e^{-\gamma t/4} \begin{bmatrix} 1 + \gamma_0 t \\ -\imath\gamma_0 t \end{bmatrix}. \tag{3.22}$$

With the form of $|\widetilde{\psi}(t)\rangle$ known, the survival probability can be obtained from EQ. (3.20). We note the explicit form of the survival probability when $|\psi(0)\rangle = |\psi_0\rangle$

$$
S(t, \lambda) = \begin{cases}
\dfrac{e^{-\frac{\gamma}{2}t}}{\beta^2} \left(\sin^2 (\beta\gamma_0 t) + \sin^2 (\beta\gamma_0 t + \phi) \right) & \text{for } 0 \leq \lambda < 1 \\[2ex]
\dfrac{e^{-\frac{\gamma}{2}t}}{\beta'^2} \left(\sinh^2 (\beta'\gamma_0 t) + \sinh^2 (\beta'\gamma_0 t + \phi') \right) & \text{for } \lambda > 1 \\[2ex]
e^{-\frac{\gamma}{2}t} \left((\gamma_0 t)^2 + (1 + \gamma_0 t)^2 \right) & \text{for } \lambda = 1
\end{cases}
\tag{3.23}
$$

Because $\beta' < \lambda$, even for $\lambda > 1$ the survival probability is a decaying exponential. In all cases $[S(t, \lambda)]_{t \to \infty} = 0$. The value $\lambda = 1$ is clearly a crossover point where the form of the functional dependence of $S(t)$ changes. Furthermore, for a fixed γ_0 and $\lambda \neq 1$ one has,

$$
\lim_{t \to \infty} \frac{S(t, 1)}{S(t, \lambda)} = 0.
\tag{3.24}
$$

Thus the survival probability decays at the fastest rate for the critical value of $\lambda = 1$.

Noting that $dN_s = 0$ for all $s \in [0, t]$ when no clicks are observed, the equation for the evolution of the normalized state $|\psi(t)\rangle$ can be obtained from EQ. (3.15) by putting $dN_t = 0$. We note this non-linear equation below

$$
\imath \partial_t |\psi(t)\rangle = \gamma_0 H_{\text{eff}} |\psi(t)\rangle + \imath 2\lambda\gamma_0 |\langle\psi_1|\psi(t)\rangle|^2 |\psi(t)\rangle.
\tag{3.25}
$$

Alternatively, the normalized state $|\psi(t)\rangle$ follows a non-linear equation when conditioned to evolve via no clicks. Noting that $|\psi(t)\rangle = \dfrac{|\widetilde{\psi}(t)\rangle}{\sqrt{S(t, \lambda)}}$, after differentiation and use of EQ. (3.19), one has

$$
\imath \partial_t |\psi(t)\rangle = \gamma_0 H_{\text{eff}} |\psi(t)\rangle - \frac{\imath}{2} \left(\frac{d}{dt} \log S(t) \right) |\psi(t)\rangle.
$$

The fact that $\langle\psi(t)|\psi(t)\rangle = 1$ and from the above equation it follows that

$$
-\imath \frac{d}{dt} \log S(t) = \gamma_0 \langle\psi(t)| \left[H_{\text{eff}}^\dagger - H_{\text{eff}} \right] |\psi(t)\rangle = \imath 4\lambda\gamma_0 |\langle\psi_1|\psi(t)\rangle|^2.
$$

Combining the above two results, one has the evolution equation EQ. (3.25).

3.2.2. Bloch sphere representation of no click dynamics. The pure state of a qubit can be represented by a point on the surface of the Bloch sphere whose North Pole is the state $|\psi_0\rangle$ and the South Pole is $|\psi_1\rangle$. For the particular choice of $H_\mathcal{S}$ (EQ. (3.2)) and the starting initial conditions, $|\psi(t = 0)\rangle = |\psi_0\rangle$, $|\psi(t = 0)\rangle = |\psi_1\rangle$ or point on the yz plane, the qubit state remains in a fixed plane at all times. In order to see this, we begin by noting that the standard representation of a qubit's state on the Bloch sphere is given by

$$
|\psi\rangle = \cos\frac{\chi}{2}|\psi_0\rangle + e^{\imath\xi} \sin\frac{\chi}{2}|\psi_1\rangle
\tag{3.26}
$$

for $0 \leq \chi \leq \pi$ and $0 \leq \xi \leq 2\pi$. In the spherical polar coordinate system, χ is the polar angle and ξ the azimuthal angle. In the yz plane, $\xi = \pi/2$ for $y > 0$ and $\xi = 3\pi/2$ for $y < 0$. ξ is undefined on the z axis. Substituting the above in EQ. (3.25), the following
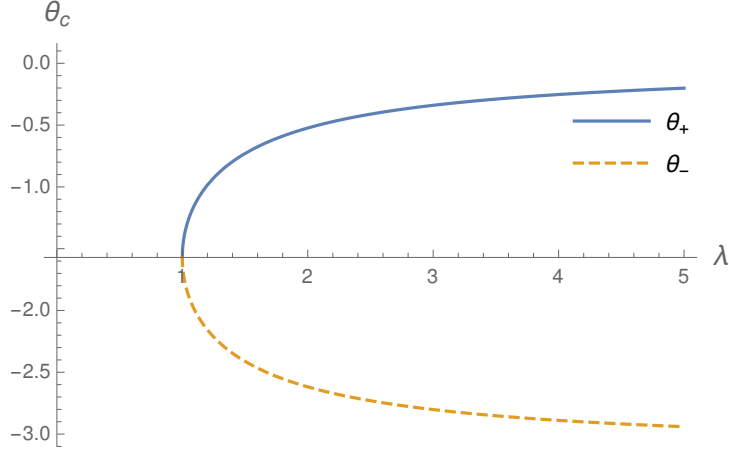
FIGURE 11. The saddle node bifurcation occurs at $\lambda = 1$ for $\theta_c = -\pi/2$. For $\lambda > 1$, two fixed points $\theta_\pm$ develop.

coupled system is obtained

$$\sin\frac{\chi}{2}\left[\imath\dot\chi + 2\gamma_0(\imath\lambda\sin\chi + e^{\imath\xi})\right] = 0,$$

$$\cos\frac{\chi}{2}\left[\imath\dot\chi - 2\gamma_0(-\imath\lambda\sin\chi + e^{-\imath\xi})\right] - 2\dot\xi\sin\frac{\chi}{2} = 0.$$

The trajectory of constant ξ is for $\cos\xi_0 = 0$ which corresponds to $\xi_0 = \pi/2$ and $\xi_0 = 3\pi/2$. For $\xi_0 = \pi/2$, χ evolves in accordance with

$$\dot\chi = -2\gamma_0(\lambda\sin\chi + 1),$$

whereas for $\xi_0 = 3\pi/2$, χ evolves in accordance with

$$\dot\chi = -2\gamma_0(\lambda\sin\chi - 1).$$

On the part of the evolution for $\xi = \pi/2$, define $\theta = \chi$ and on the part of the evolution for $\xi = 3\pi/2$, define $\theta = -\chi$. Then the state vector in EQ. (3.26) and its evolution can be described by a single angle variable $\theta \in (-\pi, \pi]$ with π and $-\pi$ identified. The general state in EQ. (3.26) can in this representation be written as

$$|\psi(t)\rangle = \begin{bmatrix} \cos(\theta_t/2) \\ \imath\sin(\theta_t/2) \end{bmatrix}, \tag{3.27}$$

and the evolution of θ_t under no click dynamics given by

$$\dot\theta = \Omega(\theta) = -2\gamma_0\left[1 + \lambda\sin\theta\right]. \tag{3.28}$$

This corresponds to the overdamped dynamics of a particle in a periodic tilted potential. For $\lambda < 1$ there are no fixed points and the particle keeps going round. At $\lambda = 1$, there is a saddle-node bifurcation (Figure 11) and two fixed points develop, one of which is stable (θ_+) and the other unstable (θ_-) and given by:

$$\theta_+ = -\sin^{-1}(1/\lambda), \qquad \theta_- = -\pi - \theta_+. \tag{3.29}$$

(a)   (b)
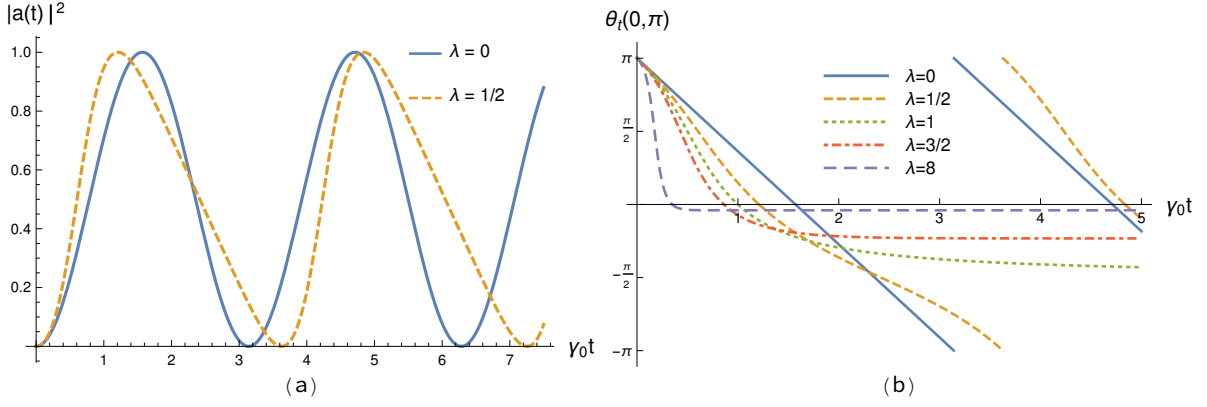
FIGURE 12. *No click dynamics*: Figure (a) compares the oscillations of the probablity $|a(t)|^2 = \cos^2(\theta_t/2)$ with $\theta_0 = 0$ for no measurement ($\lambda = 0$) and with measurement ($\lambda = 1/2$). The early half of the cycle is covered faster than the later half for $\lambda = 1/2$. (b) is the plot of θ_t for λ in various regimes. We chose initial condition $\theta_0 = \pi$ but other choices would give qualitatively the same results.

In the following, the flow notation $\theta_t(s, \theta')$ will be used to indicate the solution θ_t of the no-click dynamics $d\theta_t = \Omega(\theta_t) \, dt$ such that at the instance s, $\theta_s = \theta'$. Following are the results of integration of EQ. (3.28) in the various regimes of λ.

- For $\lambda < 1$, $\theta_0 = 0$, the equation integrates to give

$$\arctan \frac{\lambda + \tan[\theta_t(0,0)/2]}{\sqrt{1 - \lambda^2}} - \arctan \frac{\lambda}{\sqrt{1 - \lambda^2}} = -\beta\gamma_0 t. \qquad (3.30)$$

  If at t_1, $\theta_{t_1} = \pi$ and evolution happens via no click from t_1 to t then

$$\arctan \frac{\lambda + \tan[\theta_t(t_1,\pi)/2]}{\sqrt{1 - \lambda^2}} - \frac{\pi}{2} = -\beta\gamma_0(t - t_1). \qquad (3.31)$$

- For $\lambda = 1$ and $\theta(0) = 0$, the equation integrates to give

$$\tan\left(\frac{\pi}{4} - \frac{\theta_t(0,0)}{2}\right) = 1 + 2\gamma_0 t. \qquad (3.32)$$

  If at t_1, $\theta_{t_1} = \pi$ and evolution happens via no click from t_1 to t. The equation integrates to give

$$\tan\left(\frac{\pi}{4} - \frac{\theta_t(t_1,\pi)}{2}\right) = -1 + 2\gamma_0(t - t_1). \qquad (3.33)$$

- For $\lambda > 1$ and $\theta(0) = 0$, the equation integrates to give

$$\tan \frac{\theta_t(0,0)}{2} = -\frac{\sinh(\beta'\gamma_0 t)}{\sinh(\beta'\gamma_0 t + \phi')}. \qquad (3.34)$$

  If at t_1, $\theta_{t_1} = \pi$ and evolution happens via no click from t_1 to t then

$$\tan \frac{\theta_t(t_1,\pi)}{2} = -\frac{\sinh(\beta'\gamma_0(t - t_1) - \phi')}{\sinh(\beta'\gamma_0(t - t_1))}. \qquad (3.35)$$

The above equations confirm the observations made in Figs. (11, 12). For $0 < \lambda < 1$, the probability $|a(t)|^2 = \cos^2(\theta_t(0,\pi)/2)$ shows oscillations similar to Rabi oscillations, which happen for $\lambda = 0$. The frequency of these oscillations is proportional to β, whose form is given in EQ. (3.30). Figure 12(a) compares the cases $\lambda = 0$ and $\lambda = 1/2$. Figure 12(b) shows the evolution of $\theta_t(0,\pi)$ obtained from the integration of EQ. (3.28) for various values of λ. We observe that the oscillatory behaviour stops exactly at $\lambda = 1$ and increasing values of $\lambda \gg 1$ (collapsing regime of the previous section) cause rapid decay to $\theta_+ \approx 0$, which is consistent with the collapse EQ. (3.17) but conditioned on no click.

3.3. Stochastic dynamics

The continuous evolution of θ in accordance with EQ. (3.28) is interrupted whenever a click occurs. In accordance with EQ. (3.9), the system collapses to ψ_1 and hence the value of θ jumps to π (the azimuthal angle ξ is undefined for this state). The stochastic process N_t defined in EQs. (3.13, 3.14) counts the resets to the $\theta = \pi$ in the interval $[0, t]$. By mapping the evolution of the state vector on the Bloch sphere, we have thus expressed the dynamics of the object system to a classical stochastic process θ_t described by

$$d\theta_t = \Omega(\theta_t)\, dt + \left(\pi - \theta_{t_-}\right) dN_t, \tag{3.36}$$

where $\Omega(\theta)$ is as given in EQ. (3.28). The rate function α_t of N_t depends on θ_t in accordance with (3.14)

$$\mathbb{E}\left[dN_t\right] = \alpha(\theta_t)\, dt = \gamma \sin^2 \frac{\theta_t}{2}\, dt. \tag{3.37}$$

EQs. (3.36, 3.37) together define a resetting process. We note that resetting processes have gained attention in recent works in the classical context [**EM11b**, **EM11a**, **PKE16**, **EMS20**] as well as in a few studies in the quantum context [**MSM18**, **YB23**, **TDFS22**, **KM23**]. Our study provides a simple example where stochastic resetting in a quantum system appears naturally as a result of measurements.

If $P(\theta, t)$ represents the probability density of the stochastic variable θ at time t, then it was shown in [**SKR20**] that $P(\theta, t)$ obeys the forward equation

$$\frac{\partial P(\theta, t)}{\partial t} = -\frac{\partial}{\partial \theta}[\Omega(\theta)P(\theta, t)] - \gamma \sin^2\left(\frac{\theta}{2}\right) P(\theta, t) + \gamma \delta(\theta - \pi) \int_0^{2\pi} \sin^2\left(\frac{\theta'}{2}\right) P(\theta', t)\, d\theta'. \tag{3.38}$$

A similar partial integro-differential equation (PIDE) has appeared in [**WM93**] in the context of photo-detection. For an alternative derivation, please see sec. (D).

The steady state solution of EQ. (3.38) and some properties of the linear evolution operator were obtained in [**SKR20**]. It was noted that the onset of Zeno dynamics occurs in several stages, which are marked by specific values of the measurement parameter $\lambda \in \{1, \frac{2}{\sqrt{3}}, 2\}$. In EQ. (3.24), one already notices that the transition value $\lambda = 1$ makes itself apparent in the rate of decay of the survival probability. In the following, we wish to investigate how these values of λ appear in the counting statistics of the process N_t.

We also provide a complete solution of the time-evolution of $P(\theta, t)$ and a more detailed characterization of the spectrum.

From the point of view of the theory of stochastic processes, the process (θ_t, N_t) is a simple example of piecewise deterministic Markov processes [**Dav84**]. In the context of quantum measurement theory, counting processes related to arrival events of quanta at a counter were analysed in detail by E.B.Davies in [**Dav69**]. From [**BB91**] we learn that these processes are completely described by a specification of their exclusive probability densities (EPD). We now turn to the derivation of these EPDs for the process N_t and a study of the counting statistics.

3.3.1. Counting statistics. The EPD are finite dimensional probability densities in time, denoted as

$$P_0^t[0|||\psi(0)\rangle], \quad p_0^t[t_1, \ldots, t_n|||\psi(0)\rangle]. \tag{3.39}$$

$P_0^t[0|||\psi(0)\rangle]$ is the probability of obtaining no clicks in the interval $(0, t]$ when the measured system starts in the initial state $|\psi(0)\rangle$. $p_0^t[t_1, \ldots, t_n|||\psi(0)\rangle]$ is the probability density (in times $t_1, \ldots, t_n$) of exactly n counts at instances $0 < t_1 < \cdots < t_n \leq t$ where n ranges over positive integers.

One has for the non-autonomous counting process N_t [**Bré81**]

$$P_0^t[0||\psi(0)] = \exp\left[-\int_0^t \alpha(\theta_s(0, \theta_0))\, ds\right]. \tag{3.40}$$

For the 2−state system under consideration, $|\psi(0)\rangle = |\psi_0\rangle$ which corresponds to $\theta_0 = 0$ and $P_0^t[0|||\psi(0)\rangle]$ is then nothing but the survival probability in EQ. (3.23). From EQs. (3.28, 3.37) one obtains

$$\int_0^t \alpha(\theta_s(0, \theta_0))\, ds = \frac{\gamma t}{2} + \log\left|\frac{1 + \lambda \sin\theta_t(0, \theta_0)}{1 + \lambda \sin\theta_0}\right|. \tag{3.41}$$

The survival probability can now be compactly written in the form

$$P_0^t[0||\theta_0] = \frac{\Omega(\theta_0)}{\Omega(\theta_t(0, \theta_0))}\, e^{-\frac{\gamma t}{2}}. \tag{3.42}$$

From the above expression, all the expressions for survival probability in EQ. (3.23) can be recovered. For example, taking $\theta_0 = 0$ for the case $\lambda = 1$, one finds from EQ. (3.32)

$$\Omega(\theta_t) = -2\gamma_0(1 + \sin\theta_t), \qquad \tan\frac{\theta_t}{2} = -\frac{\gamma_0 t}{1 + \gamma_0 t},$$

$$\Rightarrow \Omega(\theta_t) = -\frac{2\gamma_0}{(1 + \gamma_0 t)^2 + (\gamma_0 t)^2}$$

from where the form of $S(t, 1)$ is clear.

Now consider the probability density in time $p_0^t[t_1||\theta_0 = 0]$ of exactly one click at the instance $t_1 \in (0, t]$. For this, there should be no click in $(0, t_1]$, a click in the interval

$(t_1, t_1 + \Delta t_1]$ and no click from $(t_1 + \Delta t_1, t]$. Then, in the limit $\Delta t \to 0$ one has,

$$p_0^t[t_1 || \theta_0 = 0] = e^{-\frac{\gamma t}{2}} \frac{\Omega(0)}{\Omega(\theta_{t_1-}(0,0))} \times \alpha(\theta_{t_1-}(0,0)) \times \frac{\Omega(\pi)}{\Omega(\theta_t(t_1, \pi))}. \tag{3.43}$$

Since $\theta_0 = 0$ in all further considerations, denote densities such as $p_0^t[t_1 || \theta_0 = 0]$ simply as $p_0^t[t_1]$ etc. For all $n \geq 1$, the densities $p_0^t[t_1, \ldots, t_n]$ can be obtained similarly. For different values of λ, one may note the form of $p_0^t[t_1, \ldots, t_n]$

$$p_0^t[t_1, \ldots, t_n] = \begin{cases} \frac{e^{-\frac{\gamma t}{2}}}{\beta^2} \left(\frac{\gamma}{\beta^2} \right)^n \sin^2(\beta\gamma_0 \Delta t_0) \frac{\prod_{k=1}^n \sin^2(\beta\gamma_0 \Delta t_k - \phi)}{\sin^2(\theta_t(t_n, \pi)/2)} & 0 \leq \lambda < 1 \\ \frac{e^{-\frac{\gamma t}{2}}}{\beta'^2} \left(\frac{\gamma}{\beta'^2} \right)^n \sinh^2(\beta'\gamma_0 \Delta t_0) \frac{\prod_{k=1}^n \sinh^2(\beta\gamma_0 \Delta t_k - \phi')}{\sin^2(\theta_t(t_n, \pi)/2)} & \lambda > 1 \\ e^{-\frac{\gamma t}{2}} \gamma^n (\gamma_0 \Delta t_0)^2 \frac{\prod_{k=1}^n (1 - \gamma_0 \Delta t_k)^2}{\sin^2(\theta_t(t_n, \pi)/2)} & \lambda = 1 \end{cases}$$

$$\tag{3.44}$$

In the above equation, we have $\Delta t_k = t_{k+1} - t_k$ with $t_0 = 0$ and $t_{n+1} = t$. The expressions for $\sin^2(\theta_t(t_n, \pi)/2)$ in the respective cases can be obtained from EQs. (3.31, 3.33, 3.35).

The probability of registering exactly n counts in the interval $(0, t]$ is given by

$$P_0^t[n] = \int_0^t dt_n \int_0^{t_n} dt_{n-1} \cdots \int_0^{t_2} dt_1 \, p_0^t[t_1, \ldots, t_n]. \tag{3.45}$$

EQ. (3.45) allows for writing the moment generating function of N_t. Explicitly

$$\mathbb{E}[e^{-sN_t}] = \sum_{n \geq 0} e^{-ns} P_0^t[n]. \tag{3.46}$$

In Appendix (E), it is shown that the Laplace transform with respect to time t of the moment generating function is

$$(\mathfrak{L}\mathbb{E}[e^{-sN_t}])(\sigma, s) = \frac{\mu^2 - \frac{\gamma}{2}(1 - 2e^{-s})\mu + 4\gamma_0^2}{\mu(\mu^2 + 4\beta^2\gamma_0^2) - \gamma e^{-s}\left(\mu^2 - \frac{\gamma}{2}\mu + 2\gamma_0^2\right)}, \tag{3.47}$$

where $\mu = \sigma + \gamma/2$. The denominator in the above is a third order polynomial in σ and has in general three (possibly complex) zeros $\sigma_1, \sigma_2, \sigma_3$ which depend on s, γ, γ_0. When these are distinct, then the moment generating function has the form

$$\mathbb{E}[e^{-sN_t}] = \frac{f(\sigma_1)e^{\sigma_1 t}}{(\sigma_1 - \sigma_2)(\sigma_1 - \sigma_3)} + \frac{f(\sigma_2)e^{\sigma_2 t}}{(\sigma_2 - \sigma_3)(\sigma_2 - \sigma_1)} + \frac{f(\sigma_3)e^{\sigma_3 t}}{(\sigma_3 - \sigma_1)(\sigma_3 - \sigma_2)}, \tag{3.48}$$

where $f(\sigma_i)$ is the numerator in EQ. (3.47) evaluated at the zero σ_i. In order to study the zeros, notice that the denominator factors when $s = 0$ as

$$(\mu - 2\lambda\gamma_0)(\mu^2 - 2\lambda\gamma_0\mu + 4\gamma_0^2). \tag{3.49}$$

The zeros of the denominator in EQ. (3.47) evaluated at $s = 0$ are,

$$\sigma_1(0) = 0, \quad \sigma_2(0) = \gamma_0 \left[-\lambda + \sqrt{\lambda^2 - 4} \right], \quad \sigma_3(0) = \gamma_0 \left[-\lambda - \sqrt{\lambda^2 - 4} \right]. \tag{3.50}$$
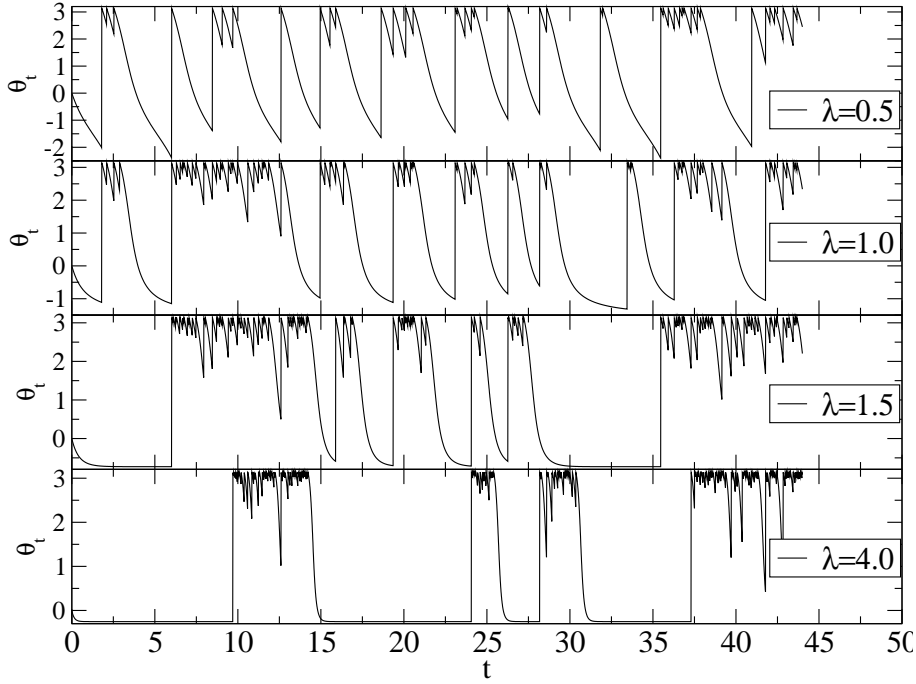
FIGURE 13. Typical realizations of stochastic trajectories, θ_t, obtained by solving eq. (3.36) for the initial condition $\theta_0 = 0$ and four different values of λ. We can see deterministic drifts and the stochastic resets to $\theta = \pi$. For trajectories starting from $\theta_0 = 0$, the whole interval $[-\pi, \pi]$ is accessible for $\lambda = 1/2$, while for $\lambda = 3/2$ (more generally for all $\lambda \geq 1$), only the interval $[\theta_+, \pi]$ is accessible. For the definition of θ_+, see eq. (3.29).

The zeros are all real for $\lambda > 2$. For $\lambda < 2$, $\sigma_2(0)$ and $\sigma_3(0)$ are complex conjugate while for $\lambda = 2$, there is a double root. When the expression in (3.49) is differentiated w.r.t. s and equated to 0, then the following are obtained

$$\left.\frac{d\sigma_1}{ds}\right|_{s=0} = -\frac{\gamma}{2}, \quad \left.\frac{d\sigma_2}{ds}\right|_{s=0} = \frac{\lambda}{\sqrt{\lambda^2 - 4}}\sigma_3(0), \quad \left.\frac{d\sigma_3}{ds}\right|_{s=0} = -\frac{\lambda}{\sqrt{\lambda^2 - 4}}\sigma_2(0). \tag{3.51}$$

For $\mathbb{E}[N_t]$, one has

$$\mathbb{E}[N_t] = -\frac{d}{ds}\mathbb{E}[e^{-sN_t}]\Big|_{s=0}. \tag{3.52}$$

A calculation using EQs. (3.48, 3.50, 3.51 3.52) then gives

$$\mathbb{E}[N_t] = \begin{cases} 2\lambda\gamma_0 t + \lambda^2\left[-1 + e^{-\lambda\gamma_0 t}\dfrac{\sin(\omega t + \varphi)}{\sin\varphi}\right] & 0 \leq \lambda < 2, \\[2mm] 2\lambda\gamma_0 t + \lambda^2\left[-1 + e^{-\lambda\gamma_0 t}\dfrac{\sinh(\omega' t + \varphi')}{\sinh\varphi'}\right] & \lambda > 2, \\[2mm] 4\left(-1 + \gamma_0 t + e^{-2\gamma_0 t}(1 + \gamma_0 t)\right) & \lambda = 2, \end{cases} \tag{3.53}$$

where $\omega^2 = -\omega'^2 = \gamma_0^2(4 - \lambda^2)$, $\tan\varphi = \frac{\lambda\sqrt{4-\lambda^2}}{\lambda^2-2}$ and $\tanh\varphi' = \frac{\lambda\sqrt{\lambda^2-4}}{\lambda^2-2}$. Here again one notices that $\lambda = 2$ is a crossover point where the form of functional dependence of $\mathbb{E}[N_t]$ changes. Furthermore, for the value of $\lambda = \sqrt{2}$, the oscillatory function $\sin(\omega t +$

$\varphi)/\sin(\varphi)$ is of minimum amplitude. In [**SKR20**], it has been pointed that there exists a transition for $\lambda = 2/\sqrt{3}$ characterised by a divergence in the steady state probability density $P_\infty(\theta)(= \lim_{t\to\infty} P(\theta, t))$. Moreover, the mean value of the transition rate α given by

$$\overline{\alpha}_t = \frac{d}{dt}\mathbb{E}[N_t] = \gamma\left[\frac{1}{2} - \frac{\gamma_0}{\omega}e^{-\lambda\gamma_0 t}\left(\frac{e^{\imath\omega t}}{\omega/\gamma_0 + \imath\lambda} + \frac{e^{-\imath\omega t}}{\omega/\gamma_0 - \imath\lambda}\right)\right] \quad (3.54)$$

has the signature of $\lambda = 2$ transition only.

It is important to note the limiting behaviour of expressions for $S(t, \lambda)$ in EQ. (3.23) and $\mathbb{E}[N_t]$ in EQ. (3.53). As defined, $\lambda = \frac{\gamma}{4\gamma_0}$ and two possible ways for $\lambda \to \infty$ are that $\gamma_0 \to 0$ for fixed γ, and that $\gamma \to \infty$ for fixed γ_0. In either case, it is easy to see that,

$$\lim_{\lambda\to\infty} S(t, \lambda) = 1. \quad (3.55)$$

As expected in the Zeno effect, for most trajectories the experimenter would detect no clicks in a finite time under strong measurement. For $\mathbb{E}[N_t]$, the behaviour is quite different, as we see in the following limits.

$$\lim_{\substack{\lambda\to\infty \\ \gamma \text{ fixed}}} \mathbb{E}[N_t] = 0, \qquad \lim_{\substack{\lambda\to\infty \\ \gamma_0 \text{ fixed}}} \mathbb{E}[N_t] = 2\gamma_0^2 t^2, \qquad \lim_{\substack{\lambda\to 0 \\ \gamma \text{ fixed}}} \mathbb{E}[N_t] = \frac{\gamma t}{2}. \quad (3.56)$$

The last panel of fig. (13) shows that under strong measurements ($\lambda \gg 1$), for most trajectories, the experimenter would detect no clicks in a finite time. This is the observation of the Zeno effect. However, after waiting for a sufficiently long time, a click is bound to occur (Since $[S(t, \lambda)]_{t\to\infty} = 0$). Immediately after the first click, $\theta = \pi$ and with a high click rate, the experimenter is likely to observe a number of subsequent clicks. Thus, for large γ, durations of no clicks (darkness) are punctuated by durations of a rapid increase in the number of clicks (brightness) [**CTD86**]. In the limit of large γ, the second limit in equation (3.56) is achievable despite the first. This can be related to the phenomenon studied in the context of spiking and collapse in the large noise limit of stochastic differential equations driven by Wiener processes [**BCC$^+$23**]. The last limit in EQ. (3.56) states that for extremely high Rabi frequency of the observed system, the clicks have the statistics of a *background* Poisson noise of intensity $\gamma/2$.

Further, consider the mean time τ_R between subsequent clicks. This is evidently given in terms of survival probability $P_0^t[0||\pi]$ and intensity α_t by the formula,

$$\tau_R = \int_0^\infty t\, P_0^t[0||\pi]\, \gamma \sin^2\frac{\theta_t(0, \pi)}{2}\, dt. \quad (3.57)$$

All the required quantities can be obtained from EQs. (3.30 - 3.35, 3.42) for various regimes of λ. For example, if $\lambda > 1$, the expression simplifies to

$$\tau_R = \frac{\gamma}{\beta'^2}\int_0^\infty t\sinh^2(\beta'\gamma_0 t - \phi')\exp(-\gamma t/2)\, dt,$$

and similar reductions can be made for the cases $\lambda \leq 1$. In all cases, the expression takes the simple form

$$\tau_R = \frac{2}{\gamma}. \tag{3.58}$$

Before indicating the connection of the above equation with results in [**TKB20**], it would help to consider another example which will further consolidate this connection. Take a 3-level system for which the system Hamiltonian H_S is given by

$$H_S = \gamma_0 \begin{bmatrix} 0 & 1 & 1 \\ 1 & 0 & 1 \\ 1 & 1 & 0 \end{bmatrix}. \tag{3.59}$$

Here γ_0 and γ (employed below) have similar significance as in the main model studied in this chapter, which was described in sec. (3.1). 2-level probes interact sequentially with the site $|1\rangle$, each interaction lasting a duration τ during which an incoming probe
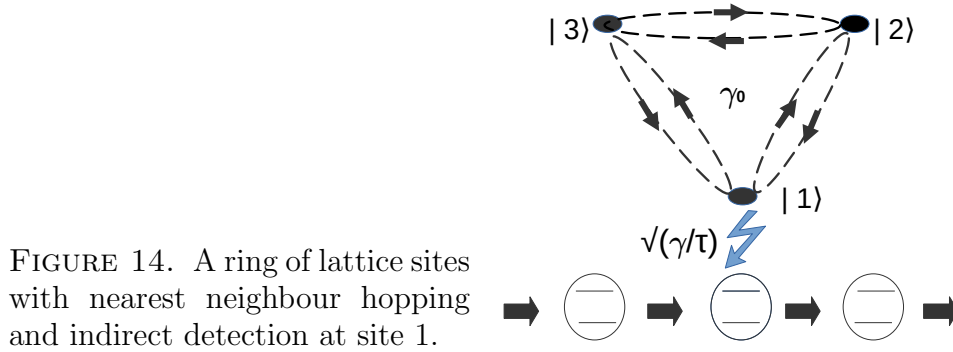
FIGURE 14. A ring of lattice sites with nearest neighbour hopping and indirect detection at site 1.

entangles with the 3-level system and the two jointly evolve in accordance with

$$H = H_S \otimes \mathbf{1} + \sqrt{\frac{\gamma}{\tau}} \pi_1 \otimes \sigma_y, \qquad \pi_1 = |1\rangle\langle 1|.$$

A time continuous limit can be obtained in much the same way as in sec. (3.1) and doing so, one obtains

$$H_{\text{eff}} = \gamma_0 H_3 = \gamma_0 \begin{bmatrix} -\imath 2\lambda & 1 & 1 \\ 1 & 0 & 1 \\ 1 & 1 & 0 \end{bmatrix}, \quad \lambda = \frac{\gamma}{4\gamma_0}, \qquad \alpha_t = \gamma |\langle 1|\psi(t)\rangle|^2. \tag{3.60}$$

The EQ. (3.58) for τ_R is generic, only that in this case the initial state is $|1\rangle = [1\ 0\ 0]^T$. The product of survival probability with $|\langle 1|\psi(t)\rangle|^2$ is nothing but the squared modulus of the un-normalized amplitude at $|1\rangle$. Therefore, one obtains

$$\tau_R = \gamma \int_0^\infty t \, |\langle 1| \exp(-\imath \gamma_0 t H_3)|1\rangle|^2 \, dt. \tag{3.61}$$

Thanks to the symmetric structure of H_3, the characteristic polynomial factorises as $(x+1)(x^2 + (-1+\imath 2\lambda)x - 2(1+\imath\lambda))$ giving eigenvalues,

$$\mu_0 = -1, \ \mu_\pm = \frac{1 - \imath 2\lambda \pm \imath \zeta(\lambda)}{2}, \qquad \zeta^2 = 4\lambda^2 - \imath 4\lambda - 9. \tag{3.62}$$

To obtain the square root in the above equation for ζ, the branch with positive imaginary part is chosen. Further notice that, for real λ, H_3 is always diagonalizable. Instead of detailing the tedious steps of diagonalization, we just note the required matrix element

$$\langle 1| \exp(-\imath\gamma_0 t H_3)|1\rangle = \frac{\exp(-\frac{\imath\gamma_0 t}{2})}{\zeta} e^{-\lambda\gamma_0 t} \left[\zeta \cosh\left(\frac{\zeta\gamma_0 t}{2}\right) + (1 - \imath 2\lambda)\sinh\left(\frac{\zeta\gamma_0 t}{2}\right) \right].$$

τ_R can now be evaluated by breaking up the integrand in several parts. For convergence of the integral, it is necessary that $|\Re\zeta| < 2\lambda$ for $\lambda > 0$. From the form of ζ in EQ. (3.62), it is in fact true the $0 < \Re\zeta < 2\lambda$ and that ζ approaches 2λ asymptotically from below. Collecting all the terms, one notes the form of τ_R arrived at after integration

$$\tau_R = \frac{\gamma}{2\gamma_0^2} \mathcal{M}(\zeta, \lambda),$$

where the radical

$$\mathcal{M}(\zeta, \lambda) = \frac{|\zeta|^2 - 1 - 4\lambda^2}{|\zeta|^2} \frac{4\lambda^2 - [\Im\zeta]^2}{(4\lambda^2 + [\Im\zeta]^2)^2} + \frac{|\zeta|^2 + 1 + 4\lambda^2}{|\zeta|^2} \frac{4\lambda^2 + [\Re\zeta]^2}{(4\lambda^2 - [\Re\zeta]^2)^2} \\ -2\frac{\Re\zeta + 2\lambda\Im\zeta}{|\zeta|^2} \frac{4\lambda\Im\zeta}{(4\lambda^2 + [\Im\zeta]^2)^2} - 2\frac{2\lambda\Re\zeta - \Im\zeta}{|\zeta|^2} \frac{4\lambda\Re\zeta}{(4\lambda^2 - [\Re\zeta]^2)^2}. \tag{3.63}$$

$\zeta(\lambda)$ defines the locus of the non-real eigenvalues of H_3 in the complex plane. It is quite surprising that $\mathcal{M}(\zeta, \lambda)$, despite having a rather involved form, actually evaluates to a very simple expression

$$\mathcal{M} \equiv \frac{1}{4\lambda^2}. \tag{3.64}$$

While a formal proof of the above hasn't been carried out, a numerical confirmation has been obtained for all tested values of λ.

Substituting for $\mathcal{M} = 1/(4\lambda^2)$ in the expression for τ_R, one gets the result in EQ. (3.58) using the fact that $\lambda = \frac{\gamma}{4\gamma_0}$. Therefore, the mean recurrence time, for both H_3 in EQ. (3.60) and the effective Hamiltonian in EQ. (3.10), is $2/\gamma$ for given sampling rate γ. This is related to the fact that the measurement does not affect the dark states. In the 2-state example, there are no dark states. In the 3-state example, the state $[0 \ -1 \ 1]^T$ is a dark state of H_3. Both these examples seem to confirm that τ_R has the general form [TKB20]

$$\frac{\text{Effective dimension of Hilbert space}}{\text{Sampling rate}},$$

where the effective dimension is equal to the dimension of the object system Hilbert space minus the number of linearly independent dark states. In [TKB20], the effective dimension was shown to have a topological interpretation as a winding number around the origin in the Laplace domain, of a function of a certain component of the resolvent of the system Hamiltonian. This component corresponds to the state for which the recurrence time is being calculated, and of course depends also on the form of the system Hamiltonian. The analysis done for the two cases in EQs. (3.10) and (3.60) here are in the direct space (time domain). For the example in EQ. (3.10), the effective Hamiltonian has an exceptional point which leads to the $\lambda = 1$ transition in the system's dynamics.

For the example in EQ. (3.60), there are no exceptional points. Despite these differences in the internal dynamics of the object system induced by measurements, we realize that the mean recurrence time τ_R has the simple form in EQ. (3.58), indicating topological protection in accordance with the conclusions in [**TKB20**]. Quantization of mean recurrence time in discrete time quantum walks was established in [**GVWW13**]. The models in EQs. (3.10) and (3.60) exhibit this quantization for systems under continuous measurements in conjunction with [**TKB20**].

3.3.2. Solution of PIDE. EQ. (3.38) can be solved for $P(\theta, t)$ directly with aid of the EPD obtained above. A given value of θ can be attained at time t after no reset, after exactly 1 reset, after exactly 2 resets and so on. These are all mutually exclusive events. Summing their contributions, one has

$$P(\theta, t) = P_0^t[0]\delta(\theta - \theta_t(0, 0)) + \sum_{n \geq 1} \int_0^t \cdots \int_0^{t_2} p_0^t[t_1, \ldots, t_n]\delta(\theta - \theta_t(0, 0)) \prod_{k=1}^n dt_k.$$

In the nth summand, suppose the last reset occurred at $t_n = t - \tau$. Then from the property in EQ. (3.43), one has

$$p_0^t[t_1, \ldots, t_n]\delta(\theta - \theta_t(0, 0)) = p_0^{t-\tau}[t_1, \ldots, t_{n-1}] \, \gamma \sin^2\left(\frac{\theta_{(t-\tau)-}(0, 0)}{2}\right) P_{t-\tau}^t[0||\pi] \, \delta(\theta - \theta_t(t - \tau, \pi))$$

$$= p_0^{t-\tau}[t_1, \ldots, t_{n-1}] \, \underbrace{\gamma \sin^2\left(\frac{\theta_{(t-\tau)-}(0, 0)}{2}\right)}_{\alpha_{t-\tau}} P_0^\tau[0||\pi] \, \delta(\theta - \theta_\tau(0, \pi)).$$

$$(3.65)$$

After substitution, one arrives at the formal solution which is in the form

$$P(\theta, t) = P_0^t[0]\delta(\theta - \theta_t(0, 0)) + \int_0^t \overline{\alpha}_{t-\tau} P_0^\tau[0||\pi] \, \delta(\theta - \theta_\tau(0, \pi)) \, d\tau, \qquad (3.66)$$

where $\overline{\alpha}_{t-\tau}$ is the mean transition rate that has already been obtained in EQ. (3.54). These type of renewal equations have been discussed in the context of stochastic resetting in [**PKE16**, **RG17**]. In sec. (D), it is shown that the proposed solution above indeed satisfies EQ. (3.38).

Alternatively, with the definition

$$\overline{\alpha}_t = \int_0^{2\pi} \gamma \sin^2\left(\frac{\theta}{2}\right) P(\theta, t) \, d\theta, \qquad (3.67)$$

when EQ. (3.66) is multiplied throughout by $\sin^2 \theta/2$, integrated w.r.t. θ and the Laplace transform is taken, one obtains

$$[\mathfrak{L}\overline{\alpha}](\sigma) = \frac{\gamma}{\beta^2} \frac{\hat{g}_0}{1 - \frac{\gamma}{\beta^2}\hat{g}_\phi}. \qquad (3.68)$$

in the notation of EQ. (E.2). Upon inversion, one recovers EQ. (3.54). One can now obtain the explicit form for $P(\theta, t)$ from EQs. (3.54,3.66) in the various regimes of λ.

3.3.3. Steady state. The evaluation of the steady state density $P_\infty(\theta) = \lim_{t\to\infty} P(\theta, t)$ is particularly simple. Since the time-dependent part of $\overline{\alpha}_t$ as well as the $P_0^t[0]\delta(\theta - \theta_t(0, 0))$ contribution to $P(\theta, t)$ are exponentially suppressed, one has

$$P_\infty(\theta) = \frac{\gamma}{2} \int_0^\infty P_0^\tau[0||\pi]\, \delta(\theta - \theta_\tau(0, \pi))\, d\tau. \tag{3.69}$$

Consider the case $\lambda < 1$. For $\theta_0 = \pi$, the no-click evolution happens via

$$\tan\frac{\theta_\tau(0, \pi)}{2} = -\frac{\sin(\beta\gamma_0\tau - \phi)}{\sin(\beta\gamma_0\tau)}, \quad P_0^\tau[0||\pi] = \frac{e^{-\frac{\gamma\tau}{2}}}{1 + \lambda\sin\theta_\tau(0, \pi)}. \tag{3.70}$$

The same value of $\theta_\tau(0, \pi) = \theta$ modulo 2π can be attained at the times $\{\tau_n\}_{n\geq 0}$ where $\tau_n = \tau_0 + \frac{n\pi}{\beta\gamma_0}$. The value of τ_0 can be worked out to be

$$\frac{\gamma\tau_0(\theta)}{2} = \frac{2\lambda}{\sqrt{1 - \lambda^2}}\left[\frac{\pi}{2} - \tan^{-1}\left(\frac{\lambda + \tan\frac{\theta}{2}}{\sqrt{1 - \lambda^2}}\right)\right].$$

In this case one also has

$$\delta(\theta - \theta_\tau(0, \pi)) = \sum_{n\geq 0} \frac{\delta(\tau - \tau_n)}{|\Omega(\theta_{\tau_n}(0, \pi))|} = \frac{1}{2\gamma_0(1 + \lambda\sin\theta)}\sum_{n\geq 0} \delta(\tau - \tau_n).$$

Integrating EQ. (3.69) with the above information one obtains for measurement parameter $\lambda < 1$

$$P_\infty(\theta) = \frac{\lambda}{(1 + \lambda\sin\theta)^2}\frac{e^{-\frac{\gamma\tau_0}{2}}}{1 - e^{-\frac{2\pi\lambda}{\sqrt{1-\lambda^2}}}}. \tag{3.71}$$

The case $\lambda \geq 1$, can be handled similarly. The main difference from $\lambda < 1$ case is that there exists only 1 instance τ_0 when a given value θ can be attained as long as θ does not lie in the no-go region. For $\lambda = 1$, one has

$$\frac{\gamma\tau_0(\theta)}{2} = \frac{2}{1 + \tan\frac{\theta}{2}}, \qquad P_\infty(\theta) = \frac{e^{-\frac{\gamma\tau_0}{2}}}{(1 + \sin\theta)^2}1_{(-\frac{\pi}{2}, \pi]}(\theta). \tag{3.72}$$

For $\lambda > 1$, one has

$$e^{-\frac{\gamma\tau_0(\theta)}{2}} = \left(\frac{\tan\frac{\theta}{2} - \tan\frac{\theta_+}{2}}{\tan\frac{\theta}{2} - \tan\frac{\theta_-}{2}}\right)^{\frac{\lambda}{\sqrt{\lambda^2 - 1}}}, \qquad \tan\frac{\theta_\pm}{2} = -\lambda \pm \sqrt{\lambda^2 - 1},$$

$$P_\infty(\theta) = \frac{\lambda e^{-\frac{\gamma\tau_0}{2}}}{(1 + \lambda\sin\theta)^2}1_{(\theta_+, \pi]}(\theta). \tag{3.73}$$

The results contained in EQs. (3.71,3.72,3.73) agree with those obtained in Ref. [SKR20] by directly finding the steady state solution of EQ. (3.38). With the resetting approach and through use of the renewal equation, we are now able to obtain the explicit time dependence of $P(\theta, t)$ in all cases. We remark that in the Zeno limit of strong measurement $\lambda \gg 1$ (coming from γ finite and $\gamma_0 \to 0$), $\theta_+ \to 0$ and we expect the steady state to converge towards a singular density concentrated near 0 and π.
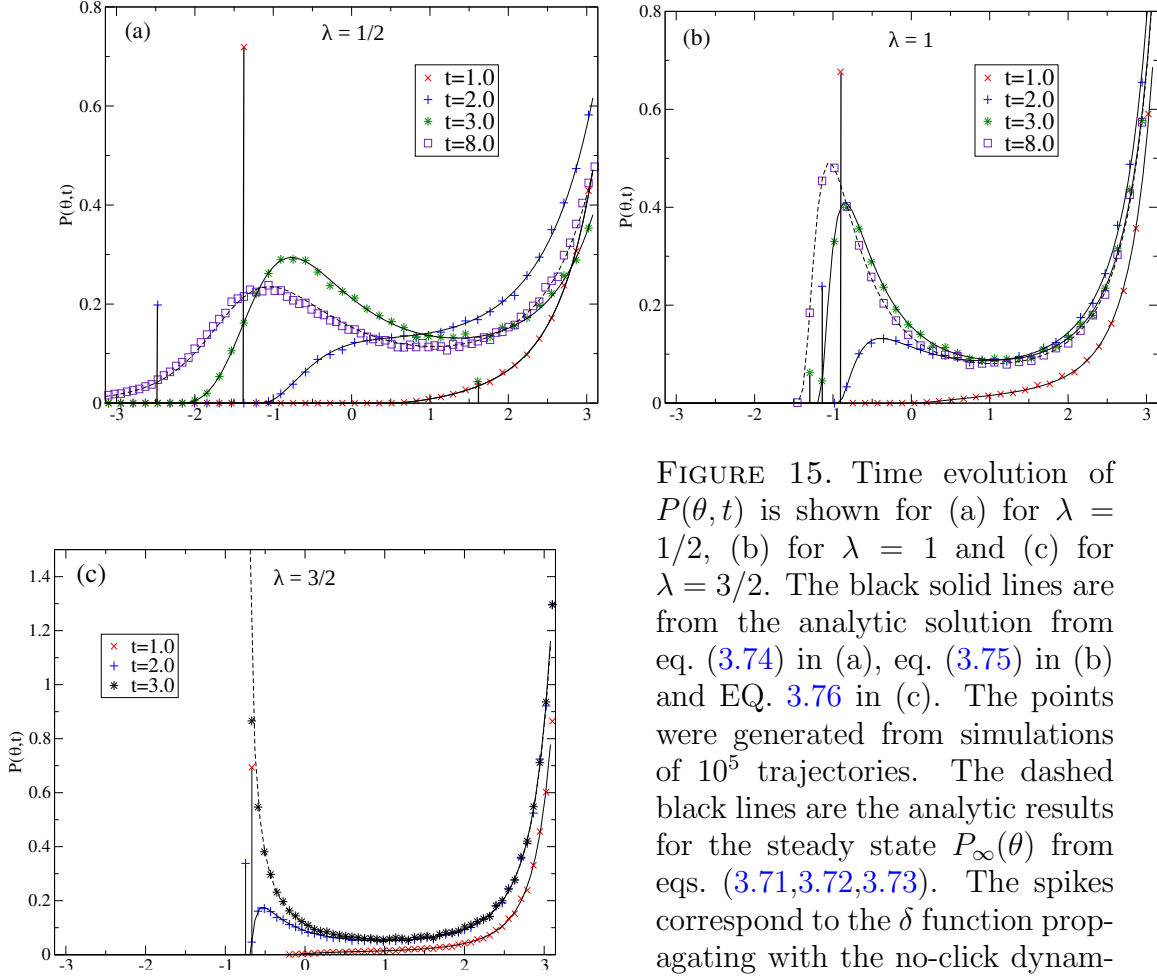
FIGURE 15. Time evolution of $P(\theta, t)$ is shown for (a) for $\lambda = 1/2$, (b) for $\lambda = 1$ and (c) for $\lambda = 3/2$. The black solid lines are from the analytic solution from eq. (3.74) in (a), eq. (3.75) in (b) and EQ. 3.76 in (c). The points were generated from simulations of 10^5 trajectories. The dashed black lines are the analytic results for the steady state $P_\infty(\theta)$ from eqs. (3.71,3.72,3.73). The spikes correspond to the δ function propagating with the no-click dynamics, and the height of the peaks equals the probability mass on the δ function.

3.3.4. Time evolution. The following equations note the result of integration of EQ. (3.66) for finite time. The integration can be carried out by use of EQs. (3.42,3.54) and the flow EQs. (3.30-3.35) for the respective cases of λ.

For $\lambda < 1$, the formula is somewhat complicated because the indicator function $1_{(\theta_t(0,\pi),\pi]}$ has to wrap properly with the number of possible visits to θ in time t starting from $\theta_0 = \pi$. For $\gamma_0 t \leq \pi/\beta$, there is only one possible visit and the expression is simpler. We give this expression:

$$
\begin{aligned}
P(\theta, t) =& P_0^t[0||0]\delta(\theta - \theta_t(0,0)) + \frac{\lambda e^{-\frac{\gamma\tau_0}{2}}}{(1 + \lambda\sin\theta)^2}\, 1_{(\theta_t(0,\pi),\pi]}(\theta) \\
& - \frac{4\lambda}{\sqrt{4 - \lambda^2}}\frac{1_{(\theta_t(0,\pi),\pi]}(\theta)}{(1 + \lambda\sin\theta)^2}\Re\left[e^{(-\lambda + \imath\sqrt{4-\lambda^2})\gamma_0 t}\frac{e^{-(\lambda + \imath\sqrt{4-\lambda^2})\gamma_0\tau_0}}{\omega/\gamma_0 + \imath\lambda}\right].
\end{aligned}
\tag{3.74}
$$

For $\lambda = 1$, we get for all times $t > 0$:

$$P(\theta, t) = P_0^t[0||0]\delta(\theta - \theta_t(0,0)) + \left[1 - \frac{2e^{-\gamma_0(t-\tau_0)}}{\sqrt{3}}\sin\left(\sqrt{3}\gamma_0(t - \tau_0) + \frac{\pi}{3}\right)\right]$$
$$\times \frac{e^{-\frac{\gamma\tau_0}{2}}}{(1 + \sin\theta)^2}1_{(\theta_t(0,\pi),\pi]}(\theta), \tag{3.75}$$

while for $\lambda > 1$, we get (for all times $t > 0$):

$$P(\theta, t) = P_0^t[0]\delta(\theta - \theta_t(0,0)) + \left[1 - \frac{2e^{-\lambda\gamma_0(t-\tau_0)}}{\sqrt{4 - \lambda^2}}\sin\left(\omega(t - \tau_0) + \arctan\sqrt{\frac{4}{\lambda^2} - 1}\right)\right]$$
$$\times \frac{\lambda e^{-\frac{\gamma\tau_0}{2}}}{(1 + \lambda\sin\theta)^2}1_{(\theta_t(0,\pi),\pi]}(\theta). \tag{3.76}$$

The three graphs in Figure 15 show good agreement between simulation and the analytic forms in EQs. (3.74,3.75 & 3.76).

3.3.5. General formulation and explicit time Laplace transform solution for the transition probability.

We consider here a more general set-up where the transition probability $P_t(\theta|\theta')$, that the process pass from θ' at time 0 to θ at time t, solves the Kolmogorov equation

$$\partial_t P_t(\theta|\theta') = L(\theta)P_t(\theta|\theta') - \gamma(\theta)P_t(\theta|\theta') + \mu(\theta)\left(\int_0^{2\pi} d\theta''\gamma(\theta'')P_t(\theta''|\theta')\right). \tag{3.77}$$

Here, $L(\theta)$ is a second (resp. first) order differential operator in θ, Markov generator, coming from a diffusion (resp. deterministic) process, and we are considering that resetting is not to a particular point but to a point θ chosen from the probability distribution $\mu(\theta)$ and the positive function $\gamma(\theta)$ is the jump rate for escape from state θ. The associated master equation for the probability density $P(\theta, t)$ is then

$$\partial_t P(\theta, t) = L(\theta)P(\theta, t) - \gamma(\theta)P(\theta, t) + \mu(\theta)\left(\int_0^{2\pi} d\theta''\gamma(\theta'')P(\theta'', t)\right). \tag{3.78}$$

Let us define the operators

$$L_0[f](\theta) \equiv L(\theta)[f](\theta) - \langle\mu, 1\rangle\gamma(\theta)f(\theta), \tag{3.79}$$

$$L_1[f](\theta) \equiv \mu(\theta)\langle\gamma, f\rangle, \tag{3.80}$$

for any function f on $[0, 2\pi]$ and where have used the following inner product definition:

$$\langle f, g\rangle = \int_0^{2\pi} d\theta f(\theta)g(\theta).$$

The master equation (3.38), and more generally the set-up of the previous section, is a particular case of this general theory when $L(\theta)[f] = -\partial_\theta[\Omega(\theta)f(\theta)]$, $\gamma(\theta) = \gamma\sin^2\left(\frac{\theta}{2}\right)$

and $\mu(\theta) = \delta(\theta - \pi)$. With these definitions, we have the formal solution of the Kolmogorov equation $P_t = \exp(t(L_0 + L_1))$ and the time Laplace transform is the resolvent

$$(\mathfrak{L}P_t)(s) \equiv \int_0^\infty dt \exp(-st) \exp(t(L_0 + L_1)) = (s - L_0 - L_1)^{-1} \tag{3.81}$$

$$= (s - L_0)^{-1} + (s - L_0)^{-1} L_1 (s - L_0 - L_1)^{-1}. \tag{3.82}$$

We thus find the auto-consistency relation

$$(\mathfrak{L}P_t)(s) = \left(\mathfrak{L}P_t^{(0)}\right)(s) + \left(\mathfrak{L}P_t^{(0)}\right)(s)L_1(\mathfrak{L}P_t)(s),$$

where $P_t^{(0)} = \exp(tL_0)$. By plugging in this relation the expression for L_1 (3.80) we obtain

$$(\mathfrak{L}P_t)(s)(\theta|\theta') = \left(\mathfrak{L}P_t^{(0)}\right)(s)(\theta|\theta') + \left\langle \left(\mathfrak{L}P_t^{(0)}\right)(s)(\theta|.), \mu(.) \right\rangle \left\langle \gamma(.), (\mathfrak{L}P_t)(s)(.|\theta') \right\rangle, \tag{3.83}$$

where . indicates the inner product integration variable. Multiplying with $\gamma(\theta)$ and integrating over θ solves for the unknown last term in the above equation,

$$\left\langle \gamma(.), (\mathfrak{L}P_t)(s)(.|\theta') \right\rangle = \frac{\left\langle \gamma(.), \left(\mathfrak{L}P_t^0\right)(s)(.|\theta') \right\rangle}{1 - \left\langle \gamma(..), \left\langle \left(\mathfrak{L}P_t^{(0)}\right)(s)(..|.), \mu(.) \right\rangle \right\rangle}. \tag{3.84}$$

Equations (3.83) and (3.84) provide a complete solution of the time evolution in the Laplace domain. We have finally the exact relation

$$(\mathfrak{L}P_t)(s)(\theta|\theta') = \left(\mathfrak{L}P_t^{(0)}\right)(s)(\theta|\theta') + \frac{\left\langle \left(\mathfrak{L}P_t^{(0)}\right)(s)(\theta|.), \mu(.) \right\rangle \left\langle \gamma(.), \left(\mathfrak{L}P_t^0\right)(s)(.|\theta') \right\rangle}{1 - \left\langle \gamma(..), \left\langle \left(\mathfrak{L}P_t^{(0)}\right)(s)(..|.), \mu(.) \right\rangle \right\rangle}, \tag{3.85}$$

which expresses $(\mathfrak{L}P_t)(s)$ in terms of $\left(\mathfrak{L}P_t^{(0)}\right)(s)$. So, in the case where the second is explicit, so is the first. It is instructive to write this equation in the time domain. To this end, we denote by $\bar{\gamma}(t)$ the inverse Laplace transform of the LHS of EQ. (3.84), which is simply,

$$\bar{\gamma}_t(\theta') = \int_0^{2\pi} d\theta''\ \gamma(\theta'')P_t(\theta''|\theta'), \tag{3.86}$$

which is just the average of transition rate $\gamma(\theta_t)$ conditioned by the initial condition $\theta_0 = \theta'$. Then EQ. 3.83 in the time domain is given by,

$$P_t(\theta|\theta') = P_t^0(\theta|\theta') + \int_0^t d\tau \langle P_\tau^0(\theta|.), \mu(.)\rangle \bar{\gamma}_{t-\tau}(\theta'), \tag{3.87}$$

which we see has the same structure as the renewal equation in EQ. (3.66). The EQ. (3.84) gives the Laplace transform of $\bar{\gamma}_t$, and is then EQ. (3.68), and for our specific example we were able to compute $\bar{\gamma}_t \equiv \bar{\alpha}_t$ explicitly (from the inverse Laplace and also using a renewal approach). In general, we would have an explicit solution for P_t from EQ. (3.83), provided we are able to evaluate $\bar{\gamma}_t$ explicitly from EQ. (3.84).

3.4. Spectral analysis

The Fokker-Planck operator corresponding to EQ. (3.38) has interesting spectral properties, which were pointed out in [**SKR20**]. In this section those studies are extended and in particular, for the case $0 < \lambda \leq 1$, some new results and some subtle features observed. One seeks solutions to EQ. (3.38) in the form $P(\theta, t) = \exp(2\gamma_0 \nu t) f_\nu(\theta)$. This leads to the following eigenvalue problem for the operator $\mathcal{L}$:

$$\mathcal{L}f_\nu = (1 + \lambda \sin \theta)\partial_\theta f_\nu + \lambda (2 \cos \theta - 1) \ f_\nu + 2\lambda\delta(\theta - \pi) \int_0^{2\pi} \sin^2(\theta'/2) f_\nu(\theta') \, d\theta' = \nu \ f_\nu. \tag{3.88}$$

Recall that π and $-\pi$ are identified. Assuming that $f_\nu(\theta)$ has no divergence at π, an integration of the above equation over a small interval across π gives a discontinuity of f_ν across π and leads to the following set of equations equivalent to the above:

$$\mathcal{L}f_\nu = (1 + \lambda \sin \theta)\partial_\theta f_\nu + \lambda (2 \cos \theta - 1) \ f_\nu = \nu \ f_\nu, \tag{3.89}$$

$$f_\nu(\pi - 0) - f_\nu(\pi + 0) = 2\lambda \int_{-\pi}^\pi \sin^2 (\theta/2) \ f_\nu(\theta) \, d\theta. \tag{3.90}$$

Define an operator $\mathcal{L}_0$ which satisfies EQ. (3.89) with condition $f(\pi - 0) = f(\pi + 0)$.

For square integrable functions $f(\theta)$, $g(\theta)$ defined on the unit circle, one has the standard inner product defined as,

$$\langle g, f \rangle := \int_{-\pi}^\pi g^* f \, d\theta, \tag{3.91}$$

where g^* is the complex conjugate of g. Then one has

$$\langle g, \mathcal{L}_0 f \rangle = \int_{-\pi}^\pi g^* \left[(1 + \lambda \sin \theta) \frac{d}{d\theta} f + 2\lambda \left(\cos \theta - \frac{1}{2} \right) f \right] d\theta$$

$$\Rightarrow \langle g, \mathcal{L}_0 f \rangle = g^*(\pi)f(\pi) - g^*(-\pi)f(-\pi) + \int_{-\pi}^\pi \left[- (1 + \lambda \sin \theta) \frac{d}{d\theta} g^* - 2\lambda \sin^2 \frac{\theta}{2} g^* \right] f \, d\theta. \tag{3.92}$$

For f in the domain of $\mathcal{L}_0$, one has $f(-\pi) = f(\pi)$. From the definition of the adjoint $\mathcal{L}_0^\dagger$ given by

$$\langle g, \mathcal{L}_0 f \rangle = \langle \mathcal{L}_0^\dagger g, f \rangle,$$

it follows that the adjoint operator $\mathcal{L}_0^\dagger$ acts on square integrable functions $g(\theta)$ as

$$\mathcal{L}_0^\dagger g = - (1 + \lambda \sin \theta) \, \partial_\theta g - 2\lambda \sin^2 (\theta/2) \, g, \quad g(\pi - 0) = g(\pi + 0). \tag{3.93}$$

A simple calculation reveals that for f in the common domain of $\mathcal{L}_0$ and $\mathcal{L}_0^\dagger$, the commutator $[\mathcal{L}_0, \mathcal{L}_0^\dagger]f = -3\lambda \sin \theta \, (1 + \lambda \sin \theta) \, f$. Thus $\mathcal{L}_0$ is not a normal operator and its eigenfunctions do not form an orthonormal basis for the Hilbert space $\mathbb{L}^2[-\pi, \pi]$.

For the operator $\mathcal{L}$ defined in EQs. (3.89, 3.90), the form of the adjoint $\mathcal{L}^\dagger$ is not immediately obvious. While $\langle g, \mathcal{L}f \rangle$ still evaluates to the RHS of EQ. (3.92), the boundary condition needs to be adjusted properly. The most direct way to do this is to employ

EQ. (3.90) to write

$$g^*(\pi)f(\pi) - g^*(-\pi)f(-\pi) = \left[g^*(\pi) - g^*(-\pi)\right]f(-\pi) + 2\lambda g^*(\pi) \int_{-\pi}^{\pi} \sin^2\left(\theta/2\right) f_\nu(\theta)\, d\theta$$

since f is in the domain of $\mathcal{L}$. Now one can write

$$\langle g, \mathcal{L}f \rangle = \left[g^*(\pi) - g^*(-\pi)\right]f(-\pi) + \int_{-\pi}^{\pi}\left[-(1 + \lambda\sin\theta)\frac{d}{d\theta}g^* - 2\lambda\sin^2\frac{\theta}{2}\left(g^* - g^*(\pi)\right)\right]f\, d\theta.$$

Once again, from the definition of adjoint, it follows from above that $\mathcal{L}^\dagger$ acts on square integrable functions $h(\theta)$ as

$$\mathcal{L}^\dagger h = -\left(1 + \lambda\sin\theta\right)\partial_\theta h - 2\lambda\sin^2\left(\theta/2\right)\left(h - h(\pi)\right), \quad h(\pi - 0) = h(\pi + 0). \qquad (3.94)$$

Like $\mathcal{L}_0$, $\mathcal{L}$ is also a non-normal operator. It will be seen below that the eigenfunctions of $\mathcal{L}_0$ (resp. $\mathcal{L}$) and $\mathcal{L}_0^\dagger$ (resp. $\mathcal{L}^\dagger$) together form a bi-orthonormal basis.

For completeness, we note the definition of a bi-orthonormal system [**RN12**]. The sequences $\{f_n\}, \{g_n\}$ of vectors in a Hilbert space $\mathfrak{H}$ form a bi-orthonormal system if

$$\langle f_m, g_n \rangle = 0 \quad \text{for } m \neq n, \qquad\qquad \langle f_n, g_n \rangle = 1. \qquad (3.95)$$

The sequences $\{f_n\}, \{g_n\}$ form a basis if each of $\{f_n\}, \{g_n\}$ are complete in $\mathfrak{H}$. Then for any $f \in \mathfrak{H}$, one has the bi-orthonormal developments

$$f = \sum_{n \geq 1}\langle g_n, f \rangle f_n, \qquad f = \sum_{n \geq 1}\langle f_n, f \rangle g_n. \qquad (3.96)$$

3.4.1. Measurement parameter $0 \leq \lambda < 1$**.** If $\bar{f}_\nu$ is an eigenfunction of $\mathcal{L}_0$ with eigenvalue, ν then it is easily seen that

$$\bar{f}_\nu(\theta) = \frac{C_\nu}{(1 + \lambda\sin\theta)^2}\exp\left[\frac{\nu + \lambda}{\sqrt{1 - \lambda^2}}\varphi(\theta, \lambda)\right], \qquad \varphi(\theta, \lambda) = 2\arctan\left(\frac{\lambda + \tan\frac{\theta}{2}}{\sqrt{1 - \lambda^2}}\right),$$
$$(3.97)$$

where C_ν is a normalization constant chosen so that $\int_{-\pi}^{\pi} \bar{f}_\nu(\theta), d\theta = 1$. The value of $\varphi(\theta, \lambda)$ are defined at the boundary by $\varphi(\pm\pi, \lambda) = \lim_{\theta \to \pm\pi\mp}\varphi(\theta, \lambda) = \pm\pi$. On imposing the boundary condition $\bar{f}_{\nu_m}(\pi) = \bar{f}_{\nu_m}(-\pi_+)$, the eigenvalues are obtained to be $\nu_m = -\lambda + \imath m\sqrt{1 - \lambda^2}$ where m ranges over the set of integers. Similar calculations for the operator $\mathcal{L}_0^\dagger$ gives its spectrum. The following equation gives a complete bi-orthonormal system, of eigenfunctions and eigenvalues, for the pair $\mathcal{L}_0$, $\mathcal{L}_0^\dagger$ with the property $\langle g_{\nu_m}, \bar{f}_{\nu_n} \rangle = \delta_{mn}$.

$$\bar{f}_{\nu_m}(\theta) = \left(\frac{1 - \lambda^2}{4\pi^2}\right)^{\frac{1}{4}}\frac{\exp[\imath m\varphi(\theta, \lambda)]}{(1 + \lambda\sin\theta)^2}, \qquad \nu_m = -\lambda + \imath m\sqrt{1 - \lambda^2}, m \in \mathbb{Z} \qquad \text{for } \mathcal{L}_0,$$

$$g_{\nu_m} = \left(\frac{1 - \lambda^2}{4\pi^2}\right)^{\frac{1}{4}}(1 + \lambda\sin\theta)\exp[\imath m\varphi(\theta, \lambda)], \quad \nu_{-m} = -\lambda - \imath m\sqrt{1 - \lambda^2}, m \in \mathbb{Z} \quad \text{for } \mathcal{L}_0^\dagger.$$
$$(3.98)$$

One can write a canonical expansion for any function $f \in \mathbb{L}^2[-\pi, \pi]$ in terms of the basis f_{ν_m}.

$$f = \sum_{m \in \mathbb{Z}} \alpha_m f_{\nu_m}, \qquad \alpha_m = \langle g_{\mu_m}, f \rangle = \int_{-\pi}^{\pi} g_{\mu_m}^* f \, d\theta. \tag{3.99}$$

For the eigenvalue problem in EQ. (3.89), the functions in EQ. (3.97) still satisfy the formal equation but the boundary condition in EQ. (3.90) leads to the condition

$$\frac{\nu(\nu^2 + \lambda\nu + 1)}{(\nu + \lambda)(\nu^2 + 2\nu\lambda + 1)} \sinh\left[\frac{\nu + \lambda}{\sqrt{1 - \lambda^2}}\pi\right] = 0. \tag{3.100}$$

From above, we infer that the eigenvalues of $\mathcal{L}$ are $\{0, \nu_+, \nu_-, \nu_m\}$ for $m \in \mathbb{Z} \setminus \{-1, 0, 1\}$ where

$$\nu_\pm = [-\lambda \pm \imath\sqrt{4 - \lambda^2}]/2. \tag{3.101}$$

The sinh function vanishes for $\nu = \nu_m$, $\forall m \in \mathbb{Z}$, however the denominator itself is $(\nu - \nu_0)(\nu - \nu_1)(\nu - \nu_{-1})$. The limiting value of the ratio for these three choices of ν is non-zero and therefore $\mathcal{L}$ does not have ν_0, ν_{-1} and ν_1 as eigenvalues. When the eigenvalue problem for adjoint $\mathcal{L}^\dagger$ in EQ. (3.94) is solved, one obtains the same constraint in EQ. (3.100). Thus, the operators $\mathcal{L}$ and $\mathcal{L}^\dagger$ have the same set of eigenvalues, just like the operators $\mathcal{L}_0$ and $\mathcal{L}_0^\dagger$. We further note that the integral boundary condition in EQ. (3.90) displaces only three eigenvalues in the spectrum of the $\mathcal{L}_0$, $\mathcal{L}_0^\dagger$ system — i.e. $f_{\nu_m} = \bar{f}_{\nu_m}$ for $m \neq 0, \pm 1$, while for these three eigenvalues $\{0, \nu_+, \nu_-\}$ we obtain three different eigenstates:

$$f_0(\theta) = \frac{\lambda}{2 \sinh\left[\frac{\pi(\lambda)}{\sqrt{1-\lambda^2}}\right]} \frac{\exp\left[\frac{\lambda}{\sqrt{1-\lambda^2}}\varphi(\theta, \lambda)\right]}{(1 + \lambda \sin\theta)^2}, \ f_{\nu_\pm}(\theta) = \frac{\nu_\mp}{2 \sinh\left[\frac{\pi\nu_\mp}{\sqrt{1-\lambda^2}}\right]} \frac{\exp\left[-\frac{\nu_\mp}{\sqrt{1-\lambda^2}}\varphi(\theta, \lambda)\right]}{(1 + \lambda \sin\theta)^2}. \tag{3.102}$$

We note that the $\nu = 0$ eigenvector $f_0(\theta)$ corresponds to the steady state solution $P_\infty(\theta)$.

For the eigenvalue problem in EQ.(3.94), with the convention $\mathcal{L}^\dagger h_{\nu^*} = \nu h_{\nu^*}$, where ν^* denotes the complex conjugation, the differential equation can be rewritten as

$$\frac{\partial}{\partial \theta}\left[\frac{h_{\nu^*}(\theta) - h_{\nu^*}(\pi)}{1 + \lambda \sin\theta} \exp\left[\frac{\lambda + \nu}{\sqrt{1 - \lambda^2}}\varphi(\theta, \lambda)\right]\right] = -\frac{\nu \, h_{\nu^*}(\pi)}{(1 + \lambda \sin\theta)^2} \exp\left[\frac{\lambda + \nu}{\sqrt{1 - \lambda^2}}\varphi(\theta, \lambda)\right].$$

Integrating the above from π to θ, one obtains, after changing the integration variable on the r.h.s $\theta \to \varphi$

$$\frac{h_{\nu^*}(\theta) - h_{\nu^*}(\pi)}{1 + \lambda \sin\theta} \exp\left[\frac{\lambda + \nu}{\sqrt{1 - \lambda^2}}\varphi(\theta, \lambda)\right] = -\frac{\nu h_{\nu^*}(\pi)}{(1 - \lambda^2)^{3/2}}$$

$$\times \int_{\pi}^{\varphi(\theta)} d\varphi \exp\left[\frac{\lambda + \nu}{\sqrt{1 - \lambda^2}}\varphi\right]\left(1 - \frac{\lambda}{2}\nu_{-1}e^{\imath\varphi} - \frac{\lambda}{2}\nu_1 e^{-\imath\varphi}\right).$$

After performing the integration and applying the boundary condition in EQ. (3.94), we obtain the eigenfunctions $\{h_0, h_{\nu_+}, h_{\nu_-}, h_{\nu_m}\}$ ($m \in \mathbb{Z} \setminus \{-1, 0, 1\}$) for $\mathcal{L}^\dagger$. They are indexed such that $\mathcal{L}^\dagger h_\nu = \nu^* h_\nu$. The bi-orthonormality condition $\langle h_a, f_b \rangle = \delta_{ab}$ can be

verified from their explicit form:

$$h_0 = 1, \quad h_{\nu_\pm}(\theta) = \mp \imath \frac{\lambda \big[\cos\theta - \nu_\mp \sin\theta \big]}{\sqrt{4 - \lambda^2}},$$

$$h_{\nu_m}(\theta) = g_{\nu_m}(\theta) + \frac{(-1)^m \lambda^2}{B_{-m}} \sum_{k \in \{-1,0,1\}} \frac{m(m^2 - 1)}{(m-k)(k^2+1)} \frac{g_{\mu_k}(\theta)}{B_k}, \tag{3.103}$$

where g_{μ_m} is defined in EQ. (3.98). The coefficients B appearing in the above expressions are

$$B_m = \nu_m(\nu_m - \nu_-)(\nu_m - \nu_+).$$

In this bi-orthonormal system, one can now expand

$$\delta(\theta) = f_0 + h_{\nu_-}(0) \, f_{\nu_+} + h_{\nu_+}(0) \, f_{\nu_-} + \sum_{m \in \mathbb{Z} \backslash \{-1,0,1\}} h_{\nu_{-m}}(0) \, f_{\nu_m}.$$

In the original problem, EQ. (3.38), $P(\theta, 0) = \delta(\theta)$. Then the time development of $P(\theta, t)$ is given by

$$P(\theta, t) = f_0(\theta) + \imath \frac{\lambda \, e^{2\nu_+ \gamma_0 t}}{\sqrt{4 - \lambda^2}} f_{\nu_+}(\theta) - \imath \frac{\lambda \, e^{2\nu_- \gamma_0 t}}{\sqrt{4 - \lambda^2}} f_{\nu_-}(\theta) + \left(\frac{1 - \lambda^2}{4\pi^2} \right)^{\frac{1}{4}} \sum_{m \in \mathbb{Z} \backslash \{-1,0,1\}} \frac{(-1)^m \lambda}{B_m} f_{\nu_m}(\theta) \, e^{2\nu_m \gamma_0 t}$$

$$+ \left(\frac{1 - \lambda^2}{4\pi^2} \right)^{\frac{1}{2}} \frac{e^{-2\lambda \gamma_0 t}}{(1 + \lambda \sin\theta)^2} \sum_{m \in \mathbb{Z} \backslash \{-1,0,1\}} \exp\left[\imath m \, \Phi(\theta, \lambda, t) \right],$$

where $\Phi(\theta, \lambda, t) = \varphi(\theta, \lambda) - \varphi(0, \lambda) + 2\gamma_0 \, t \sqrt{1 - \lambda^2}$. We note that the first series in the RHS is convergent as $B_m \sim m^3$. We write the last summation in the above equation as $2\pi \delta[\Phi(\theta, \lambda, t)] - \sum_{m \in \{-1,0,1\}} \exp\left[\imath m \, \Phi(\theta, \lambda, t) \right]$. Then, using the fact that $\Phi(\theta, \lambda, t) = 0$ solves for $\theta_t(0,0)$ (EQ. (3.30)), we obtain $\delta[\Phi(\theta, \lambda, t)] = \delta(\theta - \theta_t(0,0)) / |\Phi'(\theta, \lambda, t)|$. In conjunction with EQ. (3.42), after some simplifications, we finally get

$$P(\theta, t) = P_0^t[0] \delta(\theta - \theta_t(0,0)) + P_{\mathrm{f}}(\theta, t), \quad \text{where}$$

$$P_{\mathrm{f}}(\theta, t) = P_\infty(\theta) + \imath \frac{\lambda \, e^{2\nu_+ \gamma_0 t}}{\sqrt{4 - \lambda^2}} f_{\nu_+}(\theta) - \imath \frac{\lambda \, e^{2\nu_- \gamma_0 t}}{\sqrt{4 - \lambda^2}} f_{\nu_-}(\theta)$$

$$+ \left(\frac{1 - \lambda^2}{4\pi^2} \right)^{\frac{1}{4}} \sum_{m \in \mathbb{Z} \backslash \{-1,0,1\}} \frac{(-1)^m \lambda}{B_m} f_{\nu_m}(\theta) \, e^{2\nu_m \gamma_0 t} \tag{3.104}$$

$$- \left(\frac{1 - \lambda^2}{4\pi^2} \right)^{\frac{1}{2}} \frac{e^{-2\lambda \gamma_0 t}}{(1 + \lambda \sin\theta)^2} \frac{\sin\left[3\Phi(\theta, \lambda, t)/2 \right]}{\sin\left[\Phi(\theta, \lambda, t)/2 \right]}.$$

Here P_{f} represents the finite part of the density which was also obtained in EQ. (3.74). Fig. (16) shows agreement between EQ. (3.104), EQ. (3.74) and numerical simulation.

In $P_{\mathrm{f}}(\theta, t)$, the smallest decay rate is for the terms corresponding to f_{ν_+} and f_{ν_-}. Therefore, the approach to $P_\infty(\theta)$ (the steady state) happens as,

$$\imath \frac{\lambda \, e^{2\nu_+ \gamma_0 t}}{\sqrt{4 - \lambda^2}} f_{\nu_+}(\theta) - \imath \frac{\lambda \, e^{2\nu_- \gamma_0 t}}{\sqrt{4 - \lambda^2}} f_{\nu_-}(\theta) = \imath \frac{\lambda \, e^{-\lambda \gamma_0 t}}{\sqrt{4 - \lambda^2}} \left(f_{\nu_+}(\theta) e^{\imath \gamma_0 t \sqrt{4 - \lambda^2}} - f_{\nu_-}(\theta) e^{-\imath \gamma_0 t \sqrt{4 - \lambda^2}} \right),$$

$$\tag{3.105}$$
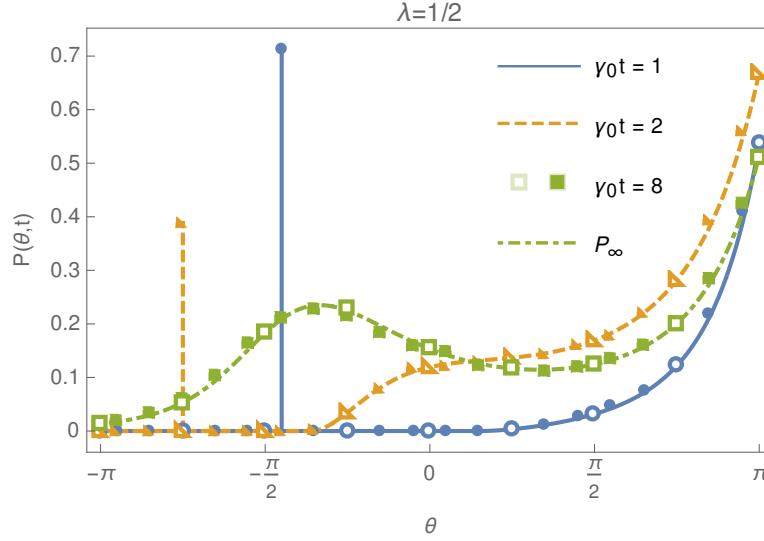
FIGURE 16. A comparison of series solution in eq. (3.104) (solid dots) truncated at $N = 150$, numerical simulation and the solution EQ. (3.74) (continuous curve) at various times for measurement strength of $\lambda = 1/2$.

which has the form of a damped oscillator of natural frequency $2\gamma_0$. Note that the spectral solution for $P(\theta, t)$ provides an easier result for the long time form than that obtained from the renewal solution.

3.4.2. Measurement parameter $\lambda = 1$. For the operators $\mathcal{L}_0$ and $\mathcal{L}_0^\dagger$ defined in EQ. (3.93), the corresponding eigenfunctions and eigenvalues are,

$$f_{\nu_k} = \frac{1}{\sqrt{2\pi}} \frac{\exp\left[\imath k \frac{-2}{1+\tan\frac{\theta}{2}}\right]}{(1+\sin\theta)^2}, \qquad \nu_k = -1 + \imath k, k \in \mathbb{R} \qquad \text{for } \mathcal{L}_0,$$

$$g_{\mu_k} = \frac{1}{\sqrt{2\pi}}(1+\sin\theta)\exp\left[\imath k \frac{-2}{1+\tan\frac{\theta}{2}}\right], \qquad \mu_k = -1 - \imath k, k \in \mathbb{R} \qquad \text{for } \mathcal{L}_0^\dagger.$$

(3.106)

Note that f_{ν_k} in EQ. (3.106) satisfies the condition $f_{\nu_k}(\pi) = f_{\nu_k}(-\pi_+)$ for any complex k. Our choice of ν_k for $k \in \mathbb{R}$ is based on the fact that this set is the limit of the set $\{\nu_m\}_{m\in\mathbb{Z}}$ (see EQ. (3.98)) as $\lambda \to 1_-$. One notices that the eigenvalues are no more discrete and therefore the bi-orthonormality condition becomes $\langle g_{\mu_k}, f_{\nu_{k'}} \rangle = \delta(k - k')$, which is easily verified. While the functions f_{ν_k} satisfy the condition $f_{\nu_k}(-\pi) = f_{\nu_k}(\pi)$, they do not belong to $\mathbb{L}^2[-\pi, \pi]$. With the substitution $x = -2/(1 + \tan\frac{\theta}{2})$, one has,

$$\int_{-\pi}^{\pi} 2\sin^2\frac{\theta}{2} f_{\nu_k} d\theta = \frac{1}{2\sqrt{2\pi}} \int_{-\infty}^{\infty} (x+2)^2 e^{\imath kx} dx = 2\sqrt{2\pi}\left[\delta(k) - \imath\delta'(k) - \delta''(k)/4\right].$$

(3.107)

We shall develop the solution $P(\theta, t)$ in the complete system of EQs.(3.106). For $\theta_0 \neq -\pi/2$, consider the integral

$$\int_{-\infty}^{\infty} g_{\mu_k}(\theta_0)^* f_{\nu_k}(\theta) \, dk = \frac{1 + \sin \theta_0}{(1 + \sin \theta)^2} \frac{1}{2\pi} \int_{-\infty}^{\infty} \exp\left[\imath k \left(\frac{2}{1 + \tan \frac{\theta_0}{2}} - \frac{2}{1 + \tan \frac{\theta}{2}} \right) \right] dk$$

$$= \left(\frac{1 + \sin \theta_0}{1 + \sin \theta} \right)^2 \delta(\theta - \theta_0).$$

Since the factor of $\delta(\theta - \theta_0)$ is continuous at θ_0, one has the following representations

$$\delta(\theta) = \frac{1}{\sqrt{2\pi}} \int_{-\infty}^{\infty} e^{\imath 2k} f_{\nu_k} \, dk, \qquad \delta(\theta - \pi) = \frac{1}{\sqrt{2\pi}} \int_{-\infty}^{\infty} f_{\nu_k} \, dk. \qquad (3.108)$$

The general function $P(\theta, t)$ can be expanded in the bi-orthonormal system of EQ. (3.106) as

$$P(\theta, t) = \int_{-\infty}^{\infty} c_k(t) \, e^{2\nu_k \gamma_0 t} f_{\nu_k} \, dk, \qquad (3.109)$$

where the time development of c_k can be ascertained after substituting the above in EQ. (3.38). Doing so, using the EQs.(3.107,3.108) and the fact that $\mathcal{L}_0 f_{\nu_k} = \nu_k f_{\nu_k}$, one has,

$$\dot{c}_k = \dot{c}_0 \, e^{-\imath k 2 \gamma_0 t}, \qquad \dot{c}_0 = 4\gamma_0 \left[\left((1 - \gamma_0 t) + \frac{\imath}{2} \frac{\partial}{\partial k} \right)^2 c_k \right]_{k=0}, \qquad c_k(0) = \frac{e^{2\imath k}}{\sqrt{2\pi}}. \quad (3.110)$$

This is a self-consistent system which can be readily solved using Laplace transform (see sec. (E)). We note the explicit solution

$$c_k(t) = \frac{1}{\sqrt{2\pi}} \left[e^{\imath 2k} + \imath \frac{\exp[-\imath 2 \gamma_0 t(k + \imath)] - 1}{k + \imath} + \frac{\nu_-}{\sqrt{3}} \frac{\exp[-\imath 2 \gamma_0 t(k - \imath\nu_-)] - 1}{k - \imath\nu_-} \right.$$

$$\left. - \frac{\nu_+}{\sqrt{3}} \frac{\exp[-\imath 2 \gamma_0 t(k - \imath\nu_+)] - 1}{k - \imath\nu_+} \right], \quad (3.111)$$

where $\nu_{\pm}$ are as defined in EQ. (3.101) for $\lambda = 1$. Substituting for c_k in EQ. (3.109) and carrying out contour integration, $P(\theta, t)$ is obtained in the form of EQ. (3.75).

The point spectrum of $\mathcal{L}$ consists of the eigenvalues $\{0, \nu_+, \nu_-\}$ with eigenfunctions,

$$f_0(\theta) = \frac{\exp\left[-\frac{2}{1 + \tan(\theta/2)} \right]}{(1 + \sin \theta)^2} 1_{[-\pi/2, \pi]}(\theta), \qquad f_{\nu_{\pm}}(\theta) = -\nu_{\mp} \frac{\exp\left[\frac{2\nu_{\mp}}{1 + \tan(\theta/2)} \right]}{(1 + \sin \theta)^2} 1_{[-\pi/2, \pi]}(\theta).$$

$$(3.112)$$

These functions properly belong to $\mathbb{L}^2[-\pi, \pi]$ and satisfy the integral boundary condition in EQ. (3.90). The continuous spectrum of $\mathcal{L}$ consists of improper eigenvalues ν_k with corresponding improper (i.e., non-normalizable) eigenfunction, f_{ν_k} as defined in EQ. (3.106) for $k \in \mathbb{R} \setminus \{0\}$. These functions satisfy the boundary condition only up to principal value, as is evident from EQ. (3.107).

Now consider the operator $\mathcal{L}^\dagger$ defined in EQ. (3.94) for the case $\lambda = 1$. An integration of the eigenvalue equation for eigenfunction h_{ν^*} of eigenvalue ν leads to the expression

$$\frac{h_{\nu^*}(\theta) - h_{\nu^*}(\pi)}{1 + \sin\theta} \exp\left[-(\nu+1)\frac{2}{1+\tan\frac{\theta}{2}}\right] = \frac{\nu h_{\nu^*}(\pi)}{(\nu+1)^3}\left[1 + \nu + \nu^2\right.$$

$$\left. -\frac{(2 + 2\nu + \nu^2 + (1+\nu)\cos\theta + \sin\theta)}{1+\sin\theta}\exp\left[-(\nu+1)\frac{2}{1+\tan\frac{\theta}{2}}\right]\right]. \qquad (3.113)$$

In case of $\nu = -1$, the RHS of the above should be evaluated as a limit. This limit is

$$-h_{\nu^*}(\pi)\frac{2\sec^2(\theta/2)(-3\sin\theta + \cos\theta - 5)}{3(\tan(\theta/2) + 1)^3}.$$

The discrete part of the spectrum of $\mathcal{L}^\dagger$ consists of $\{0, \nu_+, \nu_-\}$ (same as for $\mathcal{L}$) with corresponding eigenfunctions given by $\{h_0, h_{\nu_-}, h_{\nu_+}\}$ of the same form as in EQ. (3.103). For the continuous part of the spectrum, we take ν_k as given in EQ. (3.106). The following gives the explicit form of h_{ν_k} which are proper eigenfunctions of $\mathcal{L}^\dagger$ with eigenvalues $-1 - \imath k$, $k \in \mathbb{R} \setminus \{0\}$.

$$h_{\nu_k} = g_{\mu_k} + \frac{1}{\sqrt{2\pi}}\left[\frac{1}{\nu_{-k}} - \frac{(\nu_{-k} + 1)\cos\theta + \sin\theta}{\nu_{-k}^2 + \nu_{-k} + 1}\right], \qquad \mathcal{L}^\dagger h_{\nu_k} = \nu_{-k}h_{\nu_k}. \qquad (3.114)$$

The improper eigenfunction with improper eigenvalue -1 is give by

$$h_{\nu_0} = \frac{1}{\sqrt{2\pi}}\left[1 + \frac{2}{3}\left(\frac{3\sin\theta - \cos\theta + 5}{1 + \tan(\theta/2)}\right)\right]. \qquad (3.115)$$

In terms of the bi-orthonormal system for the pair $\mathcal{L}, \mathcal{L}^\dagger$ described above, the full expansion for $P(\theta, t)$ can be alternatively written as

$$P(\theta, t) = f_0(\theta) + \imath\frac{e^{2\nu_+ \gamma_0 t}}{\sqrt{3}}f_{\nu_+}(\theta) - \imath\frac{e^{2\nu_- \gamma_0 t}}{\sqrt{3}}f_{\nu_-}(\theta) + \int_{-\infty}^{\infty} h_{\nu_{-k}}(0)\, f_{\nu_k}(\theta)e^{2\nu_k \gamma_0 t}\, dk. \qquad (3.116)$$

3.4.3. Measurement parameter $\lambda > 1$. It is now clear that for $0 \le \lambda < 1$, the spectrum is discrete, and a series expansion is sufficient for spectral decomposition where as for $\lambda = 1$, the spectrum consists of discrete as well as continuous parts and the spectral decomposition is rather intricate. The difficulty in the $\lambda = 1$ case is clearly associated with the appearance of a singular point in the definition in EQ. (3.89) at $\theta = -\pi/2$. For $\lambda > 1$, there are two singular points at $\theta = \theta_+$ and $\theta = \theta_-$ as defined in EQ. (3.29). Furthermore, we notice that for $\lambda = 2/\sqrt{3}$, apart from the appearance of the singular point at $\theta_+ = -\pi/3$, the coefficient $(2\cos\theta - 1)$ in EQ. (3.89) also vanishes at $\theta = \theta_+$. It has been noted in [**SKR20**] that $\lambda = 2/\sqrt{3}$ corresponds to a transition point where the steady state density in EQ. (3.73) begins to show divergence at $\theta = \theta_+$. These are further interesting features of the problem at hand, however a full spectral decomposition for $\lambda > 1$ was not achieved during the course of our study.

This concludes the discussion of indirect measurements. In this chapter, indirect measurements were studied via the example of a counting measurement on a two state system. The stochastic differential equation as well as the master equation for this process

were solved through the use of standard probability theoretic means as well as through spectral analysis.

Conclusion & Outlook

Quantum mechanics is a fascinating subject and in by itself serves as motivation to conduct any study thereof. Measurement theory in quantum mechanics has been a source of interesting and sometimes puzzling questions. It was quite natural to be drawn to it and eventually make it the subject of this thesis. Thanks to the kind of problems that were studied in this development, there has been a shift in the nature of my interest in the subject. While the pursuit to understand it at a technical level continues, there is added appreciation of the intimate connection quantum measurements have with mathematical probability theory in their formulation and with quantum optics in their applications. Both the models considered in the last two chapters are simple, and they admit thorough analysis. There is a lot more ground to cover, and the subject becomes more interesting every time. In the following paragraphs, both the models are once again taken up to emphasize what was achieved in their study and what possible directions one could proceed from them.

Regarding the problems considered in chapter (2), all the solutions were obtained for one dimensional spatial lattices. However, our formulation of the problem is for a general quantum system with a separable Hilbert space. In this formulation, it was shown that repeated measurement protocol under null measurements is equivalently described by a non-Hermitian Hamiltonian. For a quantum particle on a 1D lattice with a detector at one site we then solved the corresponding Schrödinger equation with a complex potential to obtain closed form analytic results for the survival probability and the distribution of first detection time of a particle starting from an arbitrary initial lattice site. Various asymptotic cases were discussed. We then studied the limit of lattice spacing going to 0 to obtain a formulation for the continuum case. For the semi-infinite lattice with a detector at one end, we find that the effective description is in terms of free Schrödinger evolution with complex Robin boundary conditions at the detector site. Again, in this case, we provide analytic results for several objects of interest. The long time asymptotic form of the surviving wave-function was obtained. We find that while the detection time probability density generically decays as $1/t^3$, it is possible to construct special initial states for which the decay is faster. A similar dependence of decay exponent on initial states was observed in a lattice study [TKB18] and it will be interesting to relate these results. Another problem that can be investigated is to precisely describe the physical significance of the measurement parameter ζ in EQ. (2.70) in the half line case. It is conceivable that ζ simultaneously measures the initial momentum/position of the particle. In particular, if one starts with a coherent state with $p_0 = -\Re(\zeta)$ and

$x_0 = -\Im(\zeta)$, one should get a single sharp peak in $F(t)$ or consistent decay depending on how the initial momentum is directed. Here one recalls how the spectrum changes when $\Re(\zeta)$ changes sign. Setting up coherent states on half line geometry in which the origin is accessible to the particle is the main problem to solve.

In chapter (3), we studied the dynamics of a qubit that is continuously monitored via measurements on a detector qubit with which it interacts strongly to avoid the Zeno limit. For the special choice of system Hamiltonian and initial conditions that we considered here, the qubit state remains confined at all times on the yz plane of the Bloch sphere so that it can represented by a single angle variable. The state $|\psi(t)\rangle$ follows a stochastic dynamics with drift and jump terms. We obtained various results for this dynamics. We pointed out that the stochastic wave function dynamics can be naturally interpreted as a resetting process, with a resetting rate that depends on the instantaneous state. The strength of the resetting rate λ quantifies the strength of measurements. We obtain exact results on the number of resetting events, N_t, in a specified time t. We show that the form of the time-dependence, of the mean number of events EQs. (3.53), has a transition at $\lambda = 2$. Using two different approaches, a renewal approach and one based on non-perturbative resolvent (or Green's function) approach, we obtain the exact form of the probability distribution $P(\theta, t)$ for the system to be in the quantum state, $|\theta\rangle = \begin{bmatrix} \cos(\theta/2) \\ \imath \sin(\theta/2) \end{bmatrix}$, at time t. At long times we recovered the steady state form known from earlier studies. We showed that as for the steady state, the time evolution has three different forms for the regimes $0 \leq \lambda < 1$, $\lambda = 1$ and $\lambda > 1$. For the cases $0 \leq \lambda < 1$ and $\lambda = 1$ we evaluated the complete spectrum of the Fokker-Planck operator which forms a bi-orthonormal set. This provides another solution for the time evolution of $P(\theta, t)$, that is especially useful at long times. Despite a few attempts after publication of our result, the problem of spectral resolution for the case $\lambda > 1$ remains unsolved. It may be possible that a few simple things have been overlooked, but it seems more likely that spectral resolution for this case may have to be done in the space of distributions. We note that the average density matrix of the qubit is given by $\hat{\rho}(t) = \int_0^{2\pi} d\theta P(\theta, t) |\theta\rangle\langle\theta|$. We identify this decomposition of the density matrix as the Glauber-Sudarshan P-representation in terms of spin coherent states [Per12]. However, this density matrix contains much less information about the system. For example, in the steady state we have $\hat{\rho}(t) \to (1/2)\hat{I}$, while the distribution of states $P_\infty(\theta)$ is highly non-trivial. The mean number of detector clicks and the complete distribution $P(\theta, t)$ is experimentally accessible using the methods of quantum tomography, and our results could be experimentally verified.

Root locus study for finite lattice

Consider the effective Hamiltonian in EQ. (2.21) for the case $w = \alpha$. The diagonal entries of 2 only shift the spectrum by -2, therefore it is sufficient to consider the matrix

$$
h_N(\alpha) = \begin{bmatrix} -\iota\alpha & -1 & & & & \\ -1 & 0 & -1 & & & \\ & -1 & 0 & -1 & & \\ & & & \ddots & -1 & \\ & & & -1 & 0 \end{bmatrix}_{N \times N}.
$$

With the definition $p_N(\lambda; \alpha) = \mathrm{Det}\,[\lambda \mathbf{1}_N - h_N(\alpha)]$, we first observe that

$$
\mathrm{Det}\,[\lambda \mathbf{1}_N - h_N(\alpha)] = 0 \Leftrightarrow \mathrm{Det}\,[h_N(\alpha) - (-\lambda^*)\,\mathbf{1}_N] = 0.
$$

Therefore, if $\lambda(\alpha)$ is an eigenvalue of $h_N(\alpha)$, then so is $-[\lambda(\alpha)]^*$. Of course, these coincide when λ is purely imaginary. For $2 \leq N$, and $p_1(\lambda; \alpha) = \lambda + \iota\alpha$, the characteristic polynomials satisfy the recursion

$$
\lambda p_N(\lambda; \alpha) = p_{N-1}(\lambda; \alpha) + p_{N+1}(\lambda; \alpha).
$$

It follows from here that if λ is an eigenvalue of $h_N(\alpha)$, then the right eigenvector corresponding to λ is

$$
\begin{bmatrix} p_{N-1}(\lambda; 0) \\ \vdots \\ p_2(\lambda; 0) \\ p_1(\lambda; 0) \\ 1 \end{bmatrix}, \quad (\lambda + \iota\alpha)p_{N-1}(\lambda; 0) = p_{N-2}(\lambda; 0). \tag{A.1}
$$

The N solutions of the equation above $\{\lambda_j(\alpha)\}_{j=1}^N$ are the eigenvalues of $h_N(\alpha)$. For $\alpha = 0$, one has $\lambda_j(0) = 2\cos\varphi_j^N$ where $\varphi_j^N = \left(\dfrac{j\pi}{N+1}\right)$. Also $p_k(\lambda_j; 0) = \dfrac{\sin\left[(k+1)\,\varphi_j^N\right]}{\sin\varphi_j^N}$. For $\alpha \neq 0$, the eigenvalues $\lambda_j(\alpha) = 2\cos\varphi_j^N(\alpha)$ so that the phases φ_j^N in general become functions of α. The form of $\varphi_j^N(\alpha)$ can be taken as

$$
\varphi_j^N(\alpha) = \left(\frac{j\pi}{N+1}\right) + r_j(\alpha) + \iota f_j(\alpha). \tag{A.2}
$$

Here $r_j(\alpha)$ and $f_j(\alpha)$ are real valued functions such that $r_j(0) = f_j(0) = 0$. From equation (A.1) and the form of $p_k(\lambda_j; 0)$ one has,

$$
\cos\left[\varphi_j^N(\alpha)\right] = -\iota\alpha - \cot\left[N\varphi_j^N(\alpha)\right]\sin\left[\varphi_j^N(\alpha)\right].
$$
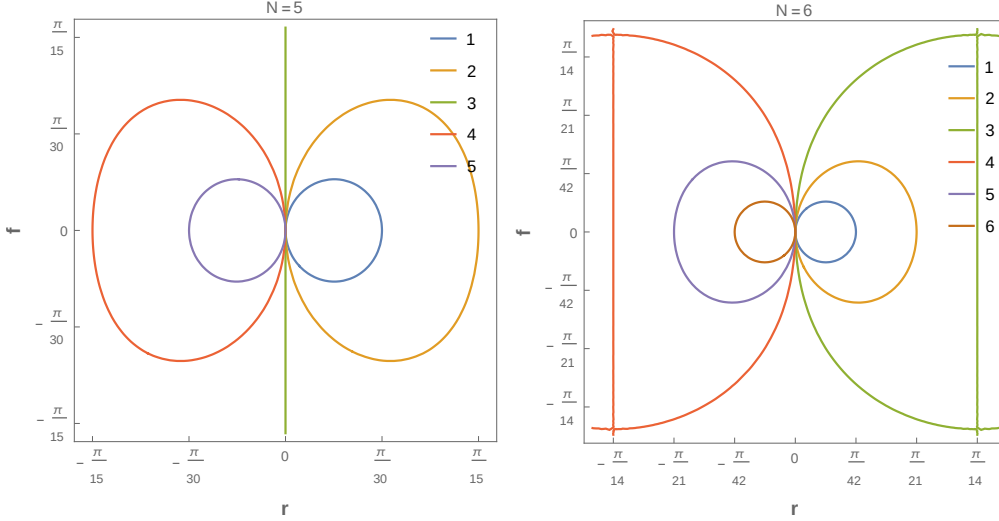
FIGURE 17. Contour Plots of first equation (A.3) for $N = 5$ and $N = 6$.

Upon substituting $\varphi_j^N(\alpha)$ from equation (A.2) in the above and separating the real and imaginary parts, we obtain the equations satisfied by $r_j(\alpha)$ and $f_j(\alpha)$.

$$\cosh(f_j)\cos[(2N+1)x_j] - \cosh[(2N+1)f_j]\cos(x_j) = 0,$$

$$\sinh(f_j)\sin[(2N+1)x_j] - \sinh[(2N+1)f_j]\sin(x_j) = \qquad\text{(A.3)}$$

$$\alpha[\cos(2Nx_j) - \cosh(2Nf_j)]$$

where $x_j = r_j + \varphi_j^N(0)$. The curves defined by the above equations in (r, f) plane can have multiple intersections for a given value of α. As α is continuously varied, these intersection points move continuously, defining various branches of functions $r_j(\alpha)$ and $f_j(\alpha)$. The branch of interest is the one for which $r_j(0) = f_j(0) = 0$. In this regard, we notice that for $\alpha = 0$; $f_j = 0$ and $r_j = 0$ i.e. $(x_j = \frac{j\pi}{N+1})$ is always a solution of equations (A.3), so one knows such a branch exists.

Consider the first of equations (A.3). When N is odd, the line $r_j = 0$ is a solution of the equation for $j = \frac{N+1}{2}$, as can be easily seen by substitution. For real parameter $t \in [0, 1]$, let $r_j(t) = t\frac{j\pi}{N(N+1)}$. Then one has $x_j(t) = j\pi\left[\frac{(1-t)}{N+1} + \frac{t}{N}\right]$ and the equation takes the form

$$\cosh(f_j(t))\cos\left[j\pi\left(-\frac{(1-t)}{N+1} + \frac{t}{N}\right)\right] =$$

$$\cosh[(2N+1)f_j(t)]\cos\left[j\pi\left(\frac{(1-t)}{N+1} + \frac{t}{N}\right)\right]. \qquad\text{(A.4)}$$

For $j \in \{1, \ldots, \frac{N-1}{2}\}$, $f_j(0) = f_j(1) = 0$ and there exist two solutions $f_j(t)$ (because cosh is an even function) for each $t \in (0, 1)$, both of same magnitude and opposite signs. It follows that the contours (r_j, f_j) are closed curves coinciding at $(0, 0)$. The curves are in fact seen to be tangential at $(0, 0)$ when one considers the ratio of cosines appearing in the last equation. For $j \in \{\frac{N+3}{2}, \ldots, N\}$, the same conclusion holds if one takes $r_j(t) = -t\frac{N-j+1}{N(N+1)}\pi$. Figure 17 is a contour plot of the first of EQ. (A.3) for $N = 5$
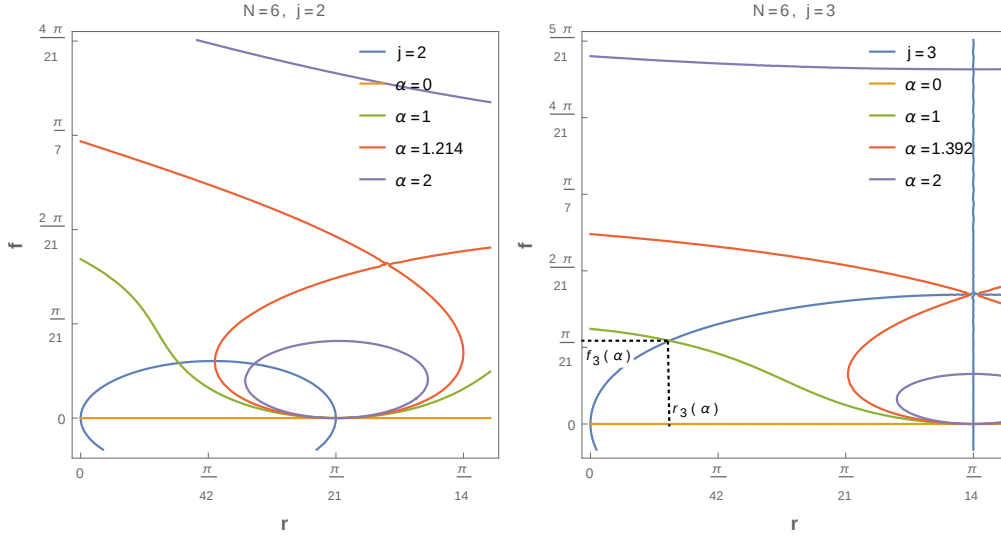
FIGURE 18. Intersection points of the system (A.3) for $N = 6$. The curves corresponding to index j (blue curves) are for the first equation in the system (A.3). Other curves indexed by α are for the second equation in the system (A.3) for various values of α.

and shows the closed curves for $j \in \{1, 2, 4, 5\}$. The $f-$axis is the solution for $j = 3$. Now let N be even. Then $r = \frac{\pi}{2(N+1)}$ and $r = -\frac{\pi}{2(N+1)}$ are solutions of the equation but neither pass through $(0, 0)$. For $j \in \{1, \dots N/2\}$ and $t \in [0, 1]$, $r_j(t) = t\frac{j\pi}{N(N+1)}$ gives required solutions along with equation (A.4). For $j \in \{N/2 + 1, \dots, N\}$ and $t \in [0, 1]$, $r_j(t) = -t\frac{N-j+1}{N(N+1)}\pi$ gives the required solutions. All the contours are closed loops except for $j \in \{N/2, N/2 + 1\}$. These contours come arbitrarily close to the lines $r = \frac{\pi}{2(N+1)}$ and $r = -\frac{\pi}{2(N+1)}$ respectively and in the limit $t \to 1$, they approach $(\pm\frac{\pi}{2(N+1)}, f_j)$ (See Figure 17) with f_j determined from equation (A.4) to be

$$\frac{\cosh\left[(2N + 1) f_j\right]}{\cosh\left(f_j\right)} = 2N + 1, \quad j \in \{N/2, N/2 + 1\}. \tag{A.5}$$

Now consider the second of equations (A.3). The whole of $r-$axis in the (r, f) plane satisfies the equation for $\alpha = 0$. The point $\left(\frac{j\pi}{N} - \frac{j\pi}{N+1}, 0\right)$ in the (r, f) plane satisfies the equation for all α. This point also satisfies the first equation (A.3). Figure 18 shows the intersection points of the System (A.3) for $N = 6$ and $j = 2, 3$ for various values of α. In both cases one observes that at a certain value of α the curve corresponding to the second equation in (A.3) self intersects. For $j \in \{N/2, N/2 + 1\}$ (assuming N is even) the value of $\alpha(= \alpha_c)$ for which this happens can be found from equation (A.3) using the fact that $x_j = \pm\frac{\pi}{2}$ and that f_j satisfies equation (A.5).

$$\alpha_c = \frac{\cosh\left[(N + 1) f_j\right]}{\sinh\left[N f_j\right]}. \tag{A.6}$$

As an example, consider the case $N = 2$ for which EQs. (A.5,A.6) read

$$\frac{\cosh(5f)}{\cosh(f)} = 5, \qquad \alpha_c = \frac{\cosh(3f)}{\sinh(2f)}$$

whose solution gives $\alpha_c = 2$. It is easily checked that the matrix

$$h_2(2) = \begin{bmatrix} -\imath 2 & -1 \\ -1 & 0 \end{bmatrix}.$$

is not diagonalizable.

Further notice that for $j \in \{1, \ldots, N/2 - 1, N/2 + 2, \ldots, N\}$, f_j increases with α to a maximum value, after which it goes to 0 as $\alpha \to \infty$. For $j \in \{N/2, N/2+1\}$, f_j increases to a maximum value defined by equation (A.5) and for $\alpha > \alpha_c$, $r_j(\alpha)$ remains constant $(= \frac{N\pi}{2(N+1)})$ while f_j is two-valued, with one value approaching 0 and the other escaping to $+\infty$. Similar statements remain true when N is odd, except that $r_{\frac{N+1}{2}} = 0$ for all α and $f_{\frac{N+1}{2}}$ goes to $+\infty$.

The following picture emerges for the eigenvalue $\lambda_j(\alpha)$. Starting with an odd value of N, $-2 < \lambda_j(0) < 2$ with $\lambda_{\frac{N+1}{2}} = 0$. When α increases, the eigenvalues move in the complex plane with $\lambda_{\frac{N+1}{2}}(\alpha)$ remaining on the negative imaginary axis. Other eigenvalues acquire negative imaginary components. Each of the eigenvalues attains a minimum imaginary component after which it starts to move towards the real axis, however $\lambda_{\frac{N+1}{2}}(\alpha)$ continues to go further down the imaginary axis. In the limit $\alpha \to \infty$, $\lambda_{\frac{N+1}{2}}(\alpha)$ has departed to $-\imath\infty$ while the rest have returned to the real axis, occupying the eigenvalues corresponding to the hamiltonian $h_{N-1}(0)$. Starting with an even value of N, similar trajectories are followed by the eigenvalues in the complex plane. However $\lambda_{\frac{N}{2}}(\alpha_c) = \lambda_{\frac{N}{2}+1}(\alpha_c)$, i.e. these eigenvalues merge and upon further increasing α, one eigenvalue moves along the negative imaginary axis towards the origin and the other goes to $-\imath\infty$. Eventually, the remaining eigenvalues have returned to the real axis, occupying the eigenvalues corresponding to the hamiltonian $h_{N-1}(0)$. Figure 19 shows the spectrum of H_N for different values of α. In case of $\alpha = 2$, we observe an isolated point of the spectrum at around $\lambda_p = -1.5\imath$ for both $N = 50$ and $N = 100$.

The equations (A.3) can be also used to evaluate α_c and the isolated part of the spectrum observed in Figure 19 in the limit $N \to \infty$. As one expects to observe the same behaviour whether N goes to ∞ through odd or even values, it is simple to consider equations (A.3) for odd N and $j = \frac{N+1}{2}$. Here $r_{\frac{N+1}{2}}(\alpha) = 0$ for which the first of equations (A.3) is identically 0. Letting $f_{\frac{N+1}{2}}$ be denoted simply by f_N, the second equation takes the form

$$\tanh(f_N) + \tanh(Nf_N) = \alpha \operatorname{sech}(f_N).$$

For a given value of α, the solutions of the above equation define a decreasing sequence f_N where $f_N > 0$ by construction. Thus, this sequence has a limit, i.e. $\lim_{N\to\infty} f_N = f_\infty$ exists. For $\alpha \in [0, 1]$, $f_\infty = 0$ for otherwise, the left hand side of the equation tends to a quantity greater than 1 in the limit while the RHS approaches a value less than 1. Thus, for $\alpha \in [0, 1]$, $f_\infty = 0$ and $\lim_{N\to\infty} \tanh(Nf_N) = \alpha$. For $\alpha > 1$, $Nf_N \to \infty$ and in the limit, the equation becomes

$$\tanh(f_\infty) + 1 = \alpha \operatorname{sech}(f_\infty)$$
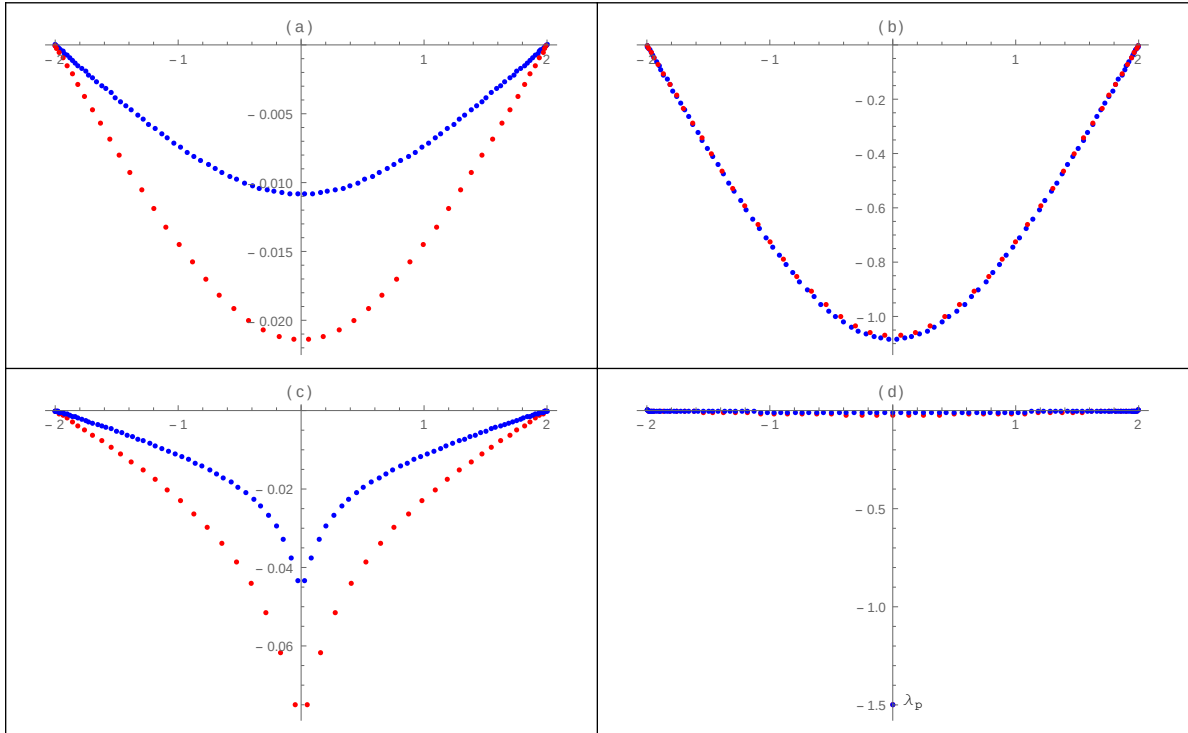
FIGURE 19. Spectrum of $H_N(\alpha)$. Red corresponds to $N = 50$ and Blue corresponds to $N = 100$. (a) $\alpha = 1/2$. (b) $\alpha = 1/2$ with imaginary parts of eigenvalues scaled by N. (c) $\alpha = 1$. (d) $\alpha = 2$.

$$\Rightarrow 2\sinh\left(f_\infty\right) = \frac{\alpha^2 - 1}{\alpha}.$$

Because $\lambda_p(\alpha) = 2\cos\varphi_j^N(\alpha) = -\imath 2\sinh\left(f_\infty\right)$, one concludes

$$\alpha_c = 1, \ \lambda_p = -\imath\left(\alpha - \frac{1}{\alpha}\right). \tag{A.7}$$

Computations to estimate survival probability

B.1. Calculation of integrals

We compute here the quantity

$$Z(w, n_0) = \imath \frac{\dfrac{2}{\pi} \displaystyle\int_0^\pi dk \, \dfrac{\sin(k)\sin(n_0 k)}{\imath s - 2(1 - \cos(k))}}{1 + \imath \dfrac{2w}{\pi} \displaystyle\int_0^\pi dk \, \dfrac{\sin^2 k}{\imath s - 2(1 - \cos(k))}} \tag{B.1}$$

where $w = \alpha + \imath\beta$. We will assume that $s \in \mathbb{C}$ satisfies $\Im(s) \neq -2$ and $s \notin \imath\mathbb{R}$.

The integral above can be evaluated by means of contour integration. We first note that

$$\int_0^\pi dk \, \frac{\sin(k)\sin(n_0 k)}{\imath s - 2(1 - \cos(k))} = \frac{1}{8}\Big[-I_{n_0+1}(s) + I_{n_0-1}(s)$$

$$+ I_{-n_0+1}(s) - I_{-n_0-1}(s)\Big]$$

where

$$I_n(s) = \int_{-\pi}^\pi dk \, \frac{\exp(\imath n k)}{\imath s - 2(1 - \cos(k))}$$

$$= -\imath \int_{\mathcal{C}} dz \, \frac{z^n}{z^2 - (2 - \imath s)z + 1}.$$

The integration contour $\mathcal{C}$ in the second integral above is the unit circle. It is easily seen that $I_n(s) = I_{-n}(s)$ so that we need only to compute $I_n(s)$ for $n \geq 0$. The poles of the integrand are

$$z_\pm(s) = \imath\theta_\pm\left(\frac{s}{2} + \imath\right)$$

where

$$\theta_\pm(z) = -z \pm \sqrt{z^2 + 1}. \tag{B.2}$$

We need first to know the positions of these poles with respect to $\mathcal{C}$.

These two functions are well-defined analytic functions in the subdomain Ω, defined as the complex plane $\mathbb{C}$ where the imaginary axis has been removed apart from the open segment of the imaginary axis between $-\imath$ and $\imath$. We claim that $|\theta_+(z)| < 1$ and $|\theta_-(z)| > 1$ for $z \in \Omega_+ = \Omega \bigcap \{z \in \mathbb{C} : \Re(z) > 0\}$ and $|\theta_+(z)| > 1$ and $|\theta_-(z)| < 1$ for $z \in \Omega_- = \Omega \bigcap \{z \in \mathbb{C} : \Re(z) < 0\}$. Since the proof of the two claims are similar, we only prove the first one. Notice that $\theta_\pm$ are analytic on the connected set Ω_+ and satisfy

$$\theta_+(z) \cdot \theta_-(z) = -1, \quad \frac{\theta_+(z) + \theta_-(z)}{2} = -z.$$

Consider $z \in \Omega_+$. If $\theta_+(z)$ or $\theta_-(z)$ belonged to $\mathcal{C}$, then both would be because of the first relation above. It would then follow that $z = -\imath \sin\left[\arg(\theta_+(z))\right]$ which is excluded since $z \in \Omega_+$. A similar ad-absurdio argument shows that $\theta_-(z)$ and $\theta_+(z)$ do not belong to the imaginary axis. Since $\theta_\pm$ are analytic on the connected set Ω_+, so is $\theta_\pm(\Omega_+)$. The imaginary axis being excluded from $\theta_\pm(\Omega_+)$, the domains $\theta_\pm(\Omega_+)$ are included into $\{z \in \mathbb{C}; \Re(z) > 0\}$ or into $\{z \in \mathbb{C}; \Re(z) < 0\}$. Since $\theta_+(1) = \sqrt{2} - 1 > 0$ and $\theta_-(1) = -\sqrt{2} - 1 < 0$ we get $\theta_+(\Omega_+) \subset \{z \in \mathbb{C}; \Re(z) > 0\}$ and $\theta_-(\Omega_+) \subset \{z \in \mathbb{C}; \Re(z) < 0\}$. Similarly, since $\theta_\pm(\Omega_+) \bigcap \mathcal{C} = \emptyset$ the domains $\theta_\pm(\Omega_+)$ are included into the interior of the unit disc or into the exterior of the unit disc. The values above of $\theta_\pm(1)$ imply that $\theta_+(\Omega_+)$ is included in the interior of unit disc and $\theta_-(\Omega_+)$ is included in the exterior of unit disc. Hence, we have that that if $\Re(s) > 0$, the pole inside the unit disc is $z_+(s)$.

It follows by the Residues Theorem that

$$I_n(s) = -\imath\pi \frac{[z_+(s)]^n}{\sqrt{\left(\frac{s}{2} + \imath\right)^2 + 1}}, \quad \Re(s) > 0. \tag{B.3}$$

This gives

$$\int_0^\pi dk \, \frac{\sin(k)\sin(n_0 k)}{\imath s - 2(1 - \cos k)} = -\frac{\pi}{2}[z_+(s)]^{n_0}, \quad \Re(s) > 0. \tag{B.4}$$

From EQ. (B.1) and EQ. (B.4)

$$Z(w, n_0) = -\imath \frac{[z_+(s)]^{n_0}}{1 - \imath w[z_+(s)]}, \quad \Re(s) > 0. \tag{B.5}$$

B.2. Expression of ψ_1 in terms of Bessel functions of first kind

The Laplace transform for ψ_1 can be expressed as

$$[\mathcal{L}\psi_1](s) = -\imath^{n_0+1}\chi\left(\frac{s}{2} + \imath\right)$$

where

$$\chi(z) = \frac{[\theta_+(z)]^{n_0}}{1 + w\theta_+(z)}$$

with the function $\theta_\pm$ defined in EQ. (B.2). We recall that this function is analytic in the subdomain Ω, defined as the complex plane $\mathbb{C}$ where the imaginary axis has been removed apart from the open segment of the imaginary axis between $-\imath$ and $\imath$. Moreover, we have seen that

$$\Re(z) > 0 \quad \text{implies} \quad |\theta_+(z)| < 1, \quad |\theta_-(z)| > 1.$$

Let us first identify $\chi(z)$ as the Laplace transform $[\mathcal{L}f](z)$ of some explicit function f. It is known that if $z \in \mathbb{C}$ satisfies $\Re(z) > 0$, then

$$\int_0^\infty dt \, e^{-zt} \frac{J_k(t)}{t} = \frac{(\theta_+(z))^k}{k}.$$

Assuming that z is such that $|w\theta_+(z)| < 1$ we have then that

$$\chi(z) = \sum_{k=0}^{\infty}(-w)^k[\theta_+(z)]^{n_0+k}$$

$$= \sum_{k=0}^{\infty}(k+n_0)(-w)^k\int_0^{\infty}dt\,e^{-zt}\frac{J_{k+n_0}(t)}{t}$$

$$= \int_0^{\infty}dt\,e^{-zt}f(t)dt = [\mathcal{L}f](z)$$

with

$$f(t) = \sum_{k=0}^{\infty}(k+n_0)(-w)^k\frac{J_{k+n_0}(t)}{t}.$$

The interchange of the sum and the integral is justified, since $J_k(2t) \sim (2\pi k)^{-1/2}(et/k)^k$ for large k. It follows that for any time $t \geq 0$

$$\psi_1(t) = -2i^{n_0+1}e^{-2it}\sum_{k=0}^{\infty}(k+n_0)(-w)^k\frac{J_{k+n_0}(2t)}{2t}$$

since the functions above have their Laplace transform coinciding on $\{s \in \mathbb{C}\,;\,\Re(s) > \sigma\}$ for some $\sigma > 0$ sufficiently large.

Computations related to half line

This appendix details some of the calculations necessary for the results in sec. (2.3.1)

C.1. Asymptotic form of the wave function on the half line

We seek the saddle point approximation of

$$\Psi(x,t) = \int_0^\infty dk\, c(k)\, \eta^k(x)\, \exp(-\imath\, k^2 t)$$

$$= \frac{\imath}{\sqrt{2\pi}}\left[\int_0^\infty dk\, c(k)\frac{(1-\imath\zeta k)e^{\imath kx - \imath k^2 t}}{\sqrt{1+\zeta^2 k^2}} - \int_0^\infty dk\, c(k)\frac{(1+\imath\zeta k)e^{-\imath kx - \imath k^2 t}}{\sqrt{1+\zeta^2 k^2}}\right]$$

$$= \frac{\imath}{\sqrt{2\pi}}\int_{-\infty}^\infty dk\, c(k)\frac{(1-\imath\zeta k)}{\sqrt{1+\zeta^2 k^2}} e^{\imath t(k\frac{x}{t} - k^2)},$$

where we used the fact that $c(-k) = -c(k)$. We now use the following result [Mil06]:
Let $g(k)$ be complex valued, $I(k)$ be real valued functions of the real variable k. Let $t > 0$ and define the integral

$$F(t) = \int_{-\infty}^\infty dk\, g(k)\, e^{\imath t\, I(k)}.$$

If k_0 is a stationary point of $I(k)$ such that $\left[\frac{dI(k)}{dk}\right]_{k=k_0} = I'(k_0) = 0$ and $\left[\frac{d^2 I(k)}{dk^2}\right]_{k=k_0} = I''(k_0) \neq 0$ then for large t, the contribution to $F(t)$ from k_0 is

$$\left[\frac{2\pi}{t\,|I''(k_0)|}\right]^{1/2} g(k_0) e^{\imath t\, I(k_0) + \imath\frac{\mathrm{sign}(I''(k_0))\pi}{4}} + o(t^{-1/2}).$$

In the current case,

$$g(k) = c(k)\frac{(1-\imath\zeta k)}{\sqrt{1+\zeta^2 k^2}} \quad \& \quad I(k) = k\frac{x}{t} - k^2.$$

We get a unique saddle point at $k_0 = x/(2t)$ and this then gives

$$[\Psi(x,t)]_{t\gg 1} \asymp \frac{\imath}{\sqrt{2t}} c\left(\frac{x}{2t}\right) \sqrt{\frac{1-\imath\zeta\frac{x}{2t}}{1+\imath\zeta\frac{x}{2t}}} e^{\imath\left(\frac{x^2}{4t} - \frac{\pi}{4}\right)}. \tag{C.1}$$

C.2. First passage time distribution on the half line

Recall EQ. (2.76) giving the expression of the solution of the Schrödinger equation on the half-line with complex Robin boundary condition and initial condition $\Psi_0(x) = \Psi(x,0)$. To simplify, we assume that Ψ_0 has compact support and has a bounded derivative defined almost everywhere. In particular, all the moments of Ψ_0 and $\frac{\partial\Psi_0}{\partial x}$ are

well-defined. After a change of variables, we can write $\Psi(0,t)$ as

$$\Psi(0,t) = \sqrt{\frac{2}{\pi}} \frac{\zeta}{t} \int_0^\infty dy \, \frac{y}{\sqrt{1 + \frac{\zeta^2}{t} y^2}} c\left(\frac{y}{\sqrt{t}}\right) \exp\left(-\imath y^2\right)$$

$$+ \sqrt{\frac{2}{\zeta}} c_b \exp\left(\imath \frac{t}{\zeta^2}\right),$$

where

$$c(k) = -\sqrt{\frac{2}{\pi(1 + \zeta^2 k^2)}} k \, H(k),$$

$$H(k) = \int_0^\infty dx \underbrace{\left[\Psi_0(x) + \zeta \frac{\partial \Psi_0}{\partial x}(x)\right]}_{\Phi(x)} \frac{\sin(k\,x)}{k}.$$

Up to factors, $H(k)$ is the sine transform of $\Phi(x)$. If $H(k)$ were to vanish identically, then $\Phi(x) \equiv 0$ and $\Psi_0(x)$ would correspond to the bound state. In this situation $\Psi(0,t)$ evolves solely by the second term and the first passage time distribution $F(t)$ defined by EQ. (2.81) has exponential decay for ζ lying in the fourth quadrant.

Assume $H(k)$ is not identically 0. Substituting for $c(k)$ one has

$$\Psi(0,t) \approx -\frac{2}{\pi} \frac{\zeta}{t^{\frac{3}{2}}} \int_0^\infty dy \, \frac{y^2}{1 + \frac{\zeta^2}{t} y^2} H\left(\frac{y}{\sqrt{t}}\right) \exp\left(-\imath y^2\right)$$

where the exponentially decaying term is neglected. By expanding $\sin(k\,x)$, and switching [1] the summation and integration for $\Phi(x)$ one can obtain an absolutely convergent series expansion for $H\left(\frac{y}{\sqrt{t}}\right)$. We get that

$$\begin{aligned}
H\left(\frac{y}{\sqrt{t}}\right) &= \sum_{s=0}^\infty \frac{(-1)^s}{t^s} \frac{y^{2s}}{(2s+1)!} \int_0^\infty dx \, x^{2s+1} \Phi(x) \\
&= \sum_{s=0}^\infty \frac{(-1)^s}{t^s} \frac{y^{2s}}{(2s+1)!} \left[M_{2s+1} - (2s+1)\zeta M_{2s}\right]
\end{aligned} \tag{C.2}$$

where $M_s = \int_0^\infty x^s \Psi_0(x) \, dx$ the sth moment of Ψ_0. In the second line, we perform an integration by parts. This allows us to finally write down the series

$$\Psi(0,t) \approx -\frac{2}{\pi} \frac{\zeta}{t^{\frac{3}{2}}} \left[\sum_{s=0}^\infty \frac{(-1)^s}{(2s+1)! \, t^s} M_{2s+1} \left(1 - \frac{\zeta}{\zeta_s}\right) I_s\left(\frac{\zeta}{\sqrt{t}}\right)\right] \tag{C.3}$$

where

$$I_s(z) = \int_0^\infty dy \, \frac{y^{2s+2}}{1 + z^2 y^2} \exp(-\imath y^2) \tag{C.4}$$

and

$$\zeta_s = \frac{1}{2s+1} \frac{M_{2s+1}}{M_{2s}} \tag{C.5}$$

---

[1] The switching is justified since Ψ_0 has compact support so that the moments of Φ grow at most geometrically.

with the convention that $\zeta_s = \infty$ if $M_{2s} = 0$. Noting that

$$\lim_{z \to 0} I_0(z) = -\frac{\sqrt{\pi}}{4} e^{\frac{\imath\pi}{4}} \quad \text{and} \quad \lim_{z \to 0} I_1(z) = -\frac{3\sqrt{\pi}}{8} e^{-\frac{\imath\pi}{4}}$$

one has then for large t,

$$\Psi(0,t) = \frac{1}{2\sqrt{\pi}} \frac{\zeta}{t^{\frac{3}{2}}} \left[\left(1 - \frac{\zeta}{\zeta_0}\right) M_1 e^{\frac{\imath\pi}{4}} - \left(1 - \frac{\zeta}{\zeta_1}\right) \frac{M_3}{4t} e^{-\frac{\imath\pi}{4}} \right] \tag{C.6}$$
$$+ O(t^{-5/2}).$$

This proves EQ. (2.83).

Consider the state

$$\Psi_0(x) = \Theta(x - 2) - \frac{\Theta(x-1) + \Theta(x-3)}{2} \tag{C.7}$$
$$+ \imath \frac{\Theta(x-1) - \Theta(x-3)}{2}$$

where $\Theta(x)$ is the Heaviside step function. Then

$$M_1 = \frac{1}{2} + 2\imath, \quad \zeta_0 = 2 - \frac{\imath}{2}$$

$$M_3 = \frac{25}{4} + 10\imath, \quad \zeta_1 = \frac{67}{82} - \frac{17i}{164}.$$

The numerical evaluation of the integral in EQ. (2.76) can be performed to obtain $\Psi(0,t)$. We choose the range $t \in (200, 750)$ which is sufficient to suppress the bound state contribution in EQ. (2.76). To begin with, let $\zeta = 1 - \imath$. Then ζ is at a sufficient distance from ζ_0 and the first term in the expansion EQ. (C.6) dominates. Therefore, one has as $t \to \infty$ that

$$F_3(t) = -2 \frac{\Im(\zeta)}{|\zeta|^2} |\Psi(0,t)|^2 \sim \frac{5}{8\pi t^3}.$$

We use this analytic estimate to compare with the numerical evaluation via EQ. (2.76) in Fig (20). This shows that the analytic estimate is quite good and indeed $F(t) \sim \frac{1}{t^3}$.

Now choose $\zeta = \zeta_0$. Doing so causes the first term in the expansion EQ. (C.6) to drop out. The estimate for $F(t)$ is obtained from EQ. (C.6) which gives

$$F_5(t) \asymp -\frac{\Im(\zeta_0)}{32\pi t^5} \left| M_3 \left(1 - \frac{\zeta_0}{\zeta_1}\right) \right|^2 = \frac{5105}{1024} \frac{1}{\pi t^5}.$$

The figure (20) shows good agreement of the above estimate with numerical values. We could now claim that if $\Psi_0(x)$ was so constructed that

$$\zeta_0 = \zeta_1 = \cdots = \zeta_{s-1} \neq \zeta_s (\neq 0)$$

then one has

$$F(t; \zeta = \zeta_0) \sim \frac{1}{t^{3+2s}}$$
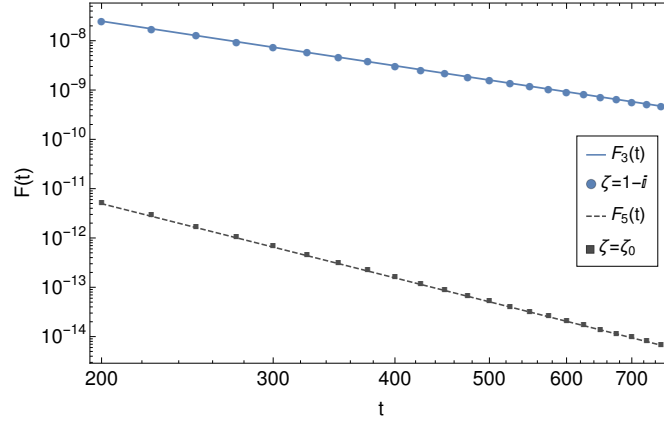
FIGURE 20. Plot comparing numerical estimates of $F(t)$ with $F_3(t)$ (resp. $F_5(t)$) for $\zeta = 1-\imath$ (resp. $\zeta(=\zeta_0) = 2-\imath/2$). The discrete points correspond to numerical values evaluated from EQ. (2.76)

.

while for other choices of ζ one has,

$$F(t, \zeta \neq \zeta_0) \sim \frac{1}{t^3}.$$

This is under the assumption that the moments $\int_0^\infty x^k \Psi_0(x)\,dx$ do not vanish up until $k = 2s+1$. Lastly, we note that for the normalized state

$$\Psi_0(x) = \sqrt{\frac{1}{\zeta_0} + \frac{1}{\zeta_0^*}}\, \exp\left(-\frac{x}{\zeta_0}\right)$$

with ζ_0 in the fourth quadrant, $\zeta_s = \zeta_0$ for all s follows from EQ. (C.5). For the measurement parameter $\zeta = \zeta_0$, the estimate in EQ. (C.3) is identically 0 and $F(t)$ falls exponentially, as has already been noted.

Master equations for indirect measurements

D.1. Lindblad equation for blind measurements

EQ. (3.18) will be derived by taking the limit $\tau \to 0$ for the evolution equation for the density matrix in the discrete time model described in sec. (3.1.1). Suppose the state density matrix for $\mathcal{S}$ at the time t is $\rho(t)$. The system is now coupled to the probe whose density matrix is $\sigma(= |\chi_0\rangle\langle\chi_0|)$. The density matrix of the entire system is the uncorrelated matrix

$$R(t) := \rho(t) \otimes \sigma.$$

Post interaction via the Hamiltonian in EQ. (3.5), the state becomes

$$R(t + \tau) = \exp\big[-\imath\tau H \big] R(t) \exp\big[\imath\tau H \big].$$

The density matrix of $\mathcal{S}$ is recovered from the above as

$$\rho(t + \tau) = \mathbf{tr}_{\mathcal{D}} R(t + \tau) = \langle\chi_0|R(t+\tau)|\chi_0\rangle + \langle\chi_1|R(t+\tau)|\chi_1\rangle.$$

From the form of H, the following relations can be inferred.

$$\langle\chi_0|R(t+\tau)|\chi_0\rangle = \rho(t) - \imath\tau\big[H_{\mathcal{S}}, \rho(t)\big] - \frac{\gamma\tau}{2}\big\{\rho(t), \pi_1\big\} + \mathcal{O}(\tau^2),$$
$$\langle\chi_1|R(t+\tau)|\chi_1\rangle = \gamma\tau\pi_1 \rho(t) \pi_1 + \mathcal{O}(\tau^{3/2}). \tag{D.1}$$

It follows from the above that

$$\frac{\rho(t+\tau) - \rho(t)}{\tau} = -\imath\big[H_{\mathcal{S}}, \rho(t)\big] + \gamma\pi_1 \rho(t) \pi_1 - \frac{\gamma}{2}\big\{\rho(t), \pi_1\big\} + \mathcal{O}(\tau^{1/2}).$$

Taking the limit $\tau \to 0$ for the case of continuous measurement, one obtains EQ. (3.18).

D.2. Derivation of the forward PIDE

The probability density $P(\theta, t)$ satisfies a generalized Fokker-Planck equation, stated in EQ. (3.38). In order to derive this, suppose $f(\theta)$ is a real-valued 2π periodic function. θ_t is a stochastic process governed by the SDE EQ. (3.36). If N_t has no jumps in the time interval $[t, t + dt]$, then $d\theta_t = \Omega(\theta_t)dt$ and

$$df = \Omega(\theta_t)\left(\frac{\partial f}{\partial\theta}\right)_t dt.$$

If N_t has a jump at t, then $d\theta_t = \pi - \theta_{t-}$. It follows that

$$df = f(\theta_{t-} + (\pi - \theta_{t-})) - f(\theta_{t-})$$
$$\Rightarrow df = f(\pi) - f(\theta_{t-}).$$

Thus, the Ito formula for the differential can be written compactly as

$$df = \Omega(\theta_t) \left(\frac{\partial f}{\partial \theta} \right)_t dt + [f(\pi) - f(\theta_{t-})] \, dN_t.$$

We rewrite the Ito formula as,

$$df = \left[\Omega(\theta_t) \left(\frac{\partial f}{\partial \theta} \right)_t + [f(\pi) - f(\theta_{t-})] \gamma \sin^2 \frac{\theta_t}{2} \right] dt + [f(\pi) - f(\theta_{t-})] \left[dN_t - \gamma \sin^2 \frac{\theta_t}{2} dt \right]$$

$$(D.2)$$

which has the advantage that the second summand in the r.h.s. has as a factor the differential of a compensated martingale [**Bjö21**, **Bré81**]. Integrating the above equation, taking expectation w.r.t. $P(\theta,t)$ and changing the order of integration in the r.h.s, one obtains

$$\int_0^{2\pi} f(\theta)P(\theta,t)d\theta - f(\theta_0) = \int_0^t \left(\int_0^{2\pi} \left[\Omega(\theta) \left(\frac{\partial f}{\partial \theta} \right) + [f(\pi) - f(\theta)] \gamma \sin^2 \frac{\theta}{2} \right] P(\theta,s)d\theta \right) ds.$$

EQ. (3.38) follows after differentiating the above equation w.r.t. t and integrating by parts in the first integral on the r.h.s.

D.3. Verification of solution for the PIDE

For the PIDE (3.38), noted here

$$\frac{\partial P(\theta,t)}{\partial t} = -\frac{\partial}{\partial \theta}[\Omega(\theta)P(\theta,t)] - \gamma \sin^2 \left(\frac{\theta}{2} \right) P(\theta,t) + \gamma \delta(\theta - \pi) \int_0^{2\pi} \sin^2 \left(\frac{\theta'}{2} \right) P(\theta',t) \, d\theta',$$

the solution proposed in EQ. (3.66) is

$$P(\theta,t) = P_0^t[0||0]\delta(\theta - \theta_t(0,0)) + \int_0^t \overline{\alpha}_{t-\tau} P_0^\tau[0||\pi] \, \delta(\theta - \theta_\tau(0,\pi)) \, d\tau. \qquad (D.3)$$

For reference, also note

$$P_0^t[0||\theta_0] = \frac{\Omega(\theta_0)}{\Omega(\theta_t(0,\theta_0))} e^{-\frac{\gamma t}{2}}, \qquad \frac{\partial}{\partial t} P_0^t[0||\theta_0] = -\gamma \sin^2 \frac{\theta_t(0,\theta_0)}{2} P_0^t[0||\theta_0]. \qquad (D.4)$$

Denote $\overline{\alpha}_{t-\tau} = \overline{\alpha}(t,\tau)$, so that one has (from EQ. (3.54)) $\frac{\partial}{\partial t}\overline{\alpha}(t,\tau) = -\frac{\partial}{\partial \tau}\overline{\alpha}(t,\tau)$. Also notice, $\overline{\alpha}(t,t) = 0$. From the Leibniz rule, one obtains

$$\frac{\partial P(\theta,t)}{\partial t} = \frac{\partial}{\partial t} \left[P_0^t[0||0] \, \delta(\theta - \theta_t(0,0)) \right] - \int_0^t \frac{\partial \overline{\alpha}(t,\tau)}{\partial \tau} P_0^\tau[0||\pi] \, \delta(\theta - \theta_\tau(0,\pi)) \, d\tau.$$

Integrating by parts in the RHS, one has

$$\frac{\partial P(\theta,t)}{\partial t} = \frac{\partial}{\partial t} \left[P_0^t[0||0] \, \delta(\theta - \theta_t(0,0)) \right] + \int_0^t \overline{\alpha}(t,\tau) \frac{\partial}{\partial \tau} \left[P_0^\tau[0||\pi] \, \delta(\theta - \theta_\tau(0,\pi)) \right] d\tau$$

$$+ \gamma \delta(\theta - \pi) \int_0^{2\pi} \sin^2 \frac{\varphi}{2} P(\varphi,t) \, d\varphi$$

Upon carrying out the differentiation in the RHS of the above, using EQ. (D.4) one can express

$$\frac{\partial P(\theta, t)}{\partial t} = F_1(\theta, t) - F_2(\theta, t) + \gamma \delta(\theta - \pi) \int_0^{2\pi} \sin^2 \frac{\varphi}{2} P(\varphi, t) \, d\varphi,$$

where the distributions

$$F_1(\theta, t) = P_0^t[0||0] \, \frac{\partial}{\partial t} \delta(\theta - \theta_t(0,0)) + \int_0^t \overline{\alpha}(t, \tau) \, P_0^\tau[0||\pi] \, \frac{\partial}{\partial \tau} \delta(\theta - \theta_\tau(0, \pi)) \, d\tau,$$

$$F_2(\theta, t) = \gamma \sin^2 \frac{\theta_t(0,0)}{2} P_0^t[0||0] \, \delta(\theta - \theta_t(0,0))$$
$$+ \int_0^t \overline{\alpha}(t, \tau) \, \gamma \sin^2 \frac{\theta_\tau(0, \pi)}{2} \, P_0^\tau[0||\pi] \, \delta(\theta - \theta_\tau(0, \pi)) \, d\tau.$$

In the sense of distributions, the following equivalence holds in view of EQ. (D.3)

$$F_2(\theta, t) \equiv \gamma \sin^2 \frac{\theta}{2} \, P(\theta, t).$$

The proof will be complete if one shows the following equivalence

$$F_1(\theta, t) \equiv -\frac{\partial}{\partial \theta} [\Omega(\theta) P(\theta, t)].$$

To show this, consider a 2π periodic differentiable function $f(\theta)$. Then one has

$$-\int_0^{2\pi} f(\theta) \frac{\partial}{\partial \theta} [\Omega(\theta) P(\theta, t)] d\theta = \int_0^{2\pi} \left[\Omega(\theta) \frac{\partial f(\theta)}{\partial \theta}\right] P(\theta, t) \, d\theta = \mathbb{E}[\Omega f'](t).$$

Further, one has

$$\frac{\partial}{\partial t} \delta(\theta - \theta_t) = \Omega(\theta_t) \frac{\partial}{\partial \theta_t} \delta(\theta - \theta_t) = \Omega(\theta_t) \, \delta(\theta - \theta_t) \frac{\partial}{\partial \theta}.$$

From the above property, it follows that

$$\int_0^{2\pi} F_1(\theta, t) \, f(\theta) \, d\theta = \int_0^{2\pi} \left(\Omega(\theta_t(0,0)) P_0^t[0||0] \, \delta(\theta - \theta_t(0,0)) \frac{\partial f(\theta)}{\partial \theta}\right.$$
$$\left. + \int_0^t \overline{\alpha}(t, \tau) \, \Omega(\theta_\tau(0, \pi)) P_0^\tau[0||\pi] \, \delta(\theta - \theta_\tau(0, \pi)) \frac{\partial f(\theta)}{\partial \theta} d\tau \right) d\theta$$
$$= \mathbb{E}[\Omega f'](t).$$

This shows the required equivalence and the proof is complete.

Furthermore, $P(\theta, t)$ should satisfy the normalization condition $\int_0^{2\pi} P(\theta, t) \, d\theta = 1 \, \forall t \geq 0$. For $P(\theta, t)$ given by EQ. (D.3), this amounts to showing

$$P_0^t[0||0] + \int_0^t \overline{\alpha}_{t-\tau} P_0^\tau[0||\pi] \, d\tau = 1. \tag{D.5}$$

For various values of the measurement strength λ, the above can be shown using EQs. (D.3, 3.54) by a simple integration.

Computations for indirect measurements

E.1. Laplace transform of the MGF

Consider the case $\lambda < 1$. Define the function

$$g(t, \phi) = \sin^2(\beta\gamma_0 t - \phi)$$

so that from EQs. (3.44 , 3.30, 3.31 and 3.45), one has

$$P_0^t[0] = \frac{e^{-\frac{\gamma t}{2}}}{\beta^2} \left[g(t, 0) + g(t, -\phi) \right],$$

$$P_0^t[n] = \frac{\gamma^n e^{-\frac{\gamma t}{2}}}{\beta^{2n+2}} \int_0^t dt_n \left[g(t - t_n, 0) + g(t - t_n, \phi) \right] \left[\prod_{k=n-1}^{1} \int_0^{t_{k+1}} dt_k \, g(t_{k+1} - t_k, \phi) \right] g(t_1, 0). \tag{E.1}$$

$P_0^t[n]$ has been expressed as a convolution. For the function $g(t, \phi)$, the Laplace transform is

$$\hat{g}_\phi(\sigma) = \int_0^\infty e^{-(\sigma + \frac{\gamma}{2})t} g(t, \phi) dt$$

$$= \frac{1}{2} \left[\frac{1}{\sigma + \frac{\gamma}{2}} - \frac{(\sigma + \frac{\gamma}{2}) \cos(2\phi) + 2\beta\gamma_0 \sin(2\phi)}{(\sigma + \frac{\gamma}{2})^2 + 4\beta^2\gamma_0^2} \right]. \tag{E.2}$$

From EQs. (3.46, E.1) and standard properties of Laplace transform, one has

$$(\mathfrak{L}\mathbb{E}[e^{-sN_t}])(\sigma, s) = \int_0^\infty e^{-\sigma t} \left(\sum_{n \geq 0} e^{-ns} P_0^t[n] \right) dt \tag{E.3}$$

$$= \frac{1}{\beta^2} \left[\hat{g}_{-\phi} + \hat{g}_0 + \frac{\gamma e^{-s}}{\beta^2} \frac{\hat{g}_0[\hat{g}_0 + \hat{g}_\phi]}{1 - \frac{\gamma e^{-s}}{\beta^2}\hat{g}_\phi} \right]. \tag{E.4}$$

From EQ. (E.2) and the above, EQ. (3.47) follows after simplification. The calculations for $\lambda = 1$ and $\lambda > 1$ are similar and lead to the same EQ. (3.47).

E.2. Solution for expansion coefficients

For reference, we note the EQs. (3.110) below

$$\dot{c}_k = \dot{c}_0 \, e^{-\imath k 2\gamma_0 t}, \qquad \dot{c}_0 = 4\gamma_0 \left[\left((1 - \gamma_0 t) + \frac{\imath}{2} \frac{\partial}{\partial k} \right)^2 c_k \right]_{k=0}, \qquad c_k(0) = \frac{e^{2\imath k}}{\sqrt{2\pi}}. \tag{E.5}$$

An integration for $c_k(t)$ in the first equation gives

$$c_k(t) = [c_k(0) - c_0(0)] + c_0(t)e^{-\imath k 2\gamma_0 t} + \imath k 2\gamma_0 \int_0^t c_0(s)e^{-\imath k 2\gamma_0 s} \, ds.$$

From the above, one has

$$\left[\frac{\partial}{\partial k}c_k(t)\right]_{k=0} = \frac{\imath 2}{\sqrt{2\pi}} - \imath 2\gamma_0 t\, c_0(t) + \imath 2\gamma_0 \int_0^t c_0(s)\, ds,$$

$$\left[\frac{\partial^2}{\partial k^2}c_k(t)\right]_{k=0} = \frac{(\imath 2)^2}{\sqrt{2\pi}} + (\imath 2\gamma_0 t)^2\, c_0(t) - 2(\imath 2\gamma_0)^2 \int_0^t s\, c_0(s)\, ds.$$

With the above evaluations, after substitution the middle EQ. (E.5) reads

$$\dot{c}_0(t) = 4\gamma_0 \left[(1-\gamma_0 t)^2 c_0(t) + \imath(1-\gamma_0 t)\left[\frac{\partial}{\partial k}c_k(t)\right]_{k=0} - \frac{1}{4}\left[\frac{\partial^2}{\partial k^2}c_k(t)\right]_{k=0} \right],$$

$$\Rightarrow \dot{c}_0(t) = 4\gamma_0 \left[-\frac{1}{\sqrt{2\pi}} + \gamma_0\, t\sqrt{\frac{2}{\pi}} + c_0(t) + 2\gamma_0 \int_0^t [\gamma_0(t-s)-1]\, c_0(s)\, ds \right].$$

With the Laplace transform defined as

$$[\mathcal{L}c_0](\sigma) = \int_0^\infty e^{-\sigma t}\, c_0(t)\, dt,$$

one has

$$[\mathcal{L}c_0](\sigma) = \frac{1}{\sqrt{2\pi}} \frac{\sigma^2 - 4\gamma_0\sigma + 8\gamma_0^2}{(\sigma - 2\gamma_0)(\sigma^2 - 2\gamma_0\sigma + 4\gamma_0^2)}.$$

Inverting the transform, the solution for $c_0(t)$ is obtained as

$$c_0(t) = \frac{1}{\sqrt{2\pi}} \left[e^{2\gamma_0 t} - \frac{2}{\sqrt{3}}\sin\left(\sqrt{3}\gamma_0\, t\right) e^{\gamma_0 t} \right]. \tag{E.6}$$

From the first and third equations in (E.5), it is easy to obtain the final result in EQ. (3.111).

Bibliography

[ABBH01]   S L Adler, D C Brody, T A Brun, and L P Hughston. Martingale models for quantum state reduction. *Journal of Physics A: Mathematical and General*, 34(42):8795, oct 2001.

[ABN$^+$01]   Andris Ambainis, Eric Bach, Ashwin Nayak, Ashvin Vishwanath, and John Watrous. One-dimensional quantum walks. In *Proceedings of the Thirty-Third Annual ACM Symposium on Theory of Computing*, STOC '01, page 37–49, New York, NY, USA, 2001. Association for Computing Machinery.

[AKJ65]   E. Arthurs and J. L. Kelly Jr. On the simultaneous measurement of a pair of conjugate observables. *Bell System Technical Journal*, 44(4):725–729, 1965.

[All69a]   G. R. Allcock. The time of arrival in quantum mechanics I. Formal considerations. *Annals of Physics*, 53(2):253–285, June 1969.

[All69b]   G.R. Allcock. The time of arrival in quantum mechanics ii. the individual measurement. *Annals of Physics*, 53(2):286–310, 1969.

[Bal98]   L.E. Ballentine. *Quantum Mechanics: A Modern Development*. G - Reference,Information and Interdisciplinary Subjects Series. World Scientific, 1998.

[Bar93]   A. Barchielli. Stochastic differential equations and a-posteriori states in quantum mechanics. *International Journal of Theoretical Physics*, 32(12):2221–2233, Dec 1993.

[BB91]   A. Barchielli and V. P. Belavkin. Measurements continuous in time and a posteriori states in quantum mechanics. *Journal of Physics A: Mathematical and General*, 24(7):1495–1514, Apr 1991.

[BB11]   Michel Bauer and Denis Bernard. Convergence of repeated quantum nondemolition measurements and wave-function collapse. *Phys. Rev. A*, 84:044103, Oct 2011.

[BBB12]   Michel Bauer, Denis Bernard, and Tristan Benoist. Iterated stochastic measurements. *Journal of Physics A: Mathematical and Theoretical*, 45(49):494020, 2012.

[BBB13]   Michel Bauer, Tristan Benoist, and Denis Bernard. Repeated quantum non-demolition measurements: Convergence and continuous time limit. *Annales Henri Poincaré*, 14(4):639–679, May 2013.

[BBC$^+$21]   Tristan Benoist, Cédric Bernardin, Raphaël Chetrite, Reda Chhaibi, Joseph Najnudel, and Clément Pellegrini. Emergence of jumps in quantum trajectories via homogenization. *Communications in Mathematical Physics*, 387:1821–1867, 2021.

[BBSR89]   M. Born, R.J. Blin-Stoyle, and J.M. Radcliffe. *Atomic Physics*. Dover books on physics and chemistry. Dover Publications, 1989.

[BBT15a]   Michel Bauer, Denis Bernard, and Antoine Tilloy. Computing the rates of measurement-induced quantum jumps. *Journal of Physics A: Mathematical and Theoretical*, 48(25):25FT02, jun 2015.

[BBT15b]   Michel Bauer, Denis Bernard, and Antoine Tilloy. Zooming in on quantum trajectories. *Journal of Physics A: Mathematical and Theoretical*, 49, 12 2015.

[BCC$^+$23]   Cédric Bernardin, Raphaël Chetrite, Reda Chhaibi, Joseph Najnudel, and Clément Pellegrini. Spiking and collapsing in large noise limits of SDEs. *The Annals of Applied Probability*, 33(1):417 – 446, 2023.

[BGL95]   Paul Busch, Marian Grabowski, and Pekka J. Lahti. Repeatable measurements in quantum theory: Their role and feasibility. *Foundations of Physics*, 25(9):1239–1266, Sep 1995.

[Bjö21]   T. Björk. *Point Processes and Jump Diffusions: An Introduction with Finance Applications*, chapter Connections between Stochastic Differential Equations and Partial Integro-Differential Equations, pages 56–63. Cambridge University Press, Cambridge, 2021.

[BKT92]   Vladimir B. Braginsky, Farid Ya Khalili, and Kip S. Thorne. *Quantum Measurement*. Cambridge University Press, 1992.

[BP02]   H.P. Breuer and F. Petruccione. *The Theory of Open Quantum Systems*. Oxford University Press, 2002.

[Bré81]   P. Brémaud. *Point Processes and Queues, Martingale Dynamics*. Springer series in statistics. Springer-Verlag, 1981.

[Bru02]   Todd A. Brun. A simple model of quantum trajectories. *American Journal of Physics*, 70(7):719–737, Jul 2002.

[BS21]   Alberto Biella and Marco Schiró. Many-body quantum zeno effect and measurement-induced subradiance transition. *Quantum*, 5:528, 2021.

[Bus03]   P. Busch. Quantum states and generalized observables: A simple proof of gleason's theorem. *Phys. Rev. Lett.*, 91:120403, Sep 2003.

[Car99]   H. Carmichael. *Statistical Methods in Quantum Optics 1: Master Equations and Fokker-Planck Equations*. Physics and astronomy online library. Springer, 1999.

[Car09]   H.J. Carmichael. *Statistical Methods in Quantum Optics 2: Non-Classical Fields*. Theoretical and Mathematical Physics. Springer Berlin Heidelberg, 2009.

[CE48]   A. E. Cameron and Jr. Eggers, D. F. An Ion "Velocitron". *Review of Scientific Instruments*, 19(9):605–607, September 1948.

[Coo88]   Richard J Cook. What are quantum jumps? *Physica Scripta*, 1988(T21):49, jan 1988.

[CTD86]   C. Cohen-Tannoudji and J. Dalibard. Single-atom laser spectroscopy. looking for dark periods in fluorescence light. *Europhysics Letters*, 1(9):441, may 1986.

[Dav69]   E. B. Davies. Quantum stochastic processes. *Communications in Mathematical Physics*, 15(4):277–304, Jan 1969.

[Dav84]   M. H. A. Davis. Piecewise-deterministic markov processes: A general class of non-diffusion stochastic models. *Journal of the Royal Statistical Society. Series B (Methodological)*, 46(3):353–388, 1984.

[DCM92]   Jean Dalibard, Yvan Castin, and Klaus Mølmer. Wave-function approach to dissipative processes in quantum optics. *Phys. Rev. Lett.*, 68:580–583, Feb 1992.

[DDD15]   S. Dhar, S. Dasgupta, and A. Dhar. Quantum time of arrival distribution in a simple lattice model. *J. Phys. A: Math. Theor.*, 48(11):115304, feb 2015.

[DDDS15] S. Dhar, S. Dasgupta, A. Dhar, and D. Sen. Detection of a quantum particle on a lattice under repeated projective measurements. *Phys. Rev. A*, 91:062115, Jun 2015.

[Dio86]   L. Diosi. Stochastic pure state representation for open quantum systems. *Physics Letters A*, 114(8):451–454, 1986.

[DM97]   V. Delgado and J. G. Muga. Arrival time in quantum mechanics. *Phys. Rev. A*, 56:3425–3435, Nov 1997.

[EM11a]   Martin R Evans and Satya N Majumdar. Diffusion with optimal resetting. *Journal of Physics A: Mathematical and Theoretical*, 44(43):435001, 2011.

[EM11b]   Martin R Evans and Satya N Majumdar. Diffusion with stochastic resetting. *Physical review letters*, 106(16):160601, 2011.

[EMS20]   Martin R Evans, Satya N Majumdar, and Grégory Schehr. Stochastic resetting and applications. *Journal of Physics A: Mathematical and Theoretical*, 53(19):193001, 2020.

[FG98]   Edward Farhi and Sam Gutmann. Quantum computation and decision trees. *Phys. Rev. A*,
            58:915–928, Aug 1998.

[FKB16]   H Friedman, D A Kessler, and E Barkai. Quantum renewal equation for the first detection
            time of a quantum walk. *Journal of Physics A: Mathematical and Theoretical*, 50(4):04LT01,
            dec 2016.

[FKB17]   H. Friedman, D. A. Kessler, and E. Barkai. Quantum walks: The first detected passage
            time problem. *Phys. Rev. E*, 95:032141, Mar 2017.

[GBD+07]   Christine Guerlin, Julien Bernu, Samuel Deleglise, Clement Sayrin, Sebastien Gleyzes, Ste-
            fan Kuhr, Michel Brune, Jean-Michel Raimond, and Serge Haroche. Progressive field-state
            collapse and quantum non-demolition photon counting. *Nature*, 448(7156):889–893, 2007.

[GG21]   Sarang Gopalakrishnan and Michael J. Gullans. Entanglement and purification transitions
            in non-hermitian quantum mechanics. *Phys. Rev. Lett.*, 126:170503, Apr 2021.

[GKS76]   Vittorio Gorini, Andrzej Kossakowski, and Ennackal Chandy George Sudarshan. Com-
            pletely positive dynamical semigroups of n-level systems. *Journal of Mathematical Physics*,
            17(5):821–825, 1976.

[GLE57]   ANDREW M. GLEASON. Measures on the closed subspaces of a hilbert space. *Journal of
            Mathematics and Mechanics*, 6(6):885–893, 1957.

[GVWW13]   F. A. Grünbaum, L. Velázquez, A. H. Werner, and R. F. Werner. Recurrence for discrete
            time unitary evolutions. *Communications in Mathematical Physics*, 320(2):543–569, Jun
            2013.

[Haw71]   Alan G. Hawkes. Spectra of some self-exciting and mutually exciting point processes.
            Biometrika, 58(1):83–90, 2022/05/08/ 1971. Full publication date: Apr., 1971.

[Hei04]   W D Heiss. Exceptional points of non-hermitian operators. *Journal of Physics A: Mathe-
            matical and General*, 37(6):2455, jan 2004.

[Hel76]   C. Helstrom. *Quantum Detection and Estimation Theory*. ISSN. Elsevier Science, 1976.

[HJ85]   Roger A. Horn and Charles R. Johnson. *Matrix Analysis*. Cambridge University Press, 1985.

[Hoc89]   H. Hochstadt. *Integral Equations*. Wiley Classics Library. Wiley, 1989.

[icvcvJK08] M. Štefaňák, I. Jex, and T. Kiss. Recurrence and pólya number of quantum walks. *Phys.
            Rev. Lett.*, 100:020501, Jan 2008.

[IGG+21]   Matteo Ippoliti, Michael J Gullans, Sarang Gopalakrishnan, David A Huse, and Vedika
            Khemani. Entanglement phase transitions in measurement-only dynamics. *Physical Review
            X*, 11(1):011030, 2021.

[IHBW90]   Wayne M. Itano, D. J. Heinzen, J. J. Bollinger, and D. J. Wineland. Quantum zeno effect.
            Phys. Rev. A, 41:2295–2300, Mar 1990.

[JS06]   Kurt Jacobs and Daniel A. Steck. A straightforward introduction to continuous quantum
            measurement. *Contemporary Physics*, 47(5):279–303, Sep 2006.

[Kem03]   J Kempe. Quantum random walks: An introductory overview. *Contemporary Physics*,
            44(4):307–327, 2003.

[KLM14]   P. L. Krapivsky, J. M. Luck, and K. Mallick. Survival of classical and quantum particles in
            the presence of traps. *J. Stat. Phys.*, 154(6):1430–1460, 2014.

[KM23]   Manas Kulkarni and Satya N Majumdar. First detection probability in quantum resetting
            via random projective measurements. *Journal of Physics A: Mathematical and Theoretical*,
            56(38):385003, sep 2023.

[Kon02]   Norio Konno. Quantum random walks in one dimension. *Quantum Information Processing*,
            1(5):345–354, Oct 2002.

[KS88]   I. Karatzas and S.E. Shreve. *Brownian Motion and Stochastic Calculus*. Graduate texts in
            mathematics. World Piblishing Company, 1988.

[LB06]   Michel Le Bellac. *Quantum Physics*. Cambridge University Press, 2006.

[LBMW03]   D. Leibfried, R. Blatt, C. Monroe, and D. Wineland. Quantum dynamics of single trapped ions. *Rev. Mod. Phys.*, 75:281–324, Mar 2003.

[LCF18]   Yaodong Li, Xiao Chen, and Matthew PA Fisher. Quantum zeno effect and the many-body entanglement transition. *Physical Review B*, 98(20):205136, 2018.

[LD19]   S. Lahiri and A. Dhar. Return to the origin problem for a particle on a one-dimensional lattice with quasi-zeno dynamics. *Phys. Rev. A*, 99:012101, Jan 2019.

[Lin76]   G. Lindblad. On the generatos of quantum dynamical semigroups. *Communications in Mathematical Physics*, 48:119–130, 1976.

[LL77]   L.D. Landau and E.M. Lifshitz. Chapter i - the basic concepts of quantum mechanics. In L.D. Lndau and E.M. Lifshitz, editors, *Quantum Mechanics (Third Edition)*, pages 1–24. Pergamon, third edition edition, 1977.

[LRS14]   Fuxiang Li, Jie Ren, and Nikolai A. Sinitsyn. Quantum zeno effect as a topological phase transition in full counting statistics and spin noise spectroscopy. *EPL (Europhysics Letters)*, 105(2):27001, Jan 2014.

[Man71]   L. I. Mandelstam. *Lectures on optics, relativity theory and quantum mechanics*. Nauka Eds, 1971.

[Mil06]   P. D. Miller. *Applied Asymptotic Analysis*. Springer, 2006.

[ML00]   J.G. Muga and C.R. Leavens. Arrival time in quantum mechanics. *Physics Reports*, 338(4):353–438, 2000.

[MMC$^+$20] Fabrizio Minganti, Adam Miranowicz, Ravindra W. Chhajlany, Ievgen I. Arkhipov, and Franco Nori. Hybrid-liouvillian formalism connecting exceptional points of non-hermitian hamiltonians and liouvillians via postselection of quantum trajectories. *Phys. Rev. A*, 101:062112, Jun 2020.

[MMCN19]   Fabrizio Minganti, Adam Miranowicz, Ravindra W. Chhajlany, and Franco Nori. Quantum exceptional points of non-hermitian hamiltonians and liouvillians: The effects of quantum jumps. *Phys. Rev. A*, 100:062131, Dec 2019.

[MMS$^+$19] Zlatko K Minev, Shantanu O Mundhada, Shyam Shankar, Philip Reinhold, Ricardo Gutiérrez-Jáuregui, Robert J Schoelkopf, Mazyar Mirrahimi, Howard J Carmichael, and Michel H Devoret. To catch and reverse a quantum jump mid-flight. *Nature*, 570(7760):200–204, 2019.

[MS77]   B. Misra and E. C. G. Sudarshan. The zeno's paradox in quantum theory. *J. Math. Phys.*, 18(4):756–763, 1977.

[MSM18]   B Mukherjee, K Sengupta, and Satya N Majumdar. Quantum dynamics with stochastic reset. *Physical Review B*, 98(10):104309, 2018.

[MWMS13]   KW Murch, SJ Weber, Christopher Macklin, and Irfan Siddiqi. Observing single quantum trajectories of a superconducting quantum bit. *Nature*, 502(7470):211–214, 2013.

[NRSR21]   Adam Nahum, Sthitadhi Roy, Brian Skinner, and Jonathan Ruhman. Measurement and entanglement phase transitions in all-to-all quantum circuits, on quantum trees, and in landau-ginsburg theory. *PRX Quantum*, 2(1):010352, 2021.

[NSD86]   Warren Nagourney, Jon Sandberg, and Hans Dehmelt. Shelved optical electron amplifier: Observation of quantum jumps. *Phys. Rev. Lett.*, 56:2797–2799, Jun 1986.

[Oza84]   Masanao Ozawa. Quantum measuring processes of continuous observables. *Journal of Mathematical Physics*, 25(1):79–87, 01 1984.

[Per71]   A. M. Perelomov. On the completeness of a system of coherent states. *Theoretical and Mathematical Physics*, 6(2):156–164, Feb 1971.

[Per12]   A. Perelomov. *Generalized Coherent States and Their Applications*. Theoretical and Mathematical Physics. Springer Berlin Heidelberg, 2012.

[PK98]   M. B. Plenio and P. L. Knight. The quantum-jump approach to dissipative dynamics in quantum optics. *Rev. Mod. Phys.*, 70:101–144, Jan 1998.

[PKE16]   Arnab Pal, Anupam Kundu, and Martin R Evans. Diffusion under time-dependent resetting. *Journal of Physics A: Mathematical and Theoretical*, 49(22):225001, 2016.

[RBH01]   J. M. Raimond, M. Brune, and S. Haroche. Manipulating quantum entanglement with atoms and photons in a cavity. *Rev. Mod. Phys.*, 73:565–582, Aug 2001.

[RCGG20]   Sthitadhi Roy, J. T. Chalker, I. V. Gornyi, and Yuval Gefen. Measurement-induced steering of quantum systems. *Phys. Rev. Res.*, 2:033347, Sep 2020.

[Reh80]   W. Rehder. When do projections commute? *Zeitschrift für Naturforschung A*, 35(4):437–441, 1980.

[RG17]   Édgar Roldán and Shamik Gupta. Path-integral formalism for stochastic resetting: Exactly solved examples and shortcuts to confinement. *Phys. Rev. E*, 96:022130, Aug 2017.

[RN12]   F. Riesz and B.S. Nagy. *Functional Analysis*. Dover Books on Mathematics. Dover Publications, 2012.

[RSM+14]   Nicolas Roch, Mollie E Schwartz, Felix Motzoi, Christopher Macklin, Rajamani Vijay, Andrew W Eddins, Alexander N Korotkov, K Birgitta Whaley, Mohan Sarovar, and Irfan Siddiqi. Observation of measurement-induced entanglement and quantum trajectories of remote superconducting qubits. *Physical review letters*, 112(17):170501, 2014.

[RTLG18]   Dominic C. Rose, Hugo Touchette, Igor Lesanovsky, and Juan P. Garrahan. Spectral properties of simple classical and quantum reset processes. *Phys. Rev. E*, 98:022129, Aug 2018.

[SH66]   C. Y. She and H. Heffner. Simultaneous measurement of noncommuting observables. *Phys. Rev.*, 152:1103–1110, Dec 1966.

[Sha94]   R. Shankar. *Principles of Quantum Mechanics*. Springer, 1994.

[SKR20]   Kyrylo Snizhko, Parveen Kumar, and Alessandro Romito. Quantum zeno effect appears in stages. *Phys. Rev. Research*, 2:033512, Sep 2020.

[TBF+21]   Xhek Turkeshi, Alberto Biella, Rosario Fazio, Marcello Dalmonte, and Marco Schiró. Measurement-induced entanglement transitions in the quantum ising chain: From infinite to zero clicks. *Phys. Rev. B*, 103:224210, Jun 2021.

[TBK18]   Felix Thiel, Eli Barkai, and David A. Kessler. First detected arrival of a quantum walker on an infinite line. *Phys. Rev. Lett.*, 120:040502, Jan 2018.

[TDFS22]   Xhek Turkeshi, Marcello Dalmonte, Rosario Fazio, and Marco Schirò. Entanglement transitions from stochastic resetting of non-hermitian quasiparticles. *Phys. Rev. B*, 105:L241114, Jun 2022.

[TK20]   F. Thiel and D. A. Kessler. Non-hermitian and zeno limit of quantum systems under rapid measurements. *Phys. Rev. A*, 102:012218, Jul 2020.

[TKB18]   F. Thiel, D. A. Kessler, and E. Barkai. Spectral dimension controlling the decay of the quantum first-detection probability. *Phys. Rev. A*, 97:062105, Jun 2018.

[TKB20]   F. Thiel, D. A. Kessler, and E. Barkai. Quantization of the mean decay time for non-hermitian quantum systems. *Phys. Rev. A*, 102:022210, Aug 2020.

[TMKB20]   F. Thiel, I. Mualem, D. A. Kessler, and E. Barkai. Uncertainty and symmetry bounds for the quantum total detection probability. *Phys. Rev. Research*, 2:023392, Jun 2020.

[TMM+20]   Felix Thiel, Itay Mualem, Dror Meidan, Eli Barkai, and David A. Kessler. Dark states of quantum search cause imperfect detection. *Phys. Rev. Res.*, 2:043107, Oct 2020.

[Tum22a]   Roderich Tumulka. Absorbing boundary condition as limiting case of imaginary potentials. *Communications in Theoretical Physics*, 75(1):015103, dec 2022.

[Tum22b]   Roderich Tumulka. Detection-time distribution for several quantum particles. *Phys. Rev. A*, 106:042220, Oct 2022.

[Tum22c]   Roderich Tumulka. Distribution of the time at which an ideal detector clicks. *Annals of Physics*, 442:168910, 2022.

[vN18]   John von Neumann. *Mathematical Foundations of Quantum Mechanics*. Princeton University Press, Princeton, 2018.

[Wer87]   R. Werner. Arrival time observables in quantum mechanics. *Ann. Inst. Henri Poincaré*, 47(4):429–449, 1987.

[WM93]   H. M. Wiseman and G. J. Milburn. Interpretation of quantum jump and diffusion processes illustrated on the bloch sphere. *Phys. Rev. A*, 47:1652–1666, Mar 1993.

[WM09]   Howard M. Wiseman and Gerard J. Milburn. *Quantum Measurement and Control*. Cambridge University Press, 2009.

[Wol01]   E. Wolf. *Progress in Optics: Volume 42*. Progress in Optics. North-Holland Publishing Company, 2001.

[YB23]   R. Yin and E. Barkai. Restart expedites quantum walk hitting times. *Phys. Rev. Lett.*, 130:050802, Feb 2023.

[YKH⁺09]   Masami Yasuda, Takuya Kohno, Kazumoto Hosaka, Hajime Inaba, Yoshiaki Nakajima, Atsushi Onae, Hidetoshi Katori, and Feng-Lei Hong. Development of an Yb optical lattice clock using a fermionic isotope. In Tetsuya Ido and Derryck T. Reid, editors, *Time and Frequency Metrology II*, volume 7431, page 74310G. International Society for Optics and Photonics, SPIE, 2009.

Published Articles

[PubDBD21] Varun Dubey, Cédric Bernardin, and Abhishek Dhar. Quantum dynamics under continuous projective measurements: Non-hermitian description and the continuum-space limit. *Phys. Rev. A*, 103:032221, Mar 2021.

[PubDCD23] Varun Dubey, Raphael Chetrite, and Abhishek Dhar. Quantum resetting in continuous measurement induced dynamics of a qubit. *Journal of Physics A: Mathematical and Theoretical*, 56(15):154001, mar 2023.